



This is to certify that the
dissertation entitled

UREASE METALLOCENTER ASSEMBLY IN
KLEBSIELLA AEROGENES

presented by

Mary Beth C. Moncrief

has been accepted towards fulfillment
of the requirements for

Ph.D. degree in Biochemistry


Major professor

Date 10/24/96

LIBRARY
Michigan State
University

PLACE IN RETURN BOX to remove this checkout from your record.
TO AVOID FINES return on or before date due.

DATE DUE	DATE DUE	DATE DUE
_____	_____	_____
_____	_____	_____
_____	_____	_____
_____	_____	_____
_____	_____	_____
_____	_____	_____
_____	_____	_____

MSU is An Affirmative Action/Equal Opportunity Institution

UREASE METALLOCENTER ASSEMBLY IN *KLEBSIELLA AEROGENES*

By

MARY BETH C. MONCRIEF

A DISSERTATION

**Submitted to
Michigan State University
in partial fulfillment of the requirements
for the degree of**

DOCTOR OF PHILOSOPHY

Department of Biochemistry

1996

ABSTRACT

UREASE METALLOCENTER ASSEMBLY IN *KLEBSIELLA AEROGENES*

By

Mary Beth C. Moncrief

Urease is a nickel-containing enzyme that functions in nitrogen metabolism and participates as a virulence factor of several human pathogens. The protein contains a binuclear active site where the metal ions are bridged by a lysine carbamate. Metallocenter assembly in *Klebsiella aerogenes* urease requires the participation of four accessory proteins: UreD, UreE, UreF, and UreG. Previous studies suggested that UreE functions as a nickel donor, but roles for the other components were unknown.

I demonstrated that urease apoprotein could be activated *in vitro* and, using deletion derivatives, showed that UreD played a key role in this process. I overexpressed *ureF* and studied the insoluble gene product. I identified a series of complexes containing UreD, UreF, and urease apoprotein and characterized their properties. My results suggest that UreF modulates the UreD-urease apoprotein complexes activation properties by excluding nickel ions from the active site until after the carbamylated lysine metallocenter ligand forms. I purified UreG and showed that, despite having a P-loop motif, it does not bind or hydrolyze nucleotides. Site-directed mutagenesis of the motif resulted in no detectable urease activity; thus the motif is essential *in vivo*. I partially purified a complex containing UreD, UreF, and UreG and showed that, unlike UreG, it bound to an ATP-linked

resin. I showed that the UreG P-loop was not involved in UreD-UreF-UreG complex formation, but was needed for binding to an ATP-linked resin. Based on these studies, I propose a model for urease metallocenter assembly.

In other studies, I characterized the activity of crystalline urease and further examined the apoprotein. I demonstrated that the enzyme is essentially inactive in the crystal lattice and I resolved purified urease apoprotein into a series of bands by nondenaturing gel electrophoresis. I showed that these species are likely to arise, in part, by mixed disulfide formations involving Cys-319.

To my parents, John and Pat Carr, and my husband, Dan, with love.

ACKNOWLEDGMENTS

I would like to thank Dr. Robert Hausinger for being my mentor and providing an inexhaustable supply of guidance and support. I thank the members of my guidance committee: Dr. Shelagh Ferguson-Miller, Dr. Paul Kindel, Dr. Lee Kroos, and Dr. Martha Mulks for their direction, support, and advice. I appreciate the technical advice as well as support from current and previous members of the lab (Tim Brayman, Gerry Coplas, Debbie Hogan, Linda Michel, Taha Taha, and Ruth Wallace).

I would like to thank Dr. Pao-Chi Liao and Dr. Doug Gage for their work on the MALDI-mass spectrometry of UreG, and Il-Seon Park for the *Escherichia coli* (pKAUG-1) strain. A special thank you goes to Dr. Tom Deits whose lab I worked in during a rotation session and who has provided encouragement and support when needed. My appreciation also goes out to Dr. Evelyn Jabri and Dr. Andy Karplus for their crystallographic studies on urease and for providing me with their crystallization protocol that I used for the activation studies in Chapter 2.

Finally, I would like to thank my parents and my husband for all the support, understanding, and patience that they gave me during the years.

TABLE OF CONTENTS

LIST OF TABLES.....	vi
LIST OF FIGURES.....	vii
CHAPTER 1	
INTRODUCTION.....	1
Urease significance and structure.....	2
Urease metallocenter assembly.....	7
Urease metallocenter stability and <i>in vitro</i> activation of urease apoprotein.....	8
Identification of accessory genes required for bacterial urease activation.....	10
Postulated role of UreD as a urease-specific chaperone protein.....	13
Potential role of UreE as a nickel-donor.....	17
Characterization of UreF.....	20
Characterization of UreG.....	23
Current model for bacterial urease metallocenter assembly.....	27
Accessory genes required for urease activation in eukaryotes.....	31
Summary.....	32
Thesis Outline.....	33
References.....	36
CHAPTER 2	
UREASE ACTIVITY IN THE CRYSTALLINE STATE.....	46
Abstract.....	47
Introduction.....	48
Materials and Methods.....	49
Enzyme Purification and crystallization.....	49
Assays.....	49
Salt inhibition of urease activity.....	50
Results and Discussion.....	50
Activity of crystalline urease.....	50
Kinetic analysis of salt inhibition.....	54
References.....	57

CHAPTER 3	
FIRST DEMONSTRATION OF IN VITRO ACTIVATION OF UREASE	
APOPROTEIN.....	58
Abstract.....	59
Introduction.....	60
Materials and Methods.....	61
Cell growth and disruption.....	62
Urease activity assays.....	62
Results and Discussion.....	62
<i>In vitro</i> activation of urease apoprotein.....	62
References.....	67
CHAPTER 4	
PURIFICATION AND ACTIVATION PROPERTIES OF URED-UREF-UREASE	
APOPROTEIN COMPLEXES.....	
	70
Abstract.....	71
Introduction.....	72
Materials and Methods.....	74
Bacterial strains and plasmid constructions.....	74
Culture conditions and cell disruption.....	76
Purification of DF-Apo.....	76
Polyacrylamide gel electrophoresis.....	77
Urease activity assays.....	78
Activation of urease apoproteins.....	78
Results and Discussion.....	78
Purification and characterization of UreD-UreF-urease apoprotein	
complexes.....	78
Activation properties of DF-Apo.....	84
Function of UreF.....	86
References.....	92
CHAPTER 5	
CHARACTERIZATION OF UREG, IDENTIFICATION OF A URED-UREF-	
UREG COMPLEX, AND EVIDENCE THAT A FUNCTIONAL	
NUCLEOTIDE-BINDING SITE IS REQUIRED FOR IN VIVO	
METALLOCENTER ASSEMBLY OF UREASE.....	
	94
Abstract.....	95
Introduction.....	97
Materials and Methods.....	98
Bacterial strains and plasmid construction.....	98
Culture conditions.....	100
Purification of UreG.....	100
Partial purification of the DFG complex.....	101
Preparation of polyclonal antibodies against UreG.....	102

Polyacrylamide gel electrophoresis.....	103
Urease activity assays.....	103
Equilibrium dialysis determination of nucleotide binding.....	104
Chromatographic measurement of nucleotide hydrolysis.....	104
Carbonic anhydrase activity.....	105
Results.....	105
UreG purification and characterization.....	105
Site-directed mutagenesis of UreG.....	108
Partial purification of the DFG complex.....	108
Discussion.....	112
UreG purification and partial characterization.....	112
The requirement of the P-loop motif for UreG function.....	113
The DFG complex.....	114
References.....	116

CHAPTER 6

PURIFICATION OF UREF AND CHARACTERIZATION OF NON-NATIVE URED-UREF-UREG-UREASE APOPROTEIN COMPLEXES.....

Abstract.....	120
Introduction.....	121
Materials and Methods.....	122
Bacterial strains and plasmid construction.....	122
Culture conditions and cell disruption.....	123
Partial purification of UreF.....	124
Enrichment of DFG-Apo.....	125
Polyacrylamide gel electrophoresis.....	126
Urease activity assays.....	126
Activation of urease apoprotein.....	127
Results and Discussion.....	127
High level synthesis and partial purification of UreF.....	127
Enrichment of DFG-Apo.....	132
References.....	137

CHAPTER 7

ADDITIONAL STUDIES.....	139
Identification of a series of urease apoprotein forms.....	140
Incubation of Apo and UreD-UreF-UreG complex.....	145
References.....	149

CHAPTER 8

CONCLUSIONS AND FUTURE PROSPECTS.....	150
References.....	160

APPENDIX I.....	161
-----------------	-----

LIST OF TABLES

CHAPTER 2

Table 1-Specific activities of soluble and crystalline <i>K. aerogenes</i> urease.....	51
---	----

CHA

CHA

CHA

CHA

CHA

LIST OF FIGURES

CHAPTER 1

Figure 1-Model of the urease bi-nickel active site.....	5
Figure 2-The <i>K. aerogenes</i> urease gene cluster.....	12
Figure 3-Sequence comparison of selected UreD sequences.....	15
Figure 4-Sequence comparison of selected UreE sequences.....	18
Figure 5-Sequence comparison of selected UreF sequences.....	22
Figure 6-Sequence comparison of selected UreG sequences.....	25
Figure 7-Model for urease metallocenter assembly.....	30

CHAPTER 2

Figure 1-Urease activity as a function of salt concentration.....	55
Figure 2-Kinetic analysis of Li_2SO_4 inhibition of urease.....	56

CHAPTER 3

Figure 1- <i>In vitro</i> activation kinetics of urease apoprotein.....	64
Figure 2-Urease stability during incubation at 37 °C.....	66

CHAPTER 4

Figure 1-Schematic representations of several plasmids utilized in these studies.....	75
Figure 2-Partial purification of the DF-Apo as analyzed by SDS/polyacrylamide gel electrophoresis.....	80
Figure 3-Native polyacrylamide gel electrophoretic comparison of the D-Apo and DF-Apo samples.....	82
Figure 4-Nickel ion concentration dependence of activation for the DF-Apo.....	85
Figure 5-Bicarbonate ion concentration dependence of activation for the DF-Apo.....	88
Figure 6-Effect of incubation of DF-Apo with metal ions prior to activation by NiCl_2 and bicarbonate.....	90
Figure 7-Effect of zinc ion concentration on DF-Apo activation.....	91

CHAPTER 5

Figure 1-Purification of UreG as monitored by SDS/polyacrylamide	
--	--

CHAP

CHAP

CHAP

gel electrophoresis.....	107
Figure 2-Effects of alterations to the UreG P-loop on formation of urease apoprotein complexes.....	109
Figure 3-Analysis of the UreD-UreF-UreG complex bound to an ATP- linked agarose resin as analyzed by SDS/polyacrylamide gel electrophoresis.....	110
CHAPTER 6	
Figure 1-SDS/polyacrylamide gel electrophoretic analysis of UreF solubilization.....	129
Figure 2-Purification of ThioHisF as analyzed by SDS/polyacrylamide gel electrophoresis.....	130
Figure 3-Analysis of DFG-Apo complex purified from <i>E. coli</i> (pKAUD2F+) by SDS/polyacrylamide gel electrophoresis.....	133
Figure 4-Bicarbonate ion concentration dependence of activation for the DFG-Apo*.....	135
Figure 5-Nickel ion concentration dependence of activation for the DFG-Apo*.....	136
CHAPTER 7	
Figure 1-Nondenaturing polyacrylamide gel electrophoretic analysis of Apo.....	141
Figure 2-Nondenaturing polyacrylamide gel electrophoretic analysis of purified Apo from <i>E. coli</i> (pKAU17C319A Δ ureD).....	144
Figure 3-SDS/polyacrylamide electrophoretic analysis of Apo and DFG pool after Superose 12 chromatography.....	146
Figure 4-Native polyacrylamide gel electrophoretic analysis of Apo and DFG pool after Superose 12 chromatography.....	147
CHAPTER 8	
Figure 1-Proposed nucleotide hydrolysis scheme for the DFG complex.....	157
Figure 2-Model for urease metallocenter assembly.....	159

ABBREVIATIONS

Apo	urease apoprotein
D-Apo	UreD-urease apoprotein
DF-Apo	UreD-UreF-urease apoprotein
DFG	UreD-UreF-UreG
DFG-Apo	UreD-UreF-UreG-urease apoprotein
DFG-Apo*	UreD-UreF-UreG-urease apoprotein produced in <i>Escherichia coli</i> (pKAUD2F+) cells

CHAPTER 1

INTRODUCTION

This chapter represents an updated version of a review chapter that was published as Moncrief, M. B. C., and R. P. Hausinger (1996). Nickel incorporation into urease. In *Mechanisms of Metallocenter Assembly* (R. P. Hausinger, G. L. Eichhorn, and L. G. Marzilli, eds.) VCH Publishers, Inc., New York, pp. 151-171. I include a section that outlines the remainder of the thesis.

I. Urease

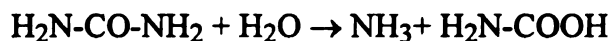
U
hydrolysis
an unstable
molecule

This act
inverteb
importa
be cryst

referenc
allows
urea an
nitroge
that ini
rumina
for uti
bacteri
these s
as a vi
shown

I. Urease Significance and Structure

Urease (EC 3.5.1.5) is a nickel-containing enzyme (1-3, 95) that catalyzes the hydrolysis of urea to give one molecule each of ammonia and carbamate. Carbamate is an unstable molecule and subsequently degrades to form carbonic acid and a second molecule of ammonia:



This activity has been found in a large number of bacterial species, several fungi, selected invertebrates, and a variety of plants. Urease from the jack bean plant has played an important historical role in the field of biochemistry (1): It was the first enzyme ever to be crystallized (4) as well as the first enzyme demonstrated to contain nickel (5).

The functional significance of urease differs for different organisms (reviewed in reference 3). For example, in many soil microorganisms, the presence of this enzyme allows cells to utilize urea as an environmentally important source of nitrogen (6). Soil urea arises from mammalian excretion, metabolism of uric acid, or degradation of other nitrogenous compounds. Similarly, urea is used as a nitrogen source by certain bacteria that inhabit the rumen (7). In this case, a portion of the urea waste product generated by a ruminant diffuses into the forestomach, urease activity of selected rumen microbes allows for utilization of this nitrogen source, bacterial growth rates are enhanced, and the bacteria ultimately serve as additional nutrient biomass for the animal. In contrast to these situations where urease provides ammonia as a nutrient, the enzyme also functions as a virulence factor in certain bacteria (3, 95). For example, urease activity has been shown to be important in the development of urinary stones (8), acute pyelonephritis (9),

urinary

urease

concent

(13). a

(review

especia

sugges

defens

genera

eukary

contai

polype

DNA

inhibi

(appro

contra

analy

subur

Furth

bean

struct

prote

residu

the si

seque

urinary catheter obstruction (10), and peptic ulceration (11, 12). In plants, the role of urease is less clear, but it does appear to have an essential function. Because toxic concentrations of urea accumulate in the leaves of plants grown in the absence of nickel (13), a pathway of nitrogen flux involving urea as an intermediate has been proposed (reviewed in reference 14). Recycling of urea-derived nitrogen by urease appears to be especially important during seed germination (87). Polacco and Holland (14) have also suggested that the embryo-specific urease of some plant seeds may play a role in chemical defense against herbivores by causing hyperammonemia to occur, similar to that generated by ureases of some pathogenic bacteria.

Urease metal contents and protein sequences are highly conserved among eukaryotic and prokaryotic organisms (2). Jack bean urease is a homohexameric protein containing two nickel ions per subunit (5). The primary sequence of the single polypeptide (M_r 90,770; 840 amino acids) has been determined by both protein (15) and DNA (16) sequencing methods. Similarly, atomic absorption analysis coupled with inhibitor studies demonstrated the presence of two nickel ions per catalytic unit (approximate M_r 100,000) in the enzyme isolated from *Klebsiella aerogenes* (17). In contrast to the plant enzyme, however, protein characterization (18) and DNA sequence analysis (19) of the genes encoding this bacterial enzyme indicates the presence of three subunits (M_r 11,086, 11,695, and 60,304 for UreA, UreB, and UreC, respectively). Furthermore, the size of the native bacterial protein is less than half that of the native jack bean urease (18). Although differing in the number of distinct subunits and in quaternary structure, the *K. aerogenes* and plant enzymes are greater than 50 percent identical in protein sequence: UreA aligns with residues 1-101 of jack bean urease, UreB matches residues 132-237, and UreC is homologous to residues 271-840.

The presence of multiple distinct subunits, each related in sequence to portions of the single subunit jack bean enzyme, also has been observed (or inferred from DNA sequence analysis) for ureases from *Proteus mirabilis* (20), *P. vulgaris* (21), *Ureaplasma*

ureally the

muscle

Bacillus

influenza

tubercu

GenBank

shown to

only two

those four

consisten

Although

that have

two nick

similarity

with the p

T

this enzy

the *K. ae*

resolution

trimer of

catalytic

and are b

to one m

distorted

include H

second n

272. Lys-

urealyticum (22, 105), *Helicobacter pylori* (23, 24), *H. felis* (25), *H. heilmannii* (26), *H. mustelae* (106), *H. nemestrinae* (107), *Yersinia enterocolitica* (27, 88), a thermophilic *Bacillus* species (28), *Rhizobium meliloti* (29), *Staphylococcus xylosus* (30), *Haemophilus influenzae* (96), *Bacillus pasteurii* (97), *Streptococcus salivarius* (99), *Mycobacterium tuberculosis* (100), and *Lactobacillus fermentum* (unpublished sequence submitted to GenBank with accession number D10605). In most cases, genes for three subunits were shown to be present, however, the five *Helicobacter* species possess genes that encode only two urease subunits, where the smaller ($\sim M_r$ 30,000) includes sequences similar to those found in both of the smaller subunits of three-subunit enzymes. These results are consistent with gene fusion or disruption events during evolution of this enzyme. Although exceptions have been noted (31-33), the metal content of most bacterial ureases that have been examined resembles that of the *K. aerogenes* enzyme [i.e., approximately two nickel ions per large subunit (reviewed in reference 2)]. The high degree of sequence similarity and the near identity in metal content observed among ureases is consistent with the presence of the same general active site in each of these proteins.

The structure of the urease active site and the detailed mechanism of action for this enzyme are best understood for the protein isolated from *K. aerogenes*. In particular, the *K. aerogenes* enzyme has been crystallized (49) and the structure determined to 2.2 Å resolution and refined to an *R* factor of 18.2 percent (89). The enzyme is a tightly packed trimer of trimers $[(\alpha\beta\gamma)_3]$ containing three bi-nickel active sites. Key features of the catalytic center are illustrated in Figure 1. The two nickel ions are located 3.5 Å apart and are bridged by a carbamate formed on Lys-217. A solvent molecule is tightly bound to one metal ion and appears to partially bridge to the second. One nickel ion possesses a distorted trigonal bipyramidyl or distorted square pyramidyl geometry and the five ligands include His-134, His-136, Asp-360, Lys-217 carbamate, and water (or hydroxide). The second nickel ion possesses pseudotetrahedral geometry and is liganded by His-246, His-272, Lys-217 carbamate, and solvent in partial occupancy.

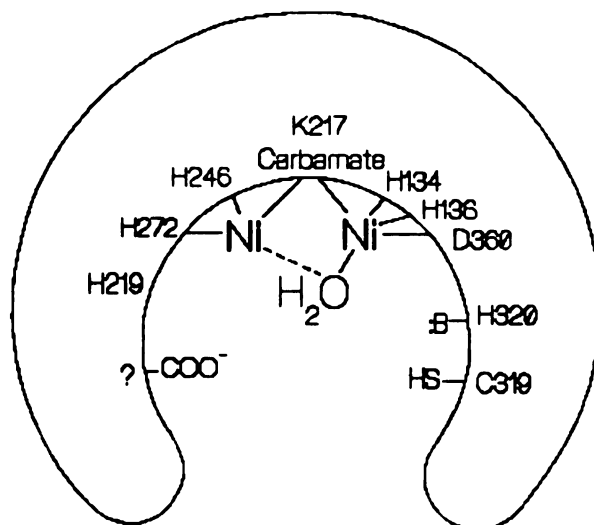


Figure 1. Model of the urease bi-nickel active site. The enzyme possesses a novel binickel center in which one nickel ion is coordinated to His-246, His-272, one oxygen atom of a lysine carbamate, and, with partial occupancy, a solvent molecule (*K. aerogenes* numbering). The second nickel ion is coordinated by His-134, His-136, Asp-360, the other oxygen atom of carbamylated Lys-217, and the solvent molecule (89). Urea is thought to coordinate to the nickel ion on the left. The metal ion acts as a Lewis acid, and the *O*-coordinated resonance form is proposed to be stabilized by interaction with His-219 and one of several carboxylate groups at the active site. The water bound to the second nickel ion, probably in its deprotonated form, carries out a nucleophilic attack on the urea carbon atom to form a tetrahedral intermediate. Ammonia is released by a general acid-assisted reaction (perhaps involving His-320), and, finally, carbamate is released.

i

fo

Th

car

Elir

invc

sight

enzy

to en

(43).

the cr

cente

bioph

nicke

imida

donor

nicke

magn

ions i

betwe

diana

obtain

In addition to the metallocenter ligands, the crystal structure reveals several additional residues worth noting. His-219 is appropriately positioned to stabilize substrate binding to the fourth ligand position of the second nickel ion. His-320 is located near the bi-nickel center and is likely to participate in catalysis. Finally, Cys-219 is within the active site environment, but does not play a catalytic role.

Catalysis has been suggested to proceed by urea binding in *O*-coordination to the fourth coordination site of the second nickel ion with stabilization rendered by His-219. The solvent molecule that is now solely coordinated to the first nickel ion is thought to carry out nucleophilic attack on the bound urea to form a tetrahedral intermediate. Elimination of ammonia from the intermediate is facilitated by proton donation, possibly involving His-320, and carbamate is released. This working model of urease catalysis is a slight modification of that originally proposed by Zerner and colleagues for the jack bean enzyme (43). The novel binuclear nickel-dependent active site of urease has been shown to enhance the degradation of urea by at least 10^{14} -fold over the uncatalyzed reaction (43). Additional studies involving *K. aerogenes* urease are discussed below in terms of the crystallographically determined structure and this mechanistic model. The binuclear center of the *K. aerogenes* enzyme has been probed by several spectroscopic and biophysical methods. On the basis of X-ray absorption spectroscopic analyses, the two nickel ions were thought to possess 5-coordinate geometry with approximately two imidazoles bound per nickel and the remainder of the ligands being oxygen or nitrogen donors (no thiols) (34). The crystal structure confirms that this is the geometry for one nickel ion, but is an overestimate for the second nickel ion (89). Saturation magnetization measurements provide no evidence for magnetic coupling of the two nickel ions in the native enzyme (35), but rather are consistent with a pH-dependent equilibrium between $S=1$ and $S=0$ metal ions. In the presence of a thiol, the metallocenter becomes diamagnetic and clear evidence for antiferromagnetic coupling of the two nickel ions was obtained by using variable temperature magnetic circular dichroism spectroscopy

(Micha

enzym

apparen

eviden

respec

direct

conse

(H13

addit

amin

invo

the

con.

ure

ha

di

sh

in

e

r

c

a

(Michael Johnson, personal communication), as previously reported for the jack bean enzyme (36). Furthermore, X-ray absorption spectroscopic analysis revealed that the apparent five-coordinate geometry is retained in thiol-inhibited enzyme and provided evidence for the presence of Ni-S and Ni-Ni scattering components at 2.23 Å and 3.26 Å, respectively (34).

Analysis of the metallocenter ligands has been examined by other methods. Site-directed mutagenesis experiments were carried out to convert independently three highly conserved histidine residues to alanine resulting in the loss of one (H134A) or both (H136A and H246A) of the nickel ions from the active site of the enzyme (37). An additional urease metallocenter ligand has been suggested to arise from reaction of an amino acid side-chain with a molecule of carbon dioxide (38). Based on precedent involving ribulose 1,5-bisphosphate carboxylase/oxygenase, a reasonable possibility for the identity of this ligand is a lysine carbamate. The crystal structure subsequently confirmed that His-134, His-136, His-246, and the carbamate of Lys-217 were ligands.

Additional studies have been used to tentatively identify other residues at the urease active site. An ionizable residue with $pK_a = 6.55$ is required for catalysis (18) and has been tentatively identified as His-320 from chemical modification studies and site-directed mutagenesis methods (37, 39). Another ionizable group with $pK_a = 8.55$ was shown to participate in catalysis (18); this group was tentatively assigned to a Cys-319 interacting with another unidentified residue (40). Chemical derivatization of Cys-319 eliminates urease activity (41); however, C319A, C319S, and C319D mutant proteins retain significant levels of activity and Cys-319 is now thought to play no catalytic role despite its location at the active site (42). Finally, the presence of an acidic group at the active site has been suggested on the basis of apparent electrostatic repulsion of negatively charged inhibitors (17) and chemical reagents (41).

II. UREASE METALLOCENTER ASSEMBLY

In

require e

discussio

the requ

demonst

activation

by four

requirem

genetic a

activation

presence

A. Urea

containi

denatur

(44, 45

protein

flexibil

site or

In vivo assembly of the urease metallocenter is a complex process that appears to require energy and the participation of several auxiliary protein components. My discussion of this topic begins by describing the stability of the urease metallocenter and the requirements for its *in vitro* assembly. Evidence will then be presented to demonstrate the presence of multiple accessory genes that are required for *in vivo* activation of bacterial urease. I will then detail known properties of the products encoded by four of these genes. By combining knowledge of the *in vitro* urease activation requirements with my understanding of the accessory protein properties gleaned from genetic and biochemical characterization studies, I will propose a model for the *in vivo* activation mechanism of urease. Finally, I summarize evidence consistent with the presence of similar accessory genes in eukaryotes.

A. Urease Metallocenter Stability and *in vitro* Activation of Urease Apoprotein

The nickel ions of urease are not removed by dialysis of the enzyme in buffers containing 1 mM EDTA at neutral pH (1, 42); however, harsh treatments with denaturants or acid conditions result in an irreversible loss of nickel and urease activity (44, 45). This evidence is consistent with the nickel metallocenter being buried in the protein. Assembly of the urease metallocenter must then require either conformational flexibility of the apoprotein to allow the nickel ions to penetrate into the metal binding site or the assistance of additional cellular factors to allow partial unfolding of the

apoprotei

address th

In:

(termed A

cultures g

activation

denaturar

achieved

nickel-de

urease g

reaching

function

More re

apoprote

it accou

sites. It

dioxide

interact

proposa

carbon

much li

apoprotein. As described later, *in vitro* and *in vivo* activation studies have been used to address this question.

In vitro activation of urease had not been achieved until 1994. Urease apoproteins (termed Apo) that are present in crude bacterial or plant cell extracts, obtained from cultures grown in nickel-depleted media, generally have been found to be incapable of activation by simple nickel ion addition or by providing nickel ion in the presence of denaturants or stabilizing compounds (46-48). Partial *in vitro* urease activation was achieved, however, by using freshly prepared, highly concentrated cell extracts from nickel-depleted *E. coli* cultures that contain and overexpress plasmid-borne *K. aerogenes* urease genes (48, Chapter 3). In this case, the activation process was both very slow, reaching maximal specific activity after approximately 1 day, and far from complete, with functional metal ion incorporation into only about 10 percent of the Apo that is present. More recently, *in vitro* urease activation was realized using purified *K. aerogenes* apoprotein (38). The observed activation was complete in approximately three hours, and it accounted for metallocenter assembly into nearly 30 percent of the total urease catalytic sites. It was remarkable at the time that the *in vitro* process was shown to require carbon dioxide in addition to nickel ion. The kinetics of activation were consistent with initial interaction between carbon dioxide and the protein, followed by nickel binding. The proposal put forward to explain this result was that an active site residue may react with carbon dioxide to form a carbamate that subsequently serves as a metal-binding ligand, much like the lysine that forms a carbamate involved in magnesium binding in ribulose

1,5-bisph

crystal str

A

Apo. it is

from the

apparent

Lee et al

nickel ic

of prote

ions

dicyclo

urease

access

B. Iden

variety

other t

51-57

K. ae

illustr

1,5-bisphosphate carboxylase/oxygenase (50). This hypothesis has been confirmed by the crystal structure of the enzyme (89).

Although conditions now have been identified to at least partially activate purified Apo, it is important to emphasize that urease activation *in vitro* is distinct in many ways from that occurring *in vivo*. One key distinguishing feature of the *in vivo* process is an apparent energy dependence for urease activation, as exemplified by studies reported by Lee *et al.* (46). Whereas preformed Apo undergoes slow activation starting 30 min after nickel ion addition to nickel-depleted *K. aerogenes* cells that are treated with an inhibitor of protein synthesis, the same cells fail to generate urease activity when exposed to nickel ions following treatment with dinitrophenol (a protonophore) or dicyclohexylcarbodiimide (an ATPase inhibitor). Moreover, as described below, *in vivo* urease activation requires the participation of several auxiliary proteins encoded by accessory genes.

B. Identification of Accessory Genes Required for Bacterial Urease Activation

Genetic analyses (e.g. deletion and transposon insertional mutagenesis) in a variety of microorganisms have provided compelling evidence that additional genes, other than those encoding the urease subunits, are required for urease activity (e.g., 28, 51-57). DNA sequencing efforts have identified several of these urease-related genes. In *K. aerogenes*, for example, seven genes make up the urease gene cluster (19, 57; illustrated in Figure 2). Three of the genes (*ureA*, *ureB*, and *ureC*) encode the structural

subunits.

structural

Homolog

[e.g., *P.*

(56), *Y.*

M. tuberc.

microbe

(28), *Y.*

H. influenzae

genes

someti

pylori

a gene

Bacil

high-

nicks

appe

low

in t

ure

er

a

subunits, whereas, an additional gene (*ureD*) is located immediately upstream of these structural genes and three genes (*ureE*, *ureF*, and *ureG*) are located downstream. Homologous urease accessory genes have been characterized for several other bacteria [e.g., *P. mirabilis* (20, 58), a thermophilic *Bacillus* species (28), *H. pylori* (55), *E. coli* (56), *Y. enterocolitica* (88), *H. influenzae* (96), *B. pasteurii* (97), *S. salivarius* (99), and *M. tuberculosis* (100)]. The urease gene organization is well conserved in these microbes, except that the *ureD* gene is positioned downstream of *ureG* in *Bacillus* TB-90 (28), *Y. enterocolitica* (88), *S. salivarius* (99), *U. urealyticum* (105), *H. pylori* (55), and in *H. influenzae* (96), (in the latter two cases the gene is designated *ureH*). In addition to the genes encoding the urease subunits and four accessory proteins, other genes are sometimes present. For example, apparent regulatory genes have been identified in *H. pylori* [termed *ureC* and *ureD* (24)], and in *P. mirabilis* [termed *ureR* (59)]. Furthermore, a gene termed *ureH* was identified downstream of the four urease accessory genes of *Bacillus* TB-90 (28). The predicted sequence of UreH is 23 percent identical to HoxN, a high-affinity nickel transport protein in *Alcaligenes eutrophus* (60). Another related nickel-transport peptide, NixA, has been partially characterized from *H. pylori* where it appears to be necessary for expression of active urease when grown in media possessing low concentrations of nickel ion (90). The putative regulatory and nickel transport genes in these microbes are not required for urease activation, whereas the *ureD*, *ureF*, and *ureG* genes are all essential for generating active urease (24, 28, 57, 59).

A major advance in understanding the role of the four urease accessory genes in enzyme activation was reported by Lee *et al.* (57) working with a plasmid-borne *K. aerogenes* urease gene cluster expressed in *E. coli*. These investigators studied the effects

D

30

Figure

aeroge

structu

that an

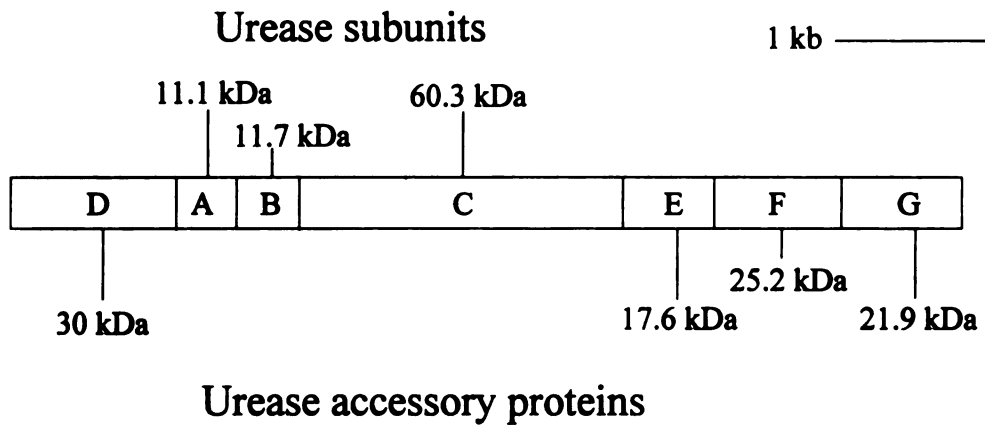


Figure 2. The *K. aerogenes* urease gene cluster (19, 57). The urease gene cluster in *K. aerogenes* is composed of seven genes. Three genes (*ureA*, *ureB*, and *ureC*) encode structural subunits, and four genes (*ureD*, *ureE*, *ureF*, and *ureG*) encode accessory genes that are required for functional assembly of the urease metallocenter.

of deletion

activity

affect ur

absence

subunit

correspo

deletion

compati

simplest

required

the foll

UreD. U

C. Post

exhibit

unrelate

sequen

protein

the *K*.

compar

of deletion mutants in each of the accessory genes on urease gene expression, enzymatic activity and nickel content. They found that deletions in *ureD*, *ureF*, and *ureG* do not affect urease subunit synthesis but result in the total loss of urease activity due to an absence of nickel in the protein. Deletions in the *ureE* gene also have no effect on subunit urease gene expression, but lead to a partial reduction in activity with a corresponding decrease in nickel content. Co-transformation of *E. coli* cells with the deletion derivatives and appropriate subclones of the missing genes located on compatible plasmids demonstrated that the genes act via *trans*-acting factors. The simplest interpretation of these results is that the four genes encode proteins that are required for the functional incorporation of nickel into the active site of urease (57). In the following sections I will detail the properties and speculate on possible roles for the UreD, UreE, UreF, and UreG accessory proteins.

C. Postulated Role of UreD as a Urease-Specific Chaperone Protein

On the basis of *ureD* DNA sequencing results, UreD proteins are predicted to exhibit limited amino acid sequence conservation (Figure 3) and they appear to be unrelated to other sequences available in GenBank or other available data bases. The sequences contain no obvious motifs that would provide insight into the function of this protein in urease activation.

The only effort to characterize the UreD protein is that reported for the product of the *K. aerogenes ureD* gene (48). In this microbe, *ureD* is expressed at very low levels compared to the other urease genes (57) making the purification and characterization of

Figur
perfo
spec
(unp
bac
yeu

Figure 3. Sequence comparison of selected UreD sequences. Sequence analysis was performed using the Pileup program (61). The UreD sequences are from the following species: kaured, *K. aerogenes* (57, M55391); kpured, *Klebsiella pneumonia* (unpublished, L07039); pmured, *P. mirabilis* (20, M31834); ecured, *E. coli* (94, L03307); bacured, *Bacillus* sp. strain TB-90 (28, D14439); hpured, *H. pylori* (55, M84338); and yeured, *Y. enterocolitica* (88, L24101).

kaure
gure
pured
edure
caure
npure
yeure

	1				50
kauredVLPPLK.K	GWQATLDFLR
kpuredVLPPLK.K	GWQRTLDFLR
pmuredMPDFSEK	GWLADIALRY
ecuredMSDFSGS	GWLAEIFLRY
bacuredM	KCTGVLQLSA
hpuredMN	TYAQESKLRL
yeured	MSEPEYRGNS	FTGSRHALGI	NAPELAQYQD	EPAQMRRRGV	GKSGYLKLR
	51				100
kaured	HQA...GGKT	VLASAQHVGP	LTVQRPFYPE	EETCHL...Y	LLHPPGGIVG
kpured	QQA...GGKT	VLASAQHVGP	LTVQRPFYPE	EETCHL...Y	LLHPPGGIVG
pmured	ELK...RGKT	CLTEKRHLGP	LMVQRPFYPE	QGVAHT...Y	LLHPPGGVVG
ecured	ELK...RGVT	RLTDKQHIGP	LMVQRPFYPE	QGIAHT...Y	LLHPPGGVVG
bacured	AKK...RQKT	IISSCYHEGA	LKVSRIPILE	KDLPFL...Y	LIHVGGGYVD
hpured	KTKIGADGRC	VIENFFTPP	FKLMAPFYPK	DDLAEI...M	LLAVSPGLMK
yeured	AKR...EHRS	ILAEMERRVP	SMVQKALYWD	EEMPELPCVT	MISTSGCILQ
	101				150
kaured	GDELTISAHL	APGCHTLITM	PGASKFYRSS	GAQALVRQQL	TLAPQATLEW
kpured	GDELTISAHL	APGCHTLITM	PGASKFYRSS	GAQALVRQQL	TLAPQATLEW
pmured	GDTLSININV	QPYAHALLTT	PGATKFYRSA	GGTASQTQTL	TVAQEGFLEW
ecured	GDKLLINIDV	QPHAHALLTT	PGATKFYRSA	GGVARQVQTL	TVAPNGFLEW
bacured	GDVYLTNLDV	EEEEELAVTT	QSATKVYKTP	KKPVVQQTNI	HLKKGSVLEY
hpured	GDAQDVQLNI	GNCKLRITS	QSFEKIHNT	DGFASRDMHI	VVGENAFLDF
yeured	GDRLATDVIV	EAGACAHVTT	QSATKVHMMN	ANYASQIQNF	TVEEGGYLEF
	151				200
kaured	LPQDAIFFPG	ANARLFTTFH	LCASSRLLAW	DLLCLGRPVI	..GETFSHGT
kpured	LPQDAIFFPG	ANARLFTTFH	LCAFSRLLAW	DLLCLGRPVI	..GETFSHGT
pmured	LPQENIFFPD	AQVCLTTHIH	LASSAKFIGW	EMQCFGRPVL	..NEWFETGK
ecured	LPQENIFFPE	AQVRLETHVR	IASSKFIW	EIQCLGRPVL	..NEQFDNGD
bacured	LLDPLISYKG	ARFIQETTIV	IEEDSGFFYS	DVITPGWA..	EDGSLFPYDW
hpured	APFPLIPFEN	AHFKGNTTIS	LRSSQLLYS	EIIVAGRV..	ARNELFKFNR
yeured	MPDPLIPHRN	SRFITDTTIN	IHPTATAIYS	EVLMSGRKYH	HADERFGFDV
	201				250
kaured	LSNRLEVWV.DNEP	LLVERLHLQ.	..EGELSSIA	ERPW..VGTL
kpured	LSNRLEVWV.DNEP	LLVERLHLQ.	..EGELSSIA	ERPW..VGTL
pmured	VKGRNLFYV.DERL	ILTESMRVE.	..GLQKQAAA	MREFPFGSL
ecured	IRGRLOFYI.DDKL	TLAESIFIE.	..GSQKQSAV	MREFPFGSL
bacured	IRSKLVY..KKDRL	VLFDHRLLEP	D.EDMSGMLQ	MDGYTHIGTF
hpured	LHTKISIL..QDEKP	IYYDNTILDP	KTTDLNMMCM	FDGYTHYLN
yeured	YSSRVAHV	LGKEQPAGKE	LFVEKYVLEP	KSESLEDAIGV	MQSFDAFGNV
	251				300
kaured	LCYPATDALL	DGVRDALA..PLGL	YAGASLTDRL	LTVRFLSDDN
kpured	LCYPATDALL	DGVRDALA..PLGL	YAGASLTDRL	LTVRFLSDDN
pmured	YIYPATDALK	EIIQHHE..	...KVNPLVE	YGLTDV.DGI	LVLRLVLTQT
ecured	YIYPASDELK	AELHESLAVF	FSTEVRL.E	YGLTDV.DGI	LVLRLVLTQT
bacured	LIFHQKADKT	FLDRLYDEME	AFDSDVRFGM	TSLP.ASG..	IILRILARST
hpured	VLVNCPIELS	GVRGLIEESE	GVDGAV....	SEIA.SSH..	LCLKALAKGS
yeured	ILLTPKEHHE	RILARVPAHF	DIKGGIASGA	TRLPNDGCG..	LVFKALGIDS
	301			332	
kaured	LICQVRMDV	WQFLRPHLTG	KSPVLPRIWL	T*	
kpured	LICQVRMDV	WQFLRPHLTG	KSPVLPRIWL	T*	
pmured	EPMMACFAQV	WQIVRQHWLG	YCPEPPIWA	T*	
ecured	EPMMACFAHI	WQATROQWLG	YCPEPPIWA	T*	
bacured	GIIENMISRA	HSFARRELLG	KNGVTWRKY*	..	
hpured	EPLLHLREKI	ARFITQTITP	KV*.....	..	
yeured	AGVKNEIRQF	WKIAREEILG	VTLPEKFLWR	*	



the
da
si
si
ov
w
w
A
p
c
th
U
a
a
l
s
P
a
r
a
c

the encoded protein very difficult. Speculating that the low expression of *ureD* may be due to the presence of a poor ribosome binding site coupled with a GTG initiation codon, site-directed mutagenesis was used to provide a more consensus-like ribosome binding site and generate an ATG initiation codon. These changes led to the successful overexpression of the *ureD* gene in *E. coli*. The UreD protein ($M_r = 29,300$) copurifies with urease apoprotein, and several UreD-urease apoprotein complexes (termed D-Apo) were shown to be formed. The results were rationalized in terms of the trimeric $[(\alpha\beta\gamma)_3]$ Apo species binding 0, 1, 2, or 3 UreD molecules. When nickel is added to the partially purified D-Apo complexes, rapid urease activation is observed with the process being complete in approximately 60 minutes and the level of activity being directly correlated to the number of UreD proteins that are associated with Apo. The complex containing 3 UreD molecules gives rise to the highest activity, but this maximal value represents only around 30 percent of that expected for fully active urease protein. Coincident with the activation of urease by added nickel, UreD dissociates from the enzyme. Based on cross-linking studies of the D-Apo complexes, UreD appears to associate with UreB (the β subunit) of the Apo species (Taha Taha, unpublished observations), and UreD was proposed to act as a chaperone protein or molecular prop that stabilizes a urease apoprotein conformation which is competent for nickel insertion (48). This role is reminiscent of that proposed for MelC1 in copper incorporation into tyrosinase (62, 63), and for NifY in iron-molybdenum cofactor insertion into apodinitrogenase (64, 65). A chaperone-type function for UreD remains a possibility, but the evidence is less

com

des

D. I

ba

Si

Me

In

wi

hi

pr

of

m

to

fr

ri

It

th

e

h

b

v

t

compelling with the recent demonstration of *in vitro* activation of purified Apo as described in the previous section.

D. Potential Role of UreE as a Nickel-Donor

UreE proteins are also predicted to be conserved to only a limited extent in the bacterial species for which *ureE* sequencing information is available (Figure 4). Similarly, these proteins are not clearly related to other proteins in sequence data bases. Most of the UreE sequences, however, do reveal several potential metal ion-binding sites. In *K. aerogenes*, for example, Cys-Tyr-His and His-His-Asp-His sequences are found within the protein and 10 of 15 residues at the carboxyl terminus are predicted to be histidinyI residues (19). The first two regions are not conserved in any other UreE proteins, but eight out of the last nine residues in the *P. mirabilis* protein (20) and 11 out of the last 22 residues in *Y. enterocolitica* UreE (88) are histidines. This polyhistidine motif was not, however, conserved in the *H. pylori* UreE sequence (24) and was limited to only two histidines out of four residues at the *Bacillus* UreE tail (28). UreE sequences from *B. pasteurii* (97), *S. salivarius* (99), and *U. urealyticum* (105) also lack a histidine-rich tail, while *H. influenza* (96) contains this motif (sequence comparisons not shown). It is possible that alternative proteins containing polyhistidine motifs can substitute for the "defective" UreE molecules in these species. For example, several *hypB* sequences, encoding proteins that participate in metallocenter assembly of the nickel-containing hydrogenases, possess polyhistidine regions (e.g., 66-70). Furthermore, the nickel-binding WHP protein from *E. coli* was shown to possess a histidine-rich region (71).

The requirement for the histidine-rich tail region of the *K. aerogenes* UreE protein was tested by generation of a truncated protein lacking 15 residues at the carboxyl terminus (102). The truncated UreE was nearly as effective as the wild-type UreE for

K
P
E
Y

K
P
E
Y

K
P
E
Y

K
P
E
Y

K
P
E
Y

K
P
E
Y

K
P
E
Y

K
P
E
Y

K
P
E
Y

K
P
E
Y

K
P
E
Y

K
P
E
Y

	1				50
kaureeMLYLTQ.RLEIP
pmureeMKKFTQI	IDQQKALELT
bacureeMMVEKV	VGNITTLEKR
hpureeMIERL	IGNLRDLNPL
yeuree	MGRPTMVGMR	GIETDFITVG	NWLLPKIQAR	SLYMILIEHI	LGNVKKDPVW
	51				100
kauree	AAATASVT..	...LPIDVRV	KSRVKVTLND	GRDAGLLLP	GLLL..RGGD
pmuree	STEKPKLT..	.LCLTMDERT	KSRLKVALSD	GQEAGLFLPR	GTVL..KEGD
bacureeVPHIE	RVYMRSDDLV	KRVKRVVDH	GKEIGIRLKE	HQELQ..DGD
hpureeDFSVD	YVDLEWFETR	KKIARFKTRQ	GKDIAVRLKD	APKLGFSQGD
yeuree	QEKLKDATFD	LLVLDQREAQ	KSRCRKLSTQ	GLDLGISLDR	HVVLA..DGD
	101				150
kauree	VLSNEEGTEF	VQV.....I	AADEEVSVVR	CDDPFMLAKA	CYHLGNRHVP
pmuree	ILLSEEG.DV	VTI.....E	AAKEQVSTVY	SDDPLLLARV	CYHLGNRHVP
bacuree	ILYMDDHNMI	VI.....S	VLEDDVLTIK	PTSMQQMGEI	AHQLGNRHLP
hpuree	ILFKEEKEII	AV.....N	ILDSEVIHIQ	AKSVAEVAKI	CYEIGNRHAA
yeuree	VLAWDEKTNV	AVVVQINLRD	VMVIDLSELK	SRSPDELIKT	CFELGHALGN
	151				200
kauree	LQIMPGEELRY	HHDHVLDDML	RQFGLTVTFG	QLPFEPEAGA	YASESHGHHH
pmuree	LQIEAGWCERY	FHDHVLDDMA	RLGATVVVG	LEKYQPEPGA	YGGSSGGHHH
bacuree	AQFEG..N..	EMIVQYDYL	EELLQKLSIP	.FTRENKMK	QAFRPIGHRH
hpuree	LYYGE..SQF	EFKTPFEKPT	LALLEKLGVO	.NRVLSSKLD	SKERLTVSMP
yeuree	QHWKAVTKNN	EVYVPLTVAT	TMMDSVMRTH	GFQHLPRFRV	KGAEILPLLS
	201				250
kauree	AHHDHHAHSH	*.....
pmuree	HHDHHH*
bacuree	E*
hpuree	HSEPNFKVSL	ASDFKVMK*
yeuree	NSEARLLFGG	AEDTDTHVHV	ASPLDEPHGS	GLHVHAIHSH	GTGHTHSHDH
	251	266			
kauree			
pmuree			
bacuree			
hpuree			
yeuree	DHSHSHGDHD	HDHKKH*			

Figure 4. Sequence comparison of selected UreE sequences. The UreE sequences, analyzed using the Pileup program (61) are from the following species: kauree, *K. aerogenes* (19, M36068); pmuree, *P. mirabilis* (20, M31834); bacuree, *Bacillus* sp. strain TB-90 (28, D14439); hpuree, *H. pylori* (55, M84338); and yeuree, *Y. enterocolitica* (88, L24101).

assisting urease activation when tested *in vivo*, and there was no difference in the sensitivity of cells containing the truncated UreE versus the wild-type protein to elevated nickel ion concentrations. These results suggest that that histidine-rich tail is not required in the urease activation pathway nor does it function to reduce nickel toxicity in the cell. It is interesting, however, that a nickel transport system has not been detected in any of the microbes possessing a UreE protein containing a histidine-rich carboxyl terminus (102). Microbes that contain a nickel permease possess a UreE protein lacking this histidine-rich motif. Although the role for this histidine-rich tail is unknown, it has been suggested that it may function in a nickel-storage role (102).

Unlike UreD, the *K. aerogenes* UreE accessory protein is synthesized at high levels in recombinant *E. coli* cells, which has made purification of the protein relatively facile (72). A single-step purification of the *P. mirabilis* protein has also been described (91). The cytoplasmic *K. aerogenes* protein appears to function as a dimer ($M_r = 35,000$) that binds approximately six nickel ions ($K_d \sim 10 \mu\text{M}$) as shown by equilibrium dialysis measurements. The protein is rather specific for binding nickel ions; competition for approximately one half of the metal-binding sites was observed with $10 \mu\text{M}$ zinc ions. Competition with copper and cobalt ions was demonstrated for selected subsites at higher concentrations. X-ray absorption and variable-temperature magnetic circular dichroism spectroscopic studies have indicated that UreE contains Ni(II) in pseudooctahedral geometry liganded with 3-5 histidine imidazole groups and the remainder of the ligands being nitrogen or oxygen donors (72). Hexagonal bipyramidal crystals of UreE apoprotein were obtained; however, these crystals diffract to only 2.9 \AA and were

obs

occl

terr

wa

sho

cor

co

co

d

p

b

Y

observed to fracture upon nickel ion addition, consistent with a conformational change occurring upon nickel addition.

The truncated *K. aerogenes* UreE protein lacking the histidine-rich carboxyl terminus mentioned above has also been purified and partially characterized. The protein was able to bind to a nickel affinity resin as observed with wild-type protein and was also shown to bind two nickel ions per dimer in a cooperative manner (102). Metal competition experiments using equilibrium dialysis methods indicated that copper competes for nickel ion binding sites at low concentrations (<50 μM), while cadmium, copper, and zinc ions compete to a lesser extent.

UreE is likely to function as a nickel donor in metallocenter assembly, possibly donating nickel to a urease-accessory protein complex (see section II.E); however, direct proof that nickel binding to UreE is important to metallocenter assembly in urease has not been obtained.

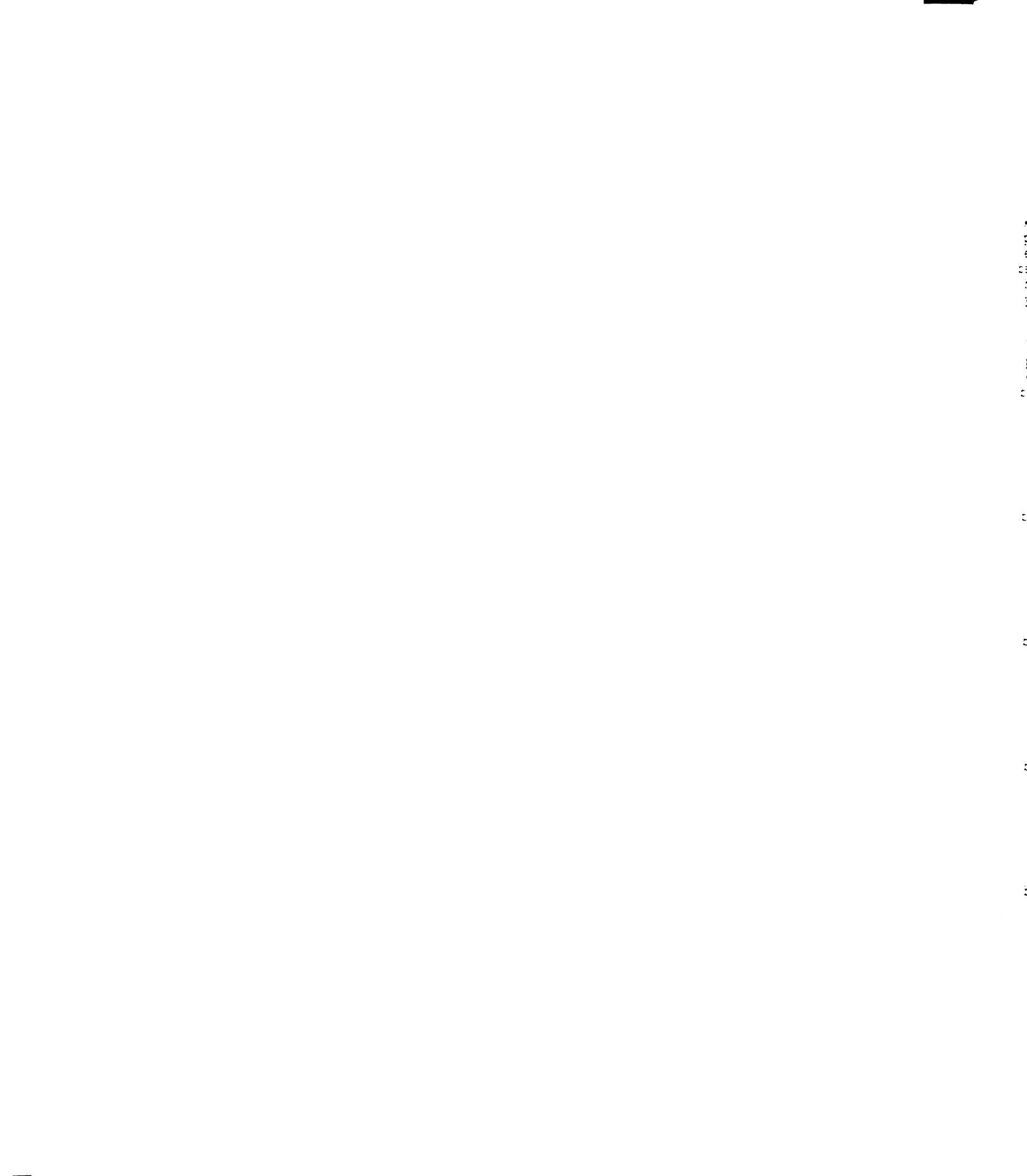
E. Characterization of UreF

UreF is the least well characterized of the urease accessory proteins. A functional UreF is absolutely essential for detecting any urease activity *in vivo*, but limited *in vitro* activation of urease in extracts of *ureF* deletion mutants was reported (48). These results highlight the important differences that are present between *in vivo* and *in vitro* Apo activation. Similar to the findings for UreD and UreE sequences, the UreF sequences are poorly conserved among the various urease gene clusters (Figure 5), and no significant

1

Fig
an
m
C
L

Figure 5. Sequence comparison of selected UreF sequences. The UreF sequences, analyzed according to (61), are from: kauref, *K. aerogenes* (19, M36068); pmuref, *P. mirabilis* (20, P17091); ecuref, *E.coli* (94, L03308); bacuref, *Bacillus* sp. strain TB-90 (28, D14439); hpuref, *H. pylori* (55, M84338); and yeuref, *Y. enterocolitica* (88, L24101).



	1				50
kaurefMSTAE	QRLRLMQLAS	SNLPVGGYSW
pmurefMML	ADLRLYQLVS	PSLPVGAFTY
ecuref
bacurefMN	RLLSLFQLCD	SNFPSGSFSH
hpuref	MDKGKSVKSI	EKSVGMLPKT	PKTDSNAHVD	NEFLILQVND	AVFPIGSYTH
yeurefMNAS	DLIRIMQFGD	SVLPVGAFTF
	51				100
kauref	SQGL..EWAV	EAGWVLDVAA	FERWQRRQMT	EGFFTVDLPL	FARLYRACEQ
pmuref	SQGL..EWAI	EKGWVCSAET	LSDWLSAQMT	GTLATLELPI	LRQLQTSLAK
ecuref
bacuref	SFGL..ETVI	QEKVITDKES	FKNAISVYIR	KQLFFTEGLA	CILAYEAMEK
hpuref	SFGLLARNLH	PAKKVTNKES	ALKYLVKANLS	SQFLYTEMLS	LKLTYESALQ
yeuref	SNGV..ESAI	QTGVVRDVPT	LKGFVLTALK	QA.ASCDGMG	VVAAHRAVVA
	101				150
kauref	GDIAAAQRWT	AYLLACRETR	ELREEERNRG	AAFARLLSDW	QPD.....C
pmuref	GSDSTVKYWC	DFMVASRETK	ELRQEERQPG	IAFPRLLPQL	GIE.....L
ecuref
bacuref	NEPSALVELD	HILFASNVAQ	ETRSGNQRMG	ERMAKLCVDL	YPSPIIEYT
hpuref	QDLKRILGVE	EIITLSTSPM	ELRLANQKLG	NRFIK.TLQA	MNELDIGAFF
yeuref	DDRDIIRAD	WAVNNRKLNE	ESRLMATRMG	KKLAEMSIHV	VEHPLISWWL
	151				200
kauref	PPWRSICQQ	SQLAGMAWLG	VRWRIALPEM	ALSLGYSWIE	SAVMAGVKLV
pmuref	DDTLQQRVKQ	TQLMAFALAA	VHWHIDSEKL	CCAYVWGWE	NTVMMSGVKLV
ecurefKLI
bacuref	NRIKEKKAYG	HSIVFAIVA	YHLKVTKETA	VGAYLFANVS	ALVQNAVIRGI
hpuref	NAYAQQTEDEP	THATSYGVFA	ASLGIELKKA	LRHYLYAQTS	NMVINCVKSV
yeuref	EQIKNGNTAG	TYPVTQAVVM	AAQGIGQREV	VVMHQYGVAM	TILSAAMRLM
	201				250
kauref	PFGQAAQQL	ILRLCDHYAA	EMPRALAAPD	GDIGSATPLA	AIASARHETQ
pmuref	PLGQSAGQKM	LFALAEQIPA	IVELSAHPQ	EDIGSLRQLK	*.....
ecuref	PLGQSAGQNI	LFTLAERIEP	VVAQSAIWPL	DDIGSFTPAQ	IIASSRHETQ
bacuref	PIGQTDGQRI	LVEIQPLLEE	GVRTISQLPK	EDLGAVSPGM	EIAQMRHERL
hpuref	PLSQNDGQKI	LLSLQSPFNQ	LIEKTLELDE	SHLCAASVQN	DIKAMQHESL
yeuref	RVTHFDTQHI	LFELNHDIK	FCDIAEIGDI	DQMSSYVPIV	DVLAAVHVKA
	251				
kauref	YSRLFRS*				
pmuref				
ecuref	YTRLFRS*				
bacuref	NVRLFMS*				
hpuref	YSRLYMS*				
yeuref	HVRLFNS*				

ho

sig

pr

ar

A

ap

co

n

U

c

C

C

a

a

e

f

Y

Y

Y

Y

Y

Y

Y

Y

Y

homology was detected between UreF and other proteins found in various data bases. No significant regions of hydrophobicity are predicted for the protein, consistent with a probable cytoplasmic location. The UreF protein ($M_r = 27,000$) is synthesized at low amounts in the cell (57), making purification and characterization of the protein difficult. Although the UreF protein has only been partially purified (Chapter 6), a peptide with the appropriate size and amino-terminal sequence for UreF has been identified as a component in several protein complexes that are found in cells grown in the absence of nickel (92, 104). In addition to UreF, one series of complexes (92) includes urease, UreD, and UreG (termed DFG-Apo, see later). UreF has also been detected in a series of complexes containing urease and UreD (termed DF-Apo) in *ureG* deletion mutants (104, Chapter 4) and in a UreD-UreF-UreG complex in urease deletion mutants (section II.F, Chapter 5). UreF in the DF-Apo species appears to preclude nickel ions from the urease active site until Lys-217 is carbamylated, but is unable to preclude other metal ions such as Co, Cu, and Zn. The precise roles of some of these complexes remains to be elucidated, but I speculate that UreF functions within several complexes rather than as the free protein.

F. Characterization of UreG

UreG is the most highly conserved accessory protein in the urease gene cluster (Figure 6). Four regions of near identity among the reported sequences can be observed: residues 16-26, 74-82, 112-150, and 157-178 (according to the numbering system shown in Figure 6). The first of these conserved regions corresponds to a sequence known as a

P-1000

where

in U

activa

two

other

hom

find

meta

aer

the

ope

E.

ger

me

hy

w

an

m

P

I

P-loop motif. The P-loop motif is typically found in ATP- and GTP-binding proteins (73) where it is known to function in nucleotide binding. The presence of this sequence motif in UreG may be related to the finding of an energy dependence for *in vivo* urease activation (46). In addition to the extensive regions of similarity within UreG sequences, two intriguing sequence relationships have been reported between UreG proteins and other proteins. In one case, the *P. mirabilis* UreG protein was found to exhibit limited homology to a 60 kDa chaperonin of the thermophilic bacterium ps-3 (58). Based on this finding, the authors suggest that UreG may function as a chaperone in the urease metallocenter assembly pathway. Of greater interest, Wu (74) noted that the *K. aerogenes* UreG sequence (19) is approximately 25 percent identical to the sequence of the *E. coli* *hypB* gene product (75). This gene is part of the *hydrogenase pleiotropic operon* that is required for activation of the three nickel-containing hydrogenases found in *E. coli*. HypB appears to have a role in nickel-ion processing since mutations in the *hypB* gene can be complemented by the addition of high levels of nickel ion to the growth medium (76). Of additional interest, HypB has been purified and found to bind and hydrolyze GTP (77). The homology between the UreG and HypB sequences is consistent with the suggestions that UreG may have nucleotide binding capabilities and that urease and hydrogenase accessory proteins may have descended from a common nickel metallocenter assembly system. Those *hypB* sequences that encode proteins containing a polyhistidine region (see section II. D) may thus represent fusions of UreE-like and UreG-like proteins.

Protein studies involving UreG have not been reported; however, selected properties of this protein have been determined. For example, the *K. aerogenes* protein has been purified and partially characterized by making use of plasmids that express relatively high levels of *ureG* in recombinant *E. coli* cells. The monomeric protein was found to be located in the cytoplasm by immunogold electron microscopic methods (Mann Hyung Lee, unpublished), consistent with the lack of significant hydrophobic

3

4

5

6

7

8

9

10

11

12

13

```

1                                     50
kaureg  ....MNSYK HPLRVGVGGP VSGKTALLE ALCKAM.RDT WQLAVVTNDI
pmureg  ....MQEYN QPLRIGVGGP VSGKTALLE VLCKAM.RDS YQIAVVTNDI
ecureg  ....MQEYN QPLRIGVGGP VSGKTALLE VLCKAM.RDT YQIAVVTNDI
bacureg  ....V EPIRIGIGGP VGAGKTM LVE KLTRAM.HKE LSI VVTNDI
hpureg  .... .MVKIGVCGP VSGKTALIE ALTRHM.SKD YDMAVITNDI
yeureg  VNSHSTDKRK KITRIGIGGP VSGKTAIE VITPILIKRG IKPLIITNDI

51                                     100
kaureg  YTKEDQRILT EA..GALAPE RIVGVETGGC PHTAIRE D AS MNLA AVEALS
pmureg  YTQEDAKILT RA..QALDAD RIIGVETGGC PHTAIRE D AS MNLA AVEELA
ecureg  YTQEDAKILT RA..EALDAD RIIGVETGGC PHTAIRE D AS MNLA AVEELA
bacureg  YTKEDAQFLL KH..GVL PAD RVIGVETGGC PHTAIRE D AS MNFP AIDELK
hpureg  YTKEDA E FMC KN..SVM PRE RIIGVETGGC PHTAIRE D AS MNLE AVEEMH
yeureg  VTTEDAKQVK RTLKGILDEE KILGVETGAC PHTAVRE D PS MNIA AVEEME

101                                    150
kaureg  EKFGNLDLIF VESGGDNLSA TFSPELADLT IYVIDVAEGE KIPRKG GPGI
pmureg  MRHKNL D I V F VESGGDNLSA TFSPELADLL FMLIDVAEGE KIPRKG GPGI
ecureg  IRHKNL D I V F VESGGDNLSA TFSPELADLT IYVIDVAEGE KIPRKG GPGI
bacureg  ERHPDLELIF IESGGDNLAA TFSPELVDFS IYIIDVAQGE KIPRKG GQGM
hpureg  GRFPNLELLL IESGGSNLSA TFPNELADFT IFVIDVAEGD KIPRKG GPGI
yeureg  ERFPDSNLIM IESGGDNLTL TFSPALADFY IYVIDVAEGE KIPRKN G PGL

151                                    200
kaureg  TKSDFLVINK TDLAPYVGAS LEVMASDTQR MRGDRPWTF T NLKQGDGLST
pmureg  THPDMMVINK IDLAPYVGAS LEVMEADTAK MRPVKPYVFT NLKEKV GLET
ecureg  THSDLLVINK IDLAPYVGAS LEVMEADTAR MRPVKPYVFT NLKKKV GLET
bacureg  IKSVLFIINK IDLAPYVGAS LEVMERDTLA ARGDKPYIFT NLKDEIGLAE
hpureg  TRSDLLVINK IDLAPYVGAD LKVMERDSKK IAAKSPFLFP NIRAKEGLDD
yeureg  VQADILVINK IDLAPYVGAS LDVMESDTKV VRGERPYILT NCKTGQ GIEE

201                                    222
kaureg  IIAFLEDKGM LGK*..... ..
pmureg  IIDFIIDKGM LRR*..... ..
ecureg  IIEFIIDKGM LGR*..... ..
bacureg  VLEWIKTNAL LYGLES*... ..
hpureg  VIAWIKRNAL LED*..... ..
yeureg  LVDMIMRDFL FTHVQPQGEH A*

```

Figure 6. Sequence comparison of selected *UreG* sequences. The *UreG* sequences, compared according to (61), are from the following species: *kaureg*, *K. aerogenes* (19, M36068); *pmureg*, *P. mirabilis* (58, Z21940); *ecureg*, *E.coli* (56, 94; L03308); *bacureg*, *Bacillus* sp. strain TB-90 (28, D14439); *hpureg*, *H. pylori* (55, M84338); and *yeureg*, *Y. enterocolitica* (88, L24101).

regio

sequ

or C

dire

exa

mu

ad

vis

ur

T

c

n

o

regions in the protein according to sequence analysis. Despite the presence of a P-loop sequence motif in this protein, purified UreG is unable to bind significant levels of ATP or GTP as shown by equilibrium dialysis measurements (Chapter 6). Nevertheless, site-directed mutants that are defective in the P-loop sequence fail to activate urease when examined *in vivo*. Apo in these site-directed P-loop mutants, similar to the *ureG* deletion mutants mentioned earlier, is able to be partially activated when CO₂ and nickel ions are added to cell extracts. This result again demonstrates the great distinction between *in vivo* and *in vitro* activation of urease (i.e., a functional UreG is crucial for detection of urease activity *in vivo* whereas partial *in vitro* activation of Apo can occur without UreG). Thus, although there is no energy dependence for *in vitro* activation of the purified Apo or D-Apo (38), nucleotide hydrolysis may be required *in vivo* and the nucleotide may bind to UreG. Rather than binding to the free protein, however, nucleotides may bind to UreG only when it is present in the DFG-Apo species (see section II.E) or a UreD-UreF-UreG complex described below.

In addition to UreG being detected in a series of DFG-Apo complexes, UreG is also present in an additional complex in urease deletion mutants. A complex containing UreD, UreF, and UreG (termed DFG) was partially purified and characterized (Chapter 6). This complex binds to an ATP-linked agarose column, while purified UreG does not. *E. coli* cells containing a mutant form of UreG, in which the conserved Thr residue in the P-loop motif was changed to an Ala (T21A), still formed the DFG complex as observed with wild-type UreG. This indicates that the P-loop is not essential for UreD, UreF, and UreG complex formation. However, the complex containing T21A did not bind to an



l
r
l
A
m
p
ex
ion

ATP-linked agarose resin which supports the hypothesis that UreG binds nucleotides and that the Thr in the P-loop motif is essential for nucleotide binding.

G. Current Model for Bacterial Urease Metallocenter Assembly

A working model describing assembly of the urease metallocenter is illustrated in Figure 7. In nickel-depleted *E. coli* cells containing the *K. aerogenes* urease gene cluster, most urease is found as the free Apo species; however, approximately 10 percent is present as the D-Apo and a smaller proportion is present as DF-Apo or DFG-Apo (48, 92, 104, Chapter 4). Although the Apo, D-Apo, and DF-Apo can be activated *in vitro* by addition of nickel ions and carbon dioxide (38, 48, 104, Chapter 4), these processes do not appear to take place *in vivo*. Rather, I propose that the DFG-Apo is the species that is activated *in vivo*. Formation of this complex may occur by a sequential binding of UreD, UreF, and UreG to the Apo species or by formation of the DFG species with subsequent binding to the Apo. The lack of *in vivo* activation of Apo, D-Apo, and DF-Apo species may be related to nickel ion sequestration and limiting levels of carbon dioxide in the cell [atmospheric CO₂ concentrations are around 0.03 percent, whereas half-maximal rates of Apo activation required sevenfold higher CO₂ levels (38)]. Alternatively, these species may bind other metal ions in the cell and the inactive metal-substituted proteins must be processed via DFG-Apo to allow productive binding of nickel ion, as suggested by experimental results in which Apo, D-Apo and DF-Apo appear to bind a range of metal ions (101, 104, Chapter 4). Thus, I speculate that the UreD, UreF, and UreG proteins

2

6

0

e

(

th

P

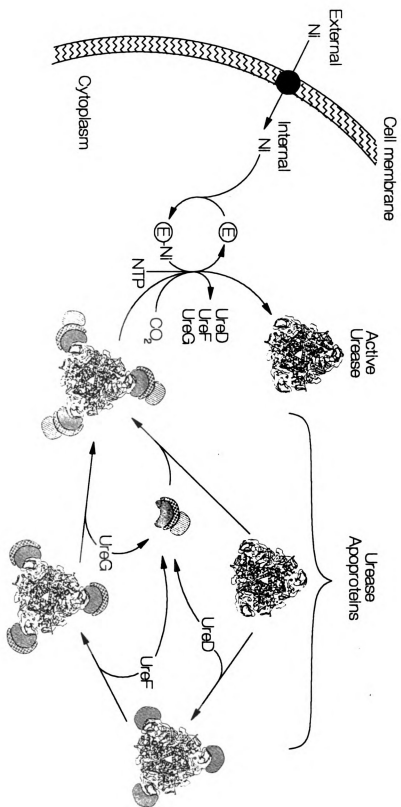
O

co

may be involved in delivery of nickel ion and/or carbon dioxide to the Apo species or in dismantling of non-productive metalcenters in the protein.

As one possibility, the accessory proteins may be required for proper docking or metal ion transfer between the UreE holoprotein and Apo complex. Although the role of UreE has not been established, its nickel-binding ability makes it an attractive candidate as the cellular nickel donor for urease activation (72, 102). As a second possibility, the UreD, UreF, and UreG proteins may function in generating carbon dioxide within or delivering CO₂ to the Apo species. For example, these proteins, as an associated unit, could have some type of decarboxylase activity, possess carbonic anhydrase activity, activate CO₂ possibly via a phosphate intermediate (e.g. HO-CO-OPO₃), or ferry CO₂ bound to biotin or other carboxyl group carrier. Whether required for UreE interaction or "CO₂" delivery, a role for nucleotide binding and hydrolysis can be postulated, consistent with the conserved UreG P-loop motif and the *in vivo* activation results. A third alternative function for the accessory proteins may involve an energy-dependent expulsion of improperly bound nickel or metal ion to the protein. This role is reminiscent of that for Rubisco activase (78), and is supported by kinetic and metal quantitation evidence that nickel can bind to Apo in the absence of CO₂ to form an inactive species (38, 101). Studies of the DF-Apo complex indicate that the presence of UreF eliminates the inhibitory binding of nickel ion to non-carbamylated protein but does not, however, prevent other divalent metal ions from binding and inactivating Apo (104, Chapter 4). Once activated in the cell, the DFG-Apo, thought to be the physiologically relevant complex, is thought to dissociate and urease holoprotein is only found as the free enzyme.

Figure 7. Model for *in vivo* urease metallocenter assembly. The incorporation of nickel into urease apoprotein *in vivo* is proposed to occur by a complex process involving four accessory proteins: UreD, UreE, UreF, and UreG. Nickel enters the cell using a nickel transport system. UreE (E) functions as the putative nickel donor and delivers nickel ions to the DFG-Apo complex. The model proposes that Apo either sequentially binds UreD, UreF, and UreG, or it binds the DFG complex to form the DFG-Apo complex. Insertion of nickel and CO_2 into the active site may require nucleotide hydrolysis in which UreG may play a role. Formation of holourease results in dissociation of the accessory proteins from the enzyme.



H. Accessory Genes Required For Urease Activation In Eukaryotes

Metallocenter accessory genes also appear to be required for urease activation in eukaryotes. The best-characterized plant urease metallocenter assembly genes identified to date are in soybean, *Glycine max* (L.) Merr. Soybean has three urease isozymes (14, 79-82): ubiquitous (leaf), embryo-specific (seed), and a background urease from an associated bacterium *Methylobacterium mesophilicum*. Pleiotropic mutations in two plant loci, *Eu2* and *Eu3*, result in the loss of all urease activity despite normal levels of urease gene expression (80). The authors suggested that the mutants are defective in a urease maturation process, such as nickel insertion into the Apo. $^{63}\text{NiCl}_2$ studies indicate that *Eu2* and *Eu3* mutants take up normal amounts of NiCl_2 , and grafting experiments indicate that transport of nickel through mutant roots and stems is unaffected. These experiments suggest that mutations in *Eu2* and *Eu3* have no effect on nickel ion uptake or transport, but somehow affect nickel incorporation into the metallocenter (80). It is surprising that mutations in soybeans at these two loci eliminate urease activity in the phylloplane-associated bacterium (79). Bacteria isolated from soybeans having these mutations lack both urease and hydrogenase activity, but these enzymatic activities can be restored by nickel addition to the isolated cultures.

An obvious interpretation of these results is that the plant mutants cause the bacteria to be deficient in nickel and unable to produce active urease and hydrogenase. It is possible that the soybean mutants somehow sequester nickel and prevent activation of all three urease isozymes. The two soybean loci have not been sequenced and their relationships to the bacterial accessory genes have not been established at this time. Partial sequences of unidentified genes from *Arabidopsis thaliana* (GenBank accession number Z18230) and barley, *Hordeum vulgare* L. (Brian Forde, personal

communication), which could be related to urease activation in plants, have sequence similarities to the UreG protein of *K. aerogenes*. Fungal species also have accessory genes that are required for functional urease activity. Four loci have been identified as being necessary for functional urease in *Aspergillus nidulans* (83), *Neurospora crassa* (84), and *Schizosaccharomyces pombe* (85). In the case of *A. nidulans*, one of the four loci, *ureA*, encodes a urea-specific transport protein. The structural subunit of urease is encoded by the *ureB* gene. Another locus, *ureC*, is required, but its function is unknown. Finally, the *ureD* gene is thought to be required for the synthesis or incorporation of the nickel cofactor based on the ability to correct a mutation in *ureD* by growing the fungus in the presence of 0.1 mM nickel sulfate (86). The fungal *ureD* gene has also been found to have sequence similarity to the UreG protein of *K. aerogenes* (Gareth Wyn Griffith, personal communication). Further research will most likely reveal other relationships between prokaryotic and eukaryotic accessory proteins as is seen with the urease enzyme itself.

III. SUMMARY

Metallocenter assembly in urease is clearly a complex and highly specific process. More extensive research has been done in prokaryotes than in eukaryotes since it is easier to grow and manipulate bacteria than most eukaryotes. In addition, the fact that urease is a virulence factor in some bacteria makes understanding bacterial urease activation an important facet of medical research. Although the players in urease metallocenter assembly have been identified, their precise roles and order of appearance in this drama have not yet been clearly identified. UreD may function as a chaperone or molecular prop that maintains a state of urease that has enhanced ability to be activated, but how the D-Apo and related complexes are formed, how their structures compare to the native urease

structure, how UreD plays this role, and how UreD is recycled are not understood. UreE is a nickel-binding protein, at least in *K. aerogenes*, but it remains unclear whether its role in metallocenter assembly is that of a nickel donor. The roles of UreF and UreG in urease activation are very poorly understood, although the presence of UreF in the DF-Apo complex prevents non-productive nickel ion-binding by the noncarbamylated urease species. We can only speculate as to the possible function for DFG-Apo species although it is thought to be the key complex *in vivo*. The putative P-loop motif in UreG may be consistent with a role for nucleotides during *in vivo* activation which is supported by the binding capabilities of the DFG complex to a nucleotide-linked resin. Hopefully some of what we learn about metallocenter assembly in urease may be applicable to activation processes in other metalloproteins.

IV. THESIS OUTLINE

The following chapters describe my studies on *Klebsiella aerogenes* urease apoprotein (Apo) and holoprotein, accessory proteins, and several Apo-accessory protein complexes. In Chapter 2, I describe crystalline urease activity and related salt inhibition studies. These studies showing that urease crystals are essentially inactive were combined with X-ray crystallographic data analysis by Evelyn Jabri and preliminary crystal activity studies by Louis G. Hom and published in *Protein Science* 4, 2234-2235 (1995) (103). In Chapter 3, I describe the first demonstration of *in vitro* activation of urease apoprotein. The *in vitro* activation process in cell extracts is slow and the highest

specific activity studies (30-40 U/mg protein) only account for activation of approximately 10% of the Apo that is present. This work was combined with UreD-urease (D-Apo) studies by Il-Seon Park and published in *Proceedings of the National Academy of Sciences USA* **91**, 3233-3237 (1994) (48). Chapter 4 describes the identification and characterization of a series of complexes containing UreD, UreF, and Apo (DF-Apo) formed in cells that overexpress *ureD* and *ureF*. These complexes exhibit activation properties that are distinct from Apo and D-Apo complexes. Unlike Apo and D-Apo, the DF-Apo complexes are resistant to inactivation by NiCl₂, exhibit a decreased bicarbonate concentration dependence, and UreD is masked, presumably by UreF, in these complexes. I propose that binding of UreF modulates the D-Apo activation properties by excluding nickel ions from the binding site until after formation of the carbamylated lysine metallocenter ligand. These studies were published in the *Journal of Bacteriology* **178**, 5417-5421 (1996) (104). In Chapter 5, I describe the purification of UreG and the identification of a UreD-UreF-UreG (DFG) complex. Purified UreG does not bind or hydrolyze nucleotides, contain biotin, or exhibit carbonic anhydrase activity. Site-directed mutagenesis of two residues in the UreG P-loop motif, known to be essential for nucleotide binding in several proteins (73), are identified as essential for *in vivo* activation of Apo. Unlike purified UreG, the DFG complex binds to an ATP-linked agarose resin. In cells containing the UreG P-loop variants, the DFG complex is still formed but doesn't bind to an ATP-linked resin. This suggests that the P-loop motif is not essential for DFG complex formation, but is essential for nucleotide binding. In Chapter 6, I describe the overexpression of *ureF* and the high insolubility of UreF in the

absence of the other urease gene products unless fused to thioredoxin. In the presence of the other urease genes, a DFG-Apo complex (termed DFG-Apo*) distinct from those described earlier (92) is produced and exhibits properties similar to Apo and D-Apo. Chapter 7 describes the identification of a series of Apo forms purified from a *ureD* deletion mutant that collapse upon incubation with 10 mM dithiothreitol. These species are not formed in a urease C319A *ureD* deletion mutant but instead form species that migrate in a manner that is coincident to forms identified when DF-Apo complexes are activated *in vitro*. This suggests that C319, the only Cys located in the active site, may play a role in formation of these species. I also include studies where Apo was incubated with DFG complex to test the urease metallocenter model proposal that DFG can bind to Apo to form DFG-Apo. A band similar in size to DFG-Apo was identified by immunoblot analysis supporting the hypothesis that the DFG complex might form first with subsequent addition of Apo to form DFG-Apo. In Chapter 8, I summarize the current model for urease metallocenter assembly and discuss future prospects. As an appendix to the thesis, I include a manuscript that I co-authored for which I supplied urease and seleno-methionine-containing urease to Evelyn Jabri and Dr. Andy Karplus at Cornell University in Ithaca, New York. This work describes the crystal structure of urease from *Klebsiella aerogenes* and was published in *Science* 268, 998-1004 (1995).

REFERENCES

1. **Zerner, B.** (1991). Recent advances in the chemistry of an old enzyme, urease. *Bioorganic Chemistry* **19**, 116-131.
2. **Hausinger, R. P.** (1993). Urease. In *Biochemistry of Nickel*, pp. 23-57. New York: Plenum Publishing Corp.
3. **Mobley, H. L. T. & Hausinger, R. P.** (1989). Microbial ureases: significance, regulation, and molecular characterization. *Microbiological Reviews* **53**, 85-108.
4. **Sumner, J. B.** (1926). The isolation and crystallization of the enzyme urease. *Journal of Biological Chemistry* **69**, 435-441.
5. **Dixon, N. E., Gazzola, C., Blakeley, R. L. & Zerner, B.** (1975). Jack bean urease (EC 3.5.1.5). A metalloenzyme. A simple biological role for nickel? *Journal of the American Chemical Society* **97**, 4131-4133.
6. **Bremner, J. M. & Mulvaney, R. L.** (1978). Urease activity in soils. In *Soil Enzymes*, pp. 149-196. Edited by R. G. Burns. New York: Academic Press.
7. **Huntington, G. B.** (1986). Uptake and transport of nonprotein nitrogen by the ruminant gut. *Federation Proceedings* **45**, 2272-2276.
8. **Griffith, D. P., Musher, D. M. & Itin, C.** (1976). Urease. The primary cause of infection-induced urinary stones. *Investigative Urology* **13**, 346-350.
9. **Braude, A. I. & Siemienski, J.** (1960). Role of bacterial urease in experimental pyelonephritis. *Journal of Bacteriology* **80**, 171-179.
10. **Mobley, H. L. T. & Warren, J. W.** (1987). Urease-positive bacteriuria and obstruction of long-term catheters. *Journal of Clinical Microbiology* **25**, 2216-2217.
11. **Segal, E. D., Shon, J. & Tompkins, L. S.** (1992). Characterization of *Helicobacter pylori* urease mutants. *Infection and Immunity* **60**, 1883-1889.
12. **Perez-Perez, G. I., Olivares, A. Z., Cover, T. L. & Blaser, M. J.** (1992). Characteristics of *Helicobacter pylori* variants selected for urease deficiency. *Infection and Immunity* **60**, 3658-3663.
13. **Eskew, D. L., Welch, R. M. & Cary, E. E.** (1983). Nickel: an essential micronutrient for legumes and possibly all higher plants. *Science* **222**, 621-623.

14. **Polacco, J. C. & Holland, M. A.** (1993). Roles of urease in plant cells. *International Review of Cytology* **145**, 65-103.
15. **Takishima, K., Suga, T. & Mamiya, G.** (1988). The structure of jack bean urease. The complete amino acid sequence, limited proteolysis and reactive cysteine residues. *European Journal of Biochemistry* **175**, 151-165.
16. **Riddles, P. W., Whan, V., Blakeley, R. L. & Zerner, B.** (1991). Cloning and sequencing of a jack bean urease-encoding cDNA. *Gene* **108**, 265-267.
17. **Todd, M. J. & Hausinger, R. P.** (1989). Competitive inhibitors of *Klebsiella aerogenes* urease. Mechanisms of interaction with the nickel active site. *Journal of Biological Chemistry* **264**, 15835-15842.
18. **Todd, M. J. & Hausinger, R. P.** (1987). Purification and characterization of the nickel-containing multicomponent urease from *Klebsiella aerogenes*. *Journal of Biological Chemistry* **262**, 5963-5967.
19. **Mulrooney, S. B. & Hausinger, R. P.** (1990). Sequence of the *Klebsiella aerogenes* urease genes and evidence for accessory proteins facilitating nickel incorporation. *Journal of Bacteriology* **172**, 5837-5843 .
20. **Jones, B. D. & Mobley, H. L. T.** (1989). *Proteus mirabilis* urease: nucleotide sequence determination and comparison with jack bean urease. *Journal of Bacteriology* **171**, 6414-6422.
21. **Mörsdorf, G. & Kaltwasser, H.** (1990). Cloning of the genes encoding urease from *Proteus vulgaris* and sequencing of the structural genes. *FEMS Microbiology Letters* **66**, 67-74.
22. **Blanchard, A.** (1990). *Ureaplasma urealyticum* urease genes; use of a UGA tryptophan codon. *Molecular Microbiology* **4**, 669-676.
23. **Clayton, C. L., Pallen, M. J., Kleanthous, H., Wren, B. W. & Tabaqchali, S.** (1990). Nucleotide sequence of two genes from *Helicobacter pylori* encoding for urease subunits. *Nucleic Acids Research* **18**, 362.
24. **Labigne, A., Cussac, V. & Courcoux, P.** (1991). Shuttle cloning and nucleotide sequences of *Helicobacter pylori* genes responsible for urease activity. *Journal of Bacteriology* **173**, 1920-1931.
25. **Ferrero, R. L. & Labigne, A.** (1993). Cloning, expression and sequencing of *Helicobacter felis* urease genes. *Molecular Microbiology* **9**, 323-333.

26. **Solnick, J. V., O'Rourke, J., Lee, A. & Tompkins, L. S. (1994).** Molecular analysis of urease genes from a newly identified uncultured species of *Helicobacter*. *Infection and Immunity* **62**, 1631-1638.
27. **Skurnick, M., Batsford, S., Mertz, A., Schiltz, E. & Toivanen, P. (1993).** The putative arthritogenic cationic 19-kilodalton antigen of *Yersinia enterocolitica* is a urease α -subunit. *Infection and Immunity* **61**, 2498-2504.
28. **Maeda, M., Hidaka, M., Nakamura, A., Masaki, H. & Uozumi, T. (1994).** Cloning, sequencing, and expression of thermophilic *Bacillus* strain TB-90 urease gene complex in *Escherichia coli*. *Journal of Bacteriology* **176**, 432-442.
29. **Miksch, G., Arnold, W., Lentzsch, P., Priefer, U. B. & Pühler, A. (1994).** A 4.6 kb DNA region of *Rhizobium meliloti* involved in determining urease and hydrogenase activities carries the structural genes for urease (*ureA*, *ureB*, *ureC*) interrupted by other open reading frames. *Molecular and General Genetics* **242**, 539-550.
30. **Jose, J., Schäfer, U. K. & Kaltwasser, H. (1994).** Threonine is present instead of cysteine at the active site of urease from *Staphylococcus xylosus*. *Archives of Microbiology* **161**, 384-392.
31. **Christians, S. & Kaltwasser, H. (1986).** Nickel-content of urease from *Bacillus pasteurii*. *Archives of Microbiology* **145**, 51-55.
32. **Nakano, H., Takenishi, S. & Watanabe, Y. (1984).** Purification and properties of urease from *Brevibacterium ammoniagenes*. *Agricultural and Biological Chemistry* **48**, 1495-1502.
33. **Schäfer, U. K. & Kaltwasser, H. (1994).** Urease from *Staphylococcus saprophyticus*: purification, characterization, and comparison to *Staphylococcus xylosus* urease. *Archives of Microbiology* **161**, 393-399.
34. **Wang, S., Lee, M. H., Hausinger, R. P., Clark, P. A., Wilcox, D. E. & Scott, R. A. (1994).** Structure of the dinuclear active site of urease. X-ray absorption spectroscopy of native and 2-mercaptoethanol-inhibited bacterial and plant enzymes. *Inorganic Chemistry* **33**, 1589-1593.
35. **Day, E. P., Peterson, J., Sendova, M. S., Todd, M. J. & Hausinger, R. P. (1993).** Saturation magnetization of ureases from *Klebsiella aerogenes* and jack bean: no evidence for coupling between the two active site nickel ions in the native enzyme. *Inorganic Chemistry* **32**, 634-638.
36. **Finnegan, M. G., Kowal, A., Werth, M. T., Clark, P. A., Wilcox, D. E. & Johnson, M. K. (1991).** Variable-temperature magnetic circular dichroism

- spectroscopy as a probe of the electronic and magnetic properties of nickel in jack bean urease. *Journal of the American Chemical Society* **113**, 4030-4032.
37. **Park, I.-S. & Hausinger, R. P. (1993).** Site-directed mutagenesis of *Klebsiella aerogenes* urease: identification of histidine residues that appear to function in nickel ligation, substrate binding, and catalysis. *Protein Science* **2**, 1034-1041.
 38. **Park, I.-S. & Hausinger, R. P. (1995).** Requirement of carbon dioxide for in vitro assembly of the urease nickel metallocenter. *Science* **267**, 1156-1158.
 39. **Park, I.-S. & Hausinger, R. P. (1993).** Diethylpyrocarbonate reactivity of *Klebsiella aerogenes* urease: effect of pH and active site ligands on the rate of inactivation. *Journal of Protein Chemistry* **12**, 51-56.
 40. **Todd, M. J. & Hausinger, R. P. (1991).** Identification of the essential cysteine residue in *Klebsiella aerogenes* urease. *Journal of Biological Chemistry* **266**, 24327-24331.
 41. **Todd, M. J. & Hausinger, R. P. (1991).** Reactivity of the essential thiol of *Klebsiella aerogenes* urease. Effect of pH and ligands on thiol modification. *Journal of Biological Chemistry* **266**, 10260-10267.
 42. **Martin, P. R. & Hausinger, R. P. (1992).** Site-directed mutagenesis of the active site cysteine in *Klebsiella aerogenes* urease. *Journal of Biological Chemistry* **267**, 20024-20027.
 43. **Dixon, N. E., Riddles, P. W., Gazzola, C., Blakeley, R. L. & Zerner, B. (1980).** Jack bean urease (EC 3.5.1.5). V. On the mechanism of action of urease on urea, formamide, *N*-methylurea, and related compounds. *Canadian Journal of Biochemistry* **58**, 1335-1344.
 44. **Dixon, N. E., Gazzola, C., Asher, C. J., Lee, D. S. W., Blakeley, R. L. & Zerner, B. (1980).** Jack bean urease (EC 3.5.1.5). II. The relationship between nickel, enzymatic activity, and the "abnormal" ultraviolet spectrum. The nickel content of jack bean seeds. *Canadian Journal of Biochemistry* **58**, 474-480.
 45. **Schneider, J. & Kaltwasser, H. (1984).** Urease from *Arthrobacter oxydans*, a nickel-containing enzyme. *Archives of Microbiology* **139**, 355-360.
 46. **Lee, M. H., Mulrooney, S. B. & Hausinger, R. P. (1990).** Purification, characterization, and in vivo reconstitution of *Klebsiella aerogenes* urease apoenzyme. *Journal of Bacteriology* **172**, 4427-4431.

47. **Winkler, R. G., Polacco, J. C., Eskew, D. L. & Welch, R. M. (1983).** Nickel is not required for apourease synthesis in soybean seeds. *Plant Physiology* **72**, 262-263.
48. **Park, I.-S., Carr, M. B. & Hausinger, R. P. (1994).** *In vitro* activation of urease apoprotein and role of UreD as a chaperone required for nickel metallocenter assembly. *Proceedings of the National Academy of Sciences* **91**, 3233-3237.
49. **Jabri, E., Lee, M. H., Hausinger, R. P. & Karplus, P. A. (1992).** Preliminary crystallographic studies of urease from jack bean and from *Klebsiella aerogenes*. *Journal of Molecular Biology* **227**, 934-937.
50. **Lorimer, G. H. & Mizioro, H. M. (1980).** Carbamate formation on the epsilon-amino group of a lysyl residue as the basis for activation of ribulosebiphosphate carboxylase by CO₂ and Mg²⁺. *Biochemistry* **19**, 5321-5328.
51. **Mulrooney, S. B., Lynch, M. J., Mobley, H. L. T. & Hausinger, R. P. (1988).** Purification, characterization, and genetic organization of recombinant *Providencia stuartii* urease expressed in *Escherichia coli*. *Journal of Bacteriology* **170**, 2202-2207.
52. **Collins, C. M. & Falkow, S. (1988).** Genetic analysis of an *Escherichia coli* urease locus: evidence of DNA rearrangement. *Journal of Bacteriology* **170**, 1041-1045.
53. **Gerlach, G.-F., Clegg, S. & Nichols, W. A. (1988).** Characterization of the genes encoding urease activity of *Klebsiella pneumoniae*. *FEMS Microbiology Letters* **50**, 131-135.
54. **Walz, S. E., Wray, S. K., Hull, S. I. & Hull, R. E. (1988).** Multiple proteins encoded within the urease gene complex of *Proteus mirabilis*. *Journal of Bacteriology* **170**, 1027-1033.
55. **Cussac, V., Ferrero, R. L. & Labigne, A. (1992).** Expression of *Helicobacter pylori* urease genes in *Escherichia coli* grown under nitrogen-limiting conditions. *Journal of Bacteriology* **174**, 2466-2473.
56. **Collins, C. M. & Gutman, D. M. (1992).** Insertional inactivation of an *Escherichia coli* urease gene by IS3411. *Journal of Bacteriology* **174**, 883-888.
57. **Lee, M. H., Mulrooney, S. B., Renner, M. J., Markowicz, Y. & Hausinger, R. P. (1992).** Sequence of *ureD* and demonstration that four accessory genes (*ureD*,

- ureE*, *ureF*, and *ureG*) are involved in nickel metallocenter biosynthesis. *Journal of Bacteriology* **174**, 4324-4330.
58. **Sriwanthana, B., Island, M. D. & Mobley, H. L. T.** (1993). Sequence of the *Proteus mirabilis* urease accessory gene *ureG*. *Gene* **129**, 103-106.
59. **Nicholson, E. B., Concaugh, E. A., Foxall, P. A., Island, M. D. & Mobley, H. L. T.** (1993). *Proteus mirabilis* urease: transcriptional regulation by UreR. *Journal of Bacteriology* **175**, 465-473.
60. **Eitinger, T. & Friedrich, B.** (1991). Cloning, nucleotide sequence, and heterologous expression of the high-affinity nickel transport gene from *Alcaligenes eutrophus*. *Journal of Biological Chemistry* **266**, 3222-3227.
61. **Devereux, J. P., Haerberli, P. & Smithies, O.** (1984). A comprehensive set of sequence analysis programs for the VAX. *Nucleic Acids Research* **12**, 387-395.
62. **Chen, L.-Y., Chen, M. Y., Leu, W. M., Tsai, T. Y. & Lee, Y. H.** (1993). Mutational study of *Streptomyces* tyrosinase trans-activator MelC1. MelC1 is likely a chaperone for apotyrosinase. *Journal of Biological Chemistry* **268**, 18710-18716.
63. **Chen, L.-Y., Leu, W. M., Wang, K. T. & Lee, Y. H.** (1992). Copper transfer and activation of the *Streptomyces* apotyrosinase are mediated through a complex formation between apotyrosinase and its trans-activator MelC1. *Journal of Biological Chemistry* **267**, 20100-20107.
64. **White, T. C., Harris, G. S. & Orme-Johnson, W. H.** (1992). Electrophoretic studies on the assembly of the nitrogenase molybdenum-iron protein from the *Klebsiella pneumoniae* *nifD* and *nifK* gene products. *Journal of Biological Chemistry* **267**, 24007-24016.
65. **Homer, M. J., Paustian, T. D., Shah, V. K. & Roberts, G. P.** (1993). The *nifY* product of *Klebsiella pneumoniae* is associated with apodinitrogenase and dissociates upon activation with the iron-molybdenum cofactor. *Journal of Bacteriology* **175**, 4907-4910.
66. **Chen, J. C. & Mortenson, L. E.** (1992). Identification of six open reading frames from a region of the *Azotobacter vinelandii* genome likely involved in dihydrogen metabolism. *Biochimica et Biophysica Acta* **1131**, 199-202.
67. **Tibelius, K. H., Du, L., Tito, D. & Stejskal, F.** (1993). The *Azotobacter chroococcum* hydrogenase gene cluster: sequences and genetic analysis of four accessory genes, *hupA*, *hupB*, *hupY*, and *hupC*. *Gene* **127**, 53-61.

68. **Xu, H.-W. & Wall, J. D. (1991).** Clustering of genes necessary for hydrogen oxidation in *Rhodobacter capsulatus*. *Journal of Bacteriology* **173**, 2401-2405.
69. **Rey, L., Murillo, J., Hernando, E., Hidalgo, E., Cabrera, E., Imperial, J. & Ruiz-Argueso, T. (1993).** Molecular analysis of a microaerobically induced operon required for hydrogenase synthesis in *Rhizobium leguminosarum biovar viciae*. *Molecular Microbiology* **8**, 471-481.
70. **Fu, C. & Maier, R. J. (1994).** Nucleotide sequences of two hydrogenase-related genes (*hypA* and *hypB*) from *Bradyrhizobium japonicum*, one of which (*hypB*) encodes an extremely histidine-rich region and guanine nucleotide-binding domains. *Biochemica et Biophysica Acta* **1184**, 135-138.
71. **Wülfing, C., Lombardero, J. & Plückthun, A. (1994).** An *Escherichia coli* protein consisting of a domain homologous to FK506-binding proteins (FKBP) and a new metal binding motif. *Journal of Biological Chemistry* **269**, 2895-2901.
72. **Lee, M. H., Pankratz, H. S., Wang, S., Scott, R. A., Finnegan, M. G., Johnson, M. K., Ippolito, J. A., Christianson, D. W. & Hausinger, R. P. (1993).** Purification and characterization of *Klebsiella aerogenes* UreE protein: a nickel-binding protein that functions in urease metallocenter assembly. *Protein Science* **2**, 1042-1052.
73. **Saraste, M., Sibbald, P. R. & Wittinghofer, A. (1990).** The P-loop—a common motif in ATP- and GTP- binding proteins. *Trends in Biochemical Sciences* **15**, 430-434.
74. **Wu, L.-F. (1992).** Putative nickel binding sites of microbial proteins. *Research in Microbiology* **143**, 347-351.
75. **Lutz, A., Jacobi, A., Schlenzog, V., Böhm, R., Sawers, G. & Böck, A. (1991).** Molecular characterization of an operon (*hyp*) necessary for the activity of the three hydrogenase isoenzymes in *Escherichia coli*. *Molecular Microbiology* **5**, 123-135.
76. **Waugh, R. & Boxer, D. H. (1986).** Pleiotropic hydrogenase mutants of *Escherichia coli* K-12: growth in the presence of nickel can restore hydrogenase activity. *Biochimie* **68**, 157-166.
77. **Maier, T., Jacobi, A., Sauter, M. & Böck, A. (1993).** The product of the *hypB* gene, which is required for nickel incorporation into hydrogenases, is a novel guanine nucleotide-binding protein. *Journal of Bacteriology* **175**, 630-635.
78. **Wang, Z. Y. & Portis, A. R. (1992).** Dissociation of ribulose-1,5-bisphosphate bound to ribulose-1,5-bisphosphate carboxylase oxygenase and its enhancement

by ribulose-1,5-bisphosphate carboxylase oxygenase activase-mediated hydrolysis of ATP. *Plant Physiology* **99**, 1348-1353.

79. **Holland, M. A. & Polacco, J. C. (1992).** Urease-null and hydrogenase-null phenotypes of a phylloplane bacterium reveal altered nickel metabolism in two soybean mutants. *Plant Physiology* **92**, 942-948.
80. **Meyer-Bothling, L. E., Polacco, J. C. & Cianzio, S. R. (1987).** Pleiotropic soybean mutants defective in both urease isozymes. *Molecular and General Genetics* **209**, 432-438.
81. **Polacco, J. C., Judd, A. K., Dybing, J. K. & Cianzio, S. R. (1989).** A new mutant class of soybean lacks urease in leaves but not in leaf-derived callus or in roots. *Molecular and General Genetics* **217**, 257-262.
82. **Stebbins, N., Holland, M. A., Cianzio, S. R. & Polacco, J. C. (1991).** Genetic tests of the roles of the embryonic ureases of soybean. *Plant Physiology* **97**, 1004-1010.
83. **Mackay, E. M. & Pateman, J. A. (1982).** The regulation of urease activity in *Aspergillus nidulans*. *Biochemical Genetics* **20**, 763-776.
84. **Benson, E. W. & Howe, H. B., Jr. (1978).** Reversion and interallelic complementation at four urease loci in *Neurospora crassa*. *Molecular and General Genetics* **165**, 277-282.
85. **Kinghorn, J. R. & Fluri, R. (1984).** Genetic studies of purine breakdown in the fission yeast *Schizosaccharomyces pombe*. *Current Genetics* **8**, 99-105.
86. **Mackay, E. M. & Pateman, J. A. (1980).** Nickel requirement of a urease-deficient mutant in *Aspergillus nidulans*. *Journal of General Microbiology* **116**, 249-251.
87. **Zonia, L. E., Stebbins, N. E. & Polacco, J. C. (1995).** Essential role of urease in germination of nitrogen-limited *Arabidopsis thaliana* seeds. *Plant Physiology* **107**, 1097-1103.
88. **de Koning-Ward, T. F., Ward, A. C. & Robins-Browne, R. M. (1994).** Characterization of the urease-encoding gene complex of *Yersinia enterocolitica*. *Gene* **145**, 25-32.
89. **Jabri, E., Carr, M. B., Hausinger, R. P. & Karplus, P. A. (1995).** The crystal structure of urease from *Klebsiella aerogenes*. *Science* **268**, 998-1004.

90. **Mobley, H. L. T., Garner, R. M. & Bauerfeind, P. (1995).** *Helicobacter pylori* nickel-transport gene *nixA*: synthesis of catalytically active urease in *Escherichia coli* independent of growth conditions. *Molecular Microbiology* **16**, 97-109.
91. **Sriwanthana, B., Island, M. D., Maneval, D. & Mobley, H. L. T. (1994).** Single-step purification of *Proteus mirabilis* urease accessory protein UreE, a protein with a naturally occurring histidine tail, by nickel chelate affinity chromatography. *Journal of Bacteriology* **176**, 6836-6841.
92. **Park, I.-S. & Hausinger, R. P. (1995).** Evidence for the presence of urease apoprotein complexes containing UreD, UreF, and UreG in cells that are competent for in vivo enzyme activation. *Journal of Bacteriology* **177**, 1947-1951.
93. **Collins, C. M. & D'Orazio, S. E. F. (1993).** Bacterial ureases: structure, regulation of expression and role in pathogenesis. *Molecular Microbiology* **9**, 907-913.
94. **D'Orazio, S. E. & Collins, C. M. (1993).** The plasmid-encoded urease gene cluster of the family *Enterobacteriaceae* is positively regulated by UreR, a member of the AraC family of transcriptional activators. *Journal of Bacteriology* **175**, 3459-3467.
95. **Mobley, H. L. T., Island, M. D. & Hausinger, R. P. (1995).** Molecular biology of microbial ureases. *Microbiological Reviews* **59**, 451-480.
96. **Fleischmann, R. D., Adams, M. D., White, O., Clayton, R. A., Kirkness, E. F., Kerlavage, A. R., Bult, C. J., Tomb, J.-F., Dougherty, B. A., Merrick, J. M., McKenney, K., Sutton, G., FitzHugh, W., Fields, C., Gocayne, J. D., Scott, J., Shirley, R., Liu, L.-I., Glodek, A., Kelley, J. M., Weidman, J. F., Phillips, C. A., Spriggs, T., Hedblom, E., Cotton, M. D., Utterback, T. R., Hanna, M. C., Nguyen, D. T., Saudek, D. M., Brandon, R. C., Fine, L. D., Fritchman, J. L., Fuhrmann, J. L., Geoghagen, N. S. M., Gnehm, C. L., McDonald, L. A., Small, K. V., Fraser, C. M., Smith, H. O. & Venter, J. C. (1995).** Whole-genome random sequencing and assembly of *Haemophilus influenzae* Rd. *Science* **269**, 496-512.
97. **You, J.-H., Song, B.-H., Kim, J.-G., Lee, M.-H. & Kim, S.-D. (1995).** Genetic organization and nucleotide sequencing of the *ure* gene cluster in *Bacillus pasteurii*. *Molecules and Cells* **5**, 359-369.
98. **Miksch, G. (1994).** The urease structural gene *ureA* in *Rhizobium meliloti* is preceded by an open reading frame necessary for urease activity. *FEMS Microbiology Letters* **124**, 185-190.

99. **Chen, Y.-Y., Clancy, K. A. & Burne, R. A. (1996).** *Streptococcus salivarius* urease: genetic and biochemical characterization and expression in a dental plaque *Streptococcus*. *Infection and Immunity* **64**, 585-592.
100. **Clemens, D. L., Lee, B.-Y. & Horwitz, M. A. (1995).** Purification, characterization, and genetic analysis of *Mycobacterium tuberculosis* urease, a potentially critical determinant of host-pathogen interaction. *Journal of Bacteriology* **177**, 5644-5652.
101. **Park, I.-S. & Hausinger, R. P. (1996).** Metal ion interactions with urease and UreD-urease apoproteins. *Biochemistry* **35**, 5345-5352.
102. **Brayman, T. G. & Hausinger, R. P. (1996).** Purification, characterization, and functional analysis of a truncated *Klebsiella aerogenes* UreE protein lacking the histidine-rich carboxyl terminus. *Journal of Bacteriology* **178**, 5410-5416.
103. **Moncrief, M. B. C., Hom, L. G., Jabri, E., Karplus, P. A. & Hausinger, R. P. (1995).** Urease activity in the crystalline state. *Protein Science* **4**, 2234-2236.
104. **Moncrief, M. B. C. & Hausinger, R. P. (1996).** Purification and activation properties of UreD-UreF-urease apoprotein complexes. *Journal of Bacteriology* **178**, 5417-5421.
105. **Neyrolles, O., Ferris, S., Behbahani, N., Montagnier, L., & Blanchard, A. (1996).** Organization of *Ureaplasma urealyticum* urease gene cluster and expression in a suppressor strain of *Escherichia coli*. *Journal of Bacteriology* **178**, 647-655.
106. **Dunn, B. E., Sung, C. C., Taylor, N. S. & Fox, J. G. (1991).** Purification and characterization of *Helicobacter mustelae* urease. *Infection and Immunity* **59**, 3343-3345.
107. **Turbett, G. R., Hoj, P. B., Horne, R. & Mee, B. J. (1992).** Purification and characterization of urease enzymes of *Helicobacter* species from humans and animals. *Infection and Immunity* **60**, 5259-5266.

CHAPTER 2

UREASE ACTIVITY IN THE CRYSTALLINE STATE

The studies reported here were combined with X-ray crystallographic data analysis by Evelyn Jabri and preliminary crystal activity studies by Louis G. Hom and published as Moncrief, M. B. C., L. G. Hom, E. Jabri, P. A. Karplus, and R. P. Hausinger. (1995). Urease activity in the crystalline state. *Protein Science*, 4:2234-2236. Information that was available as an electronic appendix to the *Protein Science* paper is integrated into this text.

ABSTRACT

Crystalline urease from *Klebsiella aerogenes* was found to have less than 0.05% of the activity observed for the soluble enzyme under standard assay conditions. Li_2SO_4 , present in the crystal storage buffer at 2 M concentration, was shown to inhibit soluble urease by a mixed inhibition mechanism (K_i 's of 0.38 ± 0.05 M for the free enzyme and 0.13 ± 0.02 M for the enzyme-urea complex). However, the activity of crystals was less than 0.5% of the expected value for the salt content in the crystal storage buffer, suggesting that salt inhibition does not account for the near absence of crystalline activity. Dissolution of crystals resulted in approximately 43% recovery of the soluble enzyme activity, demonstrating that protein denaturation during crystal growth does not cause the dramatic diminishment in the catalytic rate. Finally, crushed crystals exhibited only a three-fold increase in activity over that of intact crystals, indicating that the rate of substrate diffusion into the crystals does not significantly limit the enzyme activity. Urease is effectively inactive in this crystal form and the small amounts of activity observed likely arise from limited enzyme activity at the crystal surfaces or trace levels of enzyme dissolution into the crystal storage buffer.

INTRODUCTION

Urease (EC 3.5.1.5) is a nickel-containing enzyme (1) that catalyzes the hydrolysis of urea to yield ammonia and carbamate. Carbamate is unstable and spontaneously decomposes to yield a second molecule of ammonia and carbonic acid. The high levels of ammonia generated by these reactions and the resulting elevation of pH have important ramifications for medicine and agriculture (reviewed in 2). For example, urease is a virulence factor in pathogenic bacteria that cause gastric ulceration, urinary stone formation, pyelonephritis, and other dysfunctions. Moreover, urea-based fertilizers are rapidly decomposed by soil urease activity with consequences that include phytopathicity and loss of volatilized nitrogen.

Urease from the soil bacterium *Klebsiella aerogenes* has been crystallized (3) and the three dimensional structure has been determined (4). The structure shows that urease is a tightly associated $(\alpha\beta\gamma)_3$ trimer (α -60.3 kDa, β -11.7 kDa, γ -11.1 kDa) containing three active sites per holoenzyme and two nickel ions per active site. Thus far no binding of substrate or inhibitors soaked into the crystals has been observed. These failures raise the question of whether urease has activity in the crystalline state. This study demonstrates that crystalline urease is essentially inactive and examines the possible factors to account for the diminishment in activity.

MATERIALS AND METHODS

Enzyme purification and crystallization. Urease was purified from *K. aerogenes* CG 253 cells carrying pKAU19, a plasmid containing the *K. aerogenes* urease gene cluster, that were grown at 37 °C in MOPS-glutamine media as described previously (5). Urease crystals were grown by published procedures using the hanging drop method (3). Crystals were stored in crystal storage buffer containing 2M Li₂SO₄ and 100 mM HEPES (pH 7.75) and were used within 3.5 weeks after they were set up for growth. All experiments reported in this paper were carried out with protein from a single preparation.

Assays. Urease activity was measured by quantitating the rate of ammonia release from urea by formation of indophenol, which was monitored at 625 nm (6). One unit of urease activity was defined as the amount of enzyme required to hydrolyze 1 μmole of urea per minute at 37 °C. The standard assay buffer consisted of 25 mM HEPES (pH 7.75), 0.5 mM EDTA, and 50 mM urea. When testing whole and crushed crystal activity the assay buffer additionally included 2 M Li₂SO₄ and the solution was gently agitated on a platform shaker. All assays with crystals were carried out at 30 °C and the experimentally determined values were adjusted by a factor of 1.4 to provide 37 °C values. Whole crystals were cubes of 230-250 μm on each edge and crushed crystals had fragments of < 30 μm in the greatest dimension. For crystal dissolution, crystals were washed with crystal storage buffer, dissolved in 500 μl water, and immediately assayed.

All assays were linear over the times examined. The protein content of soluble urease was determined by the method of Lowry *et al.* (7) using bovine serum albumin as the standard. The protein content of urease crystals was determined by using the following equation:

$$\frac{\text{size } (\mu\text{m})^3}{\text{crystal}} \times \frac{\text{unit cell}}{(1.71 \times 10^{-2} \mu\text{m})^3} \times \frac{24 \alpha\beta\gamma \text{ units}}{\text{unit cell}} \times \frac{1 \text{ mole } \alpha\beta\gamma}{6.023 \times 10^{23} \alpha\beta\gamma \text{ units}} \times \frac{83,202 \text{ g}}{1 \text{ mole } \alpha\beta\gamma}$$

Using this equation a typical $(230\text{-}250 \mu\text{m})^3$ crystal contains 8.09-10.4 μg of urease.

Salt inhibition of urease activity. Since the crystal storage buffer contained 2 M Li_2SO_4 , we tested the activity of urease in the presence of varied concentrations of Li_2SO_4 , LiCl , or Na_2SO_4 , and various concentrations of urea. Kinetic data for each salt concentration were fit by using the method of Wilkinson (8) and subsequent replots of slopes and intercepts for analysis of the inhibition constants used well established methods (9).

RESULTS AND DISCUSSION

Activity of crystalline urease. Whereas freshly prepared *K. aerogenes* urease possessed a specific activity of 3,500 units/mg, the activity observed for crystalline enzyme in crystal storage buffer was only 1.54 units/mg (Table 1). Four possible reasons to account for the low activity in the urease crystals were considered: (i) a component in the crystal storage buffer may inhibit the enzyme, (ii) the crystals may represent an

Table 1. Specific activities of soluble and crystalline *K. aerogenes* urease

Sample	Specific Activity (units/mg)	
	2 M Li ₂ SO ₄	No salt
Soluble enzyme	321 ± 10	3,500 ± 100
Crystalline enzyme	1.54 ± 0.25	-
Crushed crystalline enzyme	4.3 ± 0.7	-
Dissolved crystalline enzyme	-	1,500 ± 140

irreversibly denatured and inactive state of the enzyme, (iii) the rate of substrate diffusion into the crystals may be limiting such that only the molecules exposed to the surface are active, and (iv) the crystalline enzyme is restricted from undergoing conformational changes required for catalysis. In the latter case, the observed levels of activity in crystals may correspond to enzyme molecules at the crystal surface and/or soluble enzyme arising from slight dissolution of the crystal in fresh crystal storage buffer. Experimental evidence related to these considerations are described below.

To examine the first possibility, soluble urease was added to buffer containing 2 M Li_2SO_4 to simulate crystal storage conditions. Under these conditions the enzyme possessed roughly 320 units/mg. Although Li_2SO_4 does inhibit urease (see detailed kinetics below), the approximately 11-fold decrease in activity falls far short of the 2,300-fold decrease seen in the crystals. The only other component in the crystal storage buffer is 100 mM HEPES which is known to not interfere with the urease assay. Although it is possible that atmospheric components (e.g., $\text{CO}_2/\text{HCO}_3^-$) or other unidentified factors may bind to the crystalline enzyme and reduce its activity, such factors would have to dissociate upon crystal dissolution. The active site in fresh crystals does not appear to have any unexpected ligands bound.

With regard to the second possibility, growth of urease crystals of suitable size for these studies required approximately three weeks at room temperature, thus it is conceivable that the enzyme denatured during this time and the crystals represented inactive protein. To address this concern, the urease activity of dissolved crystals was assessed. As shown in Table I, the specific activity of dissolved crystals was 1,500

units/mg, representing a recovery of 43% of the activity of fresh soluble urease. Thus, protein denaturation during crystal growth does not account for the near absence of urease activity in the crystalline state.

Although protein crystals are highly hydrated, limited rates of substrate diffusion into crystals have been shown to account for the apparent low specific activities of selected crystalline enzymes (10). Given the small size of the urea molecule, this process is not likely to be significant in the case of urease. Nevertheless, I attempted to test this possibility by observing the effect on activity of crushing individual crystals in their crystal storage buffer to form fragments where the longest dimension was less than 12.5% the size of the intact crystal. Only a slight (3-fold) increase in activity was noted (Table I), possibly arising from enhanced levels of dissolution of enzyme from the increased surface area of the crystal matrix into fresh crystal storage buffer. Thus, substrate diffusion into the crystals is not the limiting process to explain the low urease activities in the crystalline state.

Based solely on ruling out other possible explanations, the low level of urease activity in the crystalline state probably arises primarily from conformational restrictions in the crystal lattice. Indeed, I conclude that urease in this crystal form is essentially inactive. The low levels of activity observed in assays of the crystals are likely derived from trace amounts of enzyme equilibrating with the solution. Consistent with this proposal, crystal storage buffer from which a urease crystal had been removed was shown to possess significant levels of urease activity.

Kinetic analysis of salt inhibition. Because urease inhibition by Li_2SO_4 was fairly extensive, we examined it in more detail. Inhibition was not restricted to the lithium cation or the sulfate anion as similar inhibition was observed with Li_2SO_4 , LiCl , and Na_2SO_4 (Fig. 1). The inhibition is not simply due to ionic strength effects; e.g., the various concentrations of LiCl are more effective than equivalent concentrations of Na_2SO_4 . In order to characterize the mechanism of inhibition, urease activity was measured over a range of substrate and Li_2SO_4 concentrations. A subset of the data is depicted in a double-reciprocal plot in Fig. 2A. Intersection of the lines below the x-axis is consistent with a mixed type inhibition where the inhibitor binds to both free enzyme and the enzyme-substrate complex with dissociation constants of K_i and K_i' , respectively (9). This type of inhibition mechanism can be represented by the following equation:

$$v = \frac{V_{max}}{\frac{K_s}{[S]} \left(1 + \frac{[I]}{K_i} \right) + \left(1 + \frac{[I]}{K_i'} \right)}$$

The values of K_i and K_i' were obtained by replots of the slopes and the vertical axis intercepts, as shown in Fig. 2B and 2C. The K_i value of $0.38 \pm .05$ M and the K_i' value of $0.13 \pm .02$ M indicate that Li_2SO_4 binds more tightly to the enzyme-substrate complex than to the free enzyme. The crystal structure gives no evidence for sulfate binding sites near the catalytic center. Since lithium ions only have 2 electrons, they would not be easily visible in the crystal structure.

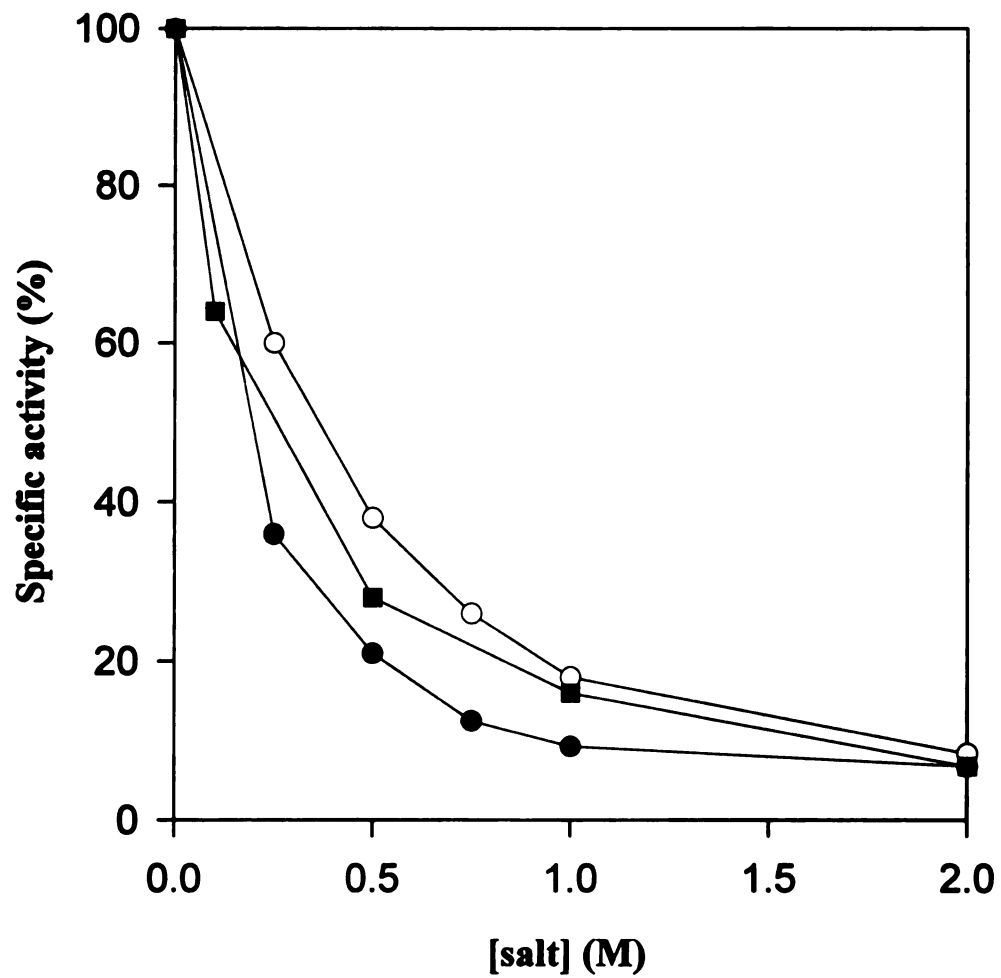


Figure 1. Urease activity as a function of salt concentration. Purified urease was assayed at 37 °C in the presence of 25 mM HEPES (pH 7.75), 0.5 mM EDTA, 50 mM urea, and the indicated concentrations of Li₂SO₄ (●), Na₂SO₄ (○), and LiCl (■).

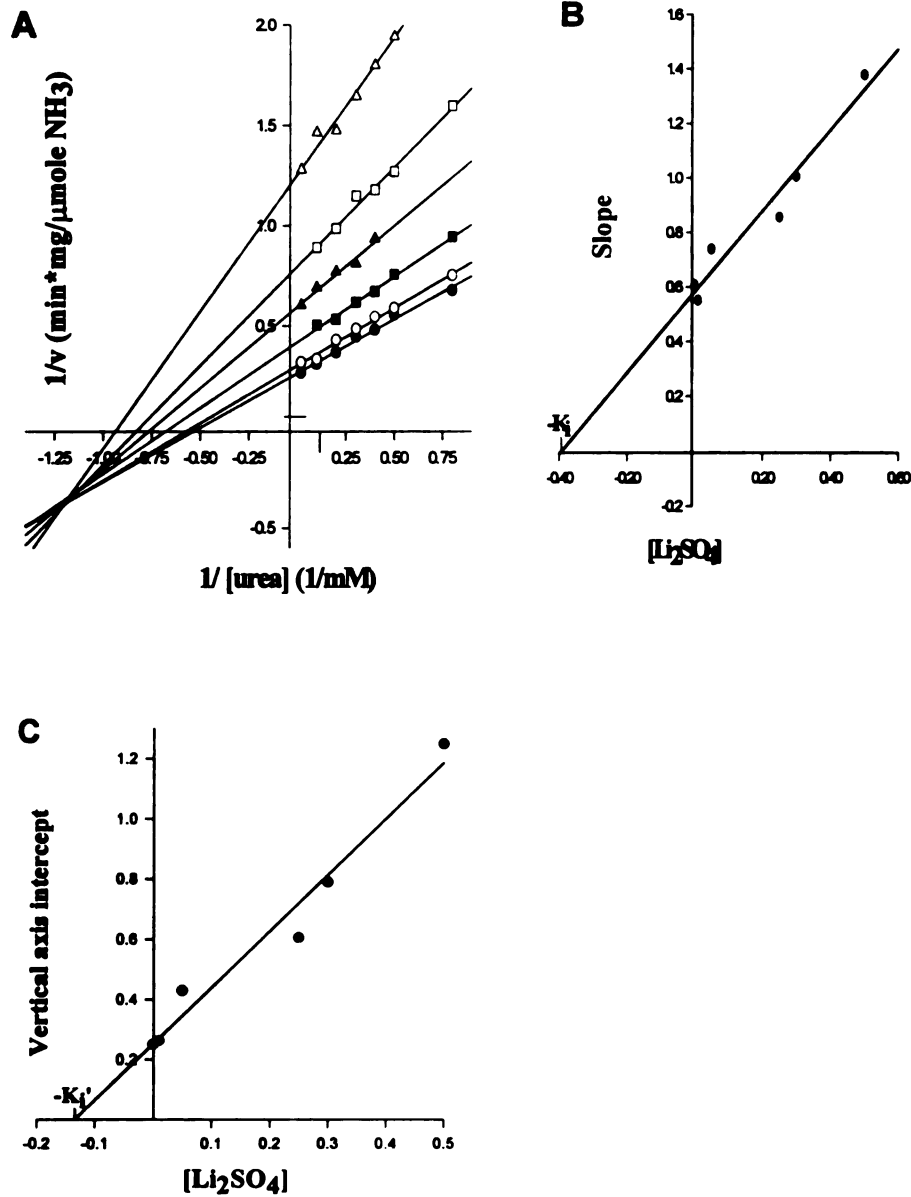


Figure 2. Kinetic analysis of Li_2SO_4 inhibition of urease. (A) An inverse plot of urease activity in the presence of Li_2SO_4 at 0 (\bullet), 0.01 M (\circ), 0.05 M (\blacksquare), 0.25 M (\blacktriangle), 0.3 M (\square), and 0.5 M (\triangle) concentrations. (B) Replot of slopes versus $[\text{Li}_2\text{SO}_4]$. (C) Replot of vertical axis intercepts versus $[\text{Li}_2\text{SO}_4]$.

REFERENCES

1. **Hausinger, R. P.** (1993). Urease. In *Biochemistry of Nickel*, pp. 23-57. New York: Plenum Publishing Corp.
2. **Mobley, H. L. T. & Hausinger, R. P.** (1989). Microbial ureases: significance, regulation, and molecular characterization. *Microbiological Reviews* **53**, 85-108.
3. **Jabri, E., Lee, M. H., Hausinger, R. P. & Karplus, P. A.** (1992). Preliminary crystallographic studies of urease from jack bean and from *Klebsiella aerogenes*. *Journal of Molecular Biology* **227**, 934-937.
4. **Jabri, E., Carr, M. B., Hausinger, R. P. & Karplus, P. A.** (1995). The crystal structure of urease from *Klebsiella aerogenes*. *Science* **268**, 998-1004.
5. **Mulrooney, S. B., Pankratz, H. S. & Hausinger, R. P.** (1989). Regulation of gene expression and cellular localization of cloned *Klebsiella aerogenes* (*K. pneumoniae*) urease. *Journal of General Microbiology* **135**, 1769-1776.
6. **Weatherburn, M. W.** (1967). Phenol-hypochlorite reaction for determination of ammonia. *Analytical Chemistry* **39**, 971-974.
7. **Lowry, O. H., Rosebrough, N. J., Farr, A. J. & Randall, R. J.** (1951). Protein measurement with the Folin phenol reagent. *Journal of Biological Chemistry* **193**, 265-275.
8. **Wilkinson, G. N.** (1961). Statistical estimations in enzyme kinetics. *Biochemical Journal* **80**, 324-332.
9. **Dixon, M. & Webb, E. C.** (1961). *Enzymes*, 3rd Ed. New York: Academic Press, Inc.
10. **Makinen, M. W. & Fink, A.** (1977). Reactivity and cryoenzymology of enzymes in the crystalline state. *Annual Review of Biophysics and Bioengineering* **6**, 301-343.

CHAPTER 3

FIRST DEMONSTRATION OF IN VITRO ACTIVATION OF UREASE

APOPROTEIN

The studies described here were combined with D-Apo studies by Il-Seon Park and published as Park, I.-S., M. B. Carr, and R. P. Hausinger (1994). In vitro activation of urease apoprotein and role of UreD as a chaperone required for nickel metallocenter assembly. *Proceedings of the National Academy of Sciences USA*, **91**: 3233-3237.

ABSTRACT

The formation of active urease in *Klebsiella aerogenes* requires the presence of three structural genes for the apoprotein (*ureA*, *ureB*, and *ureC*), as well as four accessory genes (*ureD*, *ureE*, *ureF*, and *ureG*) that are involved in functional assembly of the metallocenter in this nickel-containing enzyme. Here I report the first evidence that urease apoprotein can be activated *in vitro* in highly concentrated cell extracts. Slow and partial activation of urease apoprotein was observed after addition of nickel ions to extracts of *Escherichia coli* cells bearing a plasmid containing the *K. aerogenes* urease gene cluster or derivatives of this plasmid with deletions in *ureE*, *ureF*, or *ureG*. In contrast, extracts of cells containing a *ureD* deletion derivative failed to generate active urease, thus highlighting a key role for UreD in the metallocenter assembly process.

INTRODUCTION

Urease (EC 3.5.1.5) is a nickel-containing enzyme that catalyzes the hydrolysis of urea to form carbonic acid and two molecules of ammonia. Until recently, the best characterized urease was that from jack bean (1). This enzyme was the first ever crystallized (2) and the first shown to possess nickel (3). However, because of the ease of cell growth and genetic manipulation in bacteria compared to plants and the medical importance of bacterial urease, our understanding of the prokaryotic enzyme has outpaced knowledge of the plant enzyme (4). Importantly, the active site residues of plant and bacterial ureases are highly conserved and both enzymes possess a novel bi-nickel metallocenter.

Assembly of the urease bi-nickel metallocenter appears to be a complex process requiring the action of several accessory gene products. For example, deletion analysis of the *Klebsiella aerogenes* urease gene cluster revealed that one gene (*ureD*) located directly upstream and three genes (*ureE*, *ureF*, and *ureG*) found directly downstream of the three genes (*ureA*, *ureB*, and *ureC*) encoding the subunits of the bacterial urease are involved in the functional assembly of the urease metallocenter (5, 6). Homologs of the accessory genes have been found in several bacterial species (e.g., 7-9) and an essential role for auxiliary genes in forming active urease has been confirmed in these and many other bacteria. Genetic studies are consistent with a similar requirement for urease accessory genes in the fungi *Neurospora crassa* (10), *Schizosaccharomyces pombe* (11), and *Aspergillus nidulans* (12, 13). Finally, two loci (*Eu2* and *Eu3*) that appear to encode genes

1

associated with urease maturation factors such as nickel emplacement have been identified in soybean plants (14). Thus, accessory genes involved in metallocenter assembly may be a universal component of urease activation.

The detailed roles for the urease accessory genes are unknown. The histidine-rich *K. aerogenes* UreE protein has been purified and shown to reversibly bind six nickel ions per dimer (15); hence, it is reasonable to suggest that UreE serves as the nickel donor to urease apoprotein. UreG contains a P-loop motif that is found in many nucleotide-binding proteins (16); thus, this protein may be involved in coupling nucleotide hydrolysis to the assembly process. In this regard, *in vivo* evidence is consistent with an energy dependence for urease activation (17). Furthermore, the sequence of *K. aerogenes* UreG was shown (18) to be approximately 25% identical to that of the *Escherichia coli hypB* gene product (19). The *hyp* operon (*hydrogenase pleiotropic operon*) is required for functional activation of hydrogenase. A mutation in *hypB* was shown to be complemented, in part, by the addition of high levels of nickel (20), consistent with a role for this protein in nickel processing. Of potential significance to the function of UreG, purified HypB protein has been shown to bind guanine nucleotides and to hydrolyze GTP (21). In contrast to UreE and UreG, the sequences for UreD or UreF offer no insight into their function and these proteins have not been purified or characterized. Here I demonstrate the ability to partially activate urease apoprotein *in vitro*.

MATERIALS AND METHODS

Cell Growth and Disruption. *E. coli* DH5 or DH1 carrying pKAU17 (22) or $\Delta ureD-2$, $\Delta ureE-1$, $\Delta ureF$, or $\Delta ureG-1$ deletion derivatives of pKAU17 (6) were grown in Luria-Bertani (LB) medium to late stationary phase. The harvested cultures were resuspended in 20 mM phosphate (pH 7.0), 1 mM EDTA, and 1 mM 2-mercaptoethanol buffer and disrupted by three passages through a French pressure cell (American Instrument Co., Silver Spring MD) at 18,000 lb/in². Cell extracts were obtained after centrifugation (100,000 x g for 60 min) at 4°C. The samples were further sterilized by passage through a 0.2 μ m filter into sterile tubes.

Urease Activity Assays. Urease activities were assayed in 25 mM HEPES (pH 7.75) and 0.5 mM EDTA buffer containing 50 mM urea. Linear regression analysis of the released ammonia, determined by conversion to indophenol (23), versus time yielded initial rates. One unit of activity is defined as the amount of enzyme required to degrade 1 μ mol urea per min at 37°C. Protein concentrations were determined by a commercial assay (Bio-Rad, Hercules, CA) with a bovine serum albumin standard.

RESULTS AND DISCUSSION

***In Vitro* Activation of Urease Apoprotein.** *E. coli* (pKAU17) carries the wild-type *K. aerogenes* urease gene cluster. The urease apoprotein (Apo) in extracts from these cells (grown in the presence of nickel-free medium) is partially activated by incubation with 1 mM NiCl₂ (Fig. 1, ●). Although *in vivo* activation of Apo has been described [e.g., (17)],

the data shown in Fig. 1 represent the first evidence for *in vitro* activation of this enzyme. Similar to the *in vivo* situation, the *in vitro* activation process is very slow, in this case requiring over a day to reach its limiting activity. The highest specific activity values observed in these studies (30–40 U/mg protein) account for activation of only about 10% of the urease that is present [i.e., when grown in the presence of 1 mM NiCl₂ *E. coli*(pKAU17) cell extracts typically possess specific activity values of 300–400 U/mg (17)]. The rate and extent of activation is not affected by Apo stability as demonstrated by studies in which extracts were preincubated at 37 °C for 23 h prior to nickel addition with only partial loss of competence for activation. Similarly, the leveling off of activity is not due to simultaneous formation and inactivation of active enzyme because purified urease holoprotein is completely stable under the incubation conditions used for activation of the cell extracts (Fig. 2). Alteration of the activation conditions (varying the pH, buffer composition, ionic strength, and NiCl₂ concentration) failed to improve the extent of activation and the process was hindered by elevated nickel concentrations (4 mM) and high (> 8.0) or low (< 7.0) pH. In contrast to the *in vivo* urease activation results reported earlier (17), the *in vitro* activation process described above does not appear to require energy. Dialysis of cell extracts prior to nickel addition or inclusion of apyrase 15 min prior to the activation assay has no effect on the process. Further, inclusion of up to 1 mM magnesium and 1 mM ATP or GTP does not significantly alter the activation behavior. Higher concentrations of these nucleotides appear to inhibit activation, perhaps by sequestering nickel ion.

Analogous Apo activation experiments were carried out using extracts from cells that were defective in three of the urease accessory genes, *ureD*, *ureF*, and *ureG* (Fig. 1).

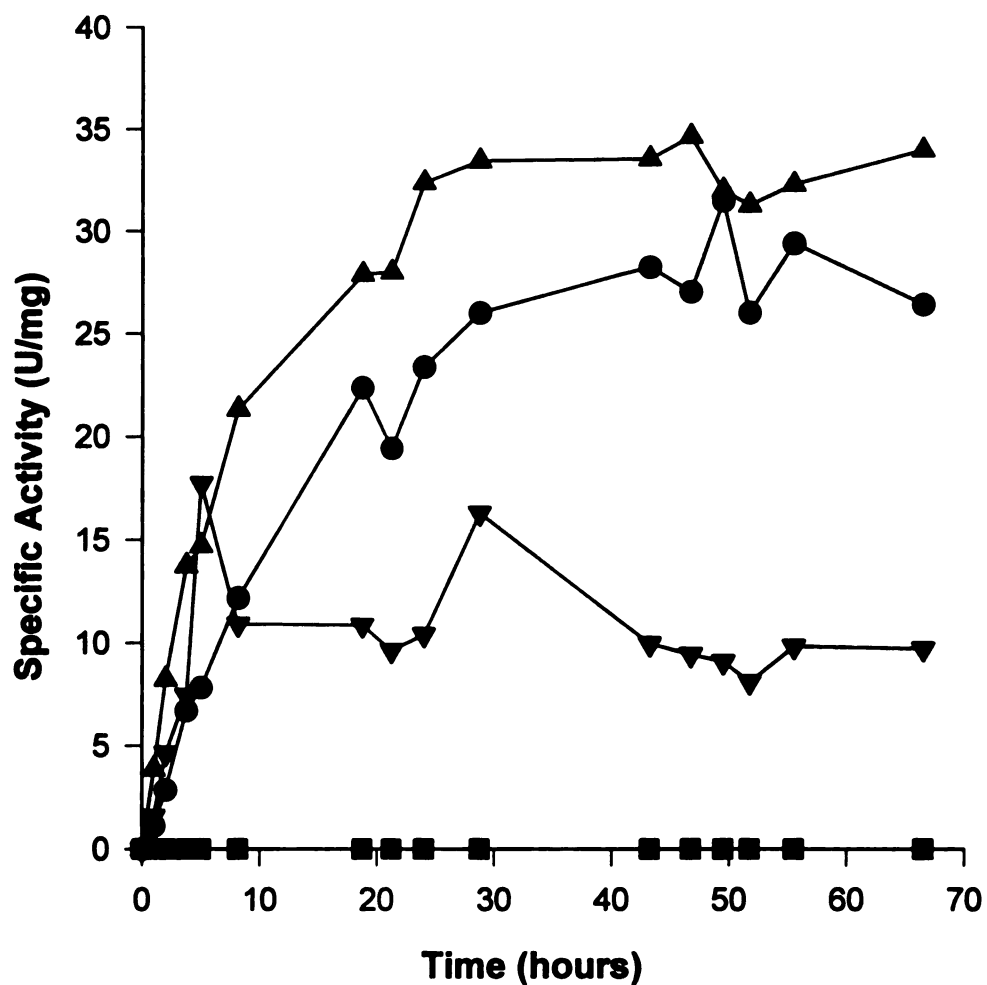


Figure 1. *In vitro* activation kinetics of urease apoprotein. Cell extracts (2 mg/ml) from *E. coli* cells carrying pKAU17 (●), or $\Delta ureD$ (■), $\Delta ureF$ (▼), or $\Delta ureG$ (▲) deletion derivatives of this plasmid were incubated in 20 mM phosphate buffer (pH 7.8) containing 1 mM EDTA, 1 mM 2-mercaptoethanol, and 1 mM $NiCl_2$ at 37 °C. Aliquots were withdrawn and assayed for urease activity and protein at the time points shown.

[UreE is known not to be essential for urease activation *in vivo* (6), hence, detailed *in vitro* activation studies were not carried out with the $\Delta ureE$ mutant. Preliminary experiments did verify the absence of a requirement for UreE *in vitro* (data not shown)]. Surprisingly, deletion of *ureG* (Fig. 1, ▲) has no inhibitory effect on the *in vitro* activation process and may lead to an increase in the rate and extent of functional metallocenter assembly. This finding is intriguing because $\Delta ureG$ cultures possess no detectable urease activity even when provided with 1 mM nickel ion in the growth medium (6). Indeed, the *in vitro* activation behavior (starting from no detectable activity and increasing at a rate and to a level similar to the control extracts) is identical for $\Delta ureG$ extracts when obtained from cells grown with or without nickel ion. The cell extracts from a *ureF* deletion mutant also exhibit activation competence (Fig. 1, ▼), but the final specific activity value reached is significantly depressed compared to the control. Again, the observation of any urease activity is surprising because $\Delta ureF$ cultures have no detectable activity even when provided with high concentrations of nickel in the growth medium. Of greatest significance, Apo in cell extracts from a $\Delta ureD$ mutant (grown in the presence or absence of nickel ion) was not competent for activation under these activation conditions.

In summary, these results provide the first evidence for *in vitro* activation of Apo and highlight a key role for UreD in the urease activation process. [Note: These experiments were carried out prior to the demonstration that CO₂ is required for *in vitro* activation (24). No bicarbonate was provided in the activation buffer, so the only CO₂ available was that which diffused into the buffer from the atmosphere. This explains, in part, the very slow kinetics of activation observed in these studies. The UreD-Apo and

UreD-UreF-Apo complexes can better incorporate trace levels of CO₂ than Apo, so the activation reported here is likely to arise predominantly from Apo that is present as complexes with accessory proteins.]

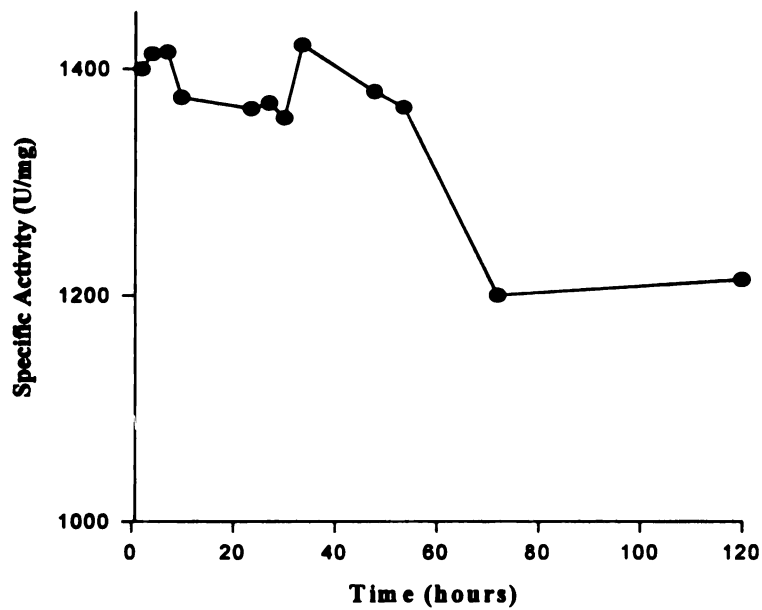


Figure 2. Urease stability during incubation at 37 °C. Purified holourease was incubated in 20 mM phosphate (pH 7.3), 1 mM EDTA, and 1 mM 2-mercaptoethanol at 37 °C and assayed for activity at the indicated timepoints.

REFERENCES

1. **Zerner, B.** (1991). Recent advances in the chemistry of an old enzyme, urease. *Bioorganic Chemistry* **19**, 116-131.
2. **Sumner, J. B.** (1926). The isolation and crystallization of the enzyme urease. *Journal of Biological Chemistry* **69**, 435-441.
3. **Dixon, N. E., Gazzola, C., Blakeley, R. L. & Zerner, B.** (1975). Jack bean urease (EC 3.5.1.5). A metalloenzyme. A simple biological role for nickel? *Journal of the American Chemical Society* **97**, 4131-4133.
4. **Mobley, H. L. T. & Hausinger, R. P.** (1989). Microbial ureases: significance, regulation, and molecular characterization. *Microbiological Reviews* **53**, 85-108.
5. **Mulrooney, S. B. & Hausinger, R. P.** (1990). Sequence of the *Klebsiella aerogenes* urease genes and evidence for accessory proteins facilitating nickel incorporation. *Journal of Bacteriology* **172**, 5837-5843.
6. **Lee, M. H., Mulrooney, S. B., Renner, M. J., Markowicz, Y. & Hausinger, R. P.** (1992). Sequence of *ureD* and demonstration that four accessory genes (*ureD*, *ureE*, *ureF*, and *ureG*) are involved in nickel metallocenter biosynthesis. *Journal of Bacteriology* **174**, 4324-4330.
7. **Cussac, V., Ferrero, R. L. & Labigne, A.** (1992). Expression of *Helicobacter pylori* urease genes in *Escherichia coli* grown under nitrogen-limiting conditions. *Journal of Bacteriology* **174**, 2466-2473.
8. **Jones, B. D. & Mobley, H. L. T.** (1989). *Proteus mirabilis* urease: nucleotide sequence determination and comparison with jack bean urease. *Journal of Bacteriology* **171**, 6414-6422.
9. **Collins, C. M. & Gutman, D. M.** (1992). Insertional inactivation of an *Escherichia coli* urease gene by IS3411. *Journal of Bacteriology* **174**, 883-888.
10. **Benson, E. W. & Howe, H. B., Jr.** (1978). Reversion and interallelic complementation at four urease loci in *Neurospora crassa*. *Molecular and General Genetics* **165**, 277-282.
11. **Kinghorn, J. R. & Fluri, R.** (1984). Genetic studies of purine breakdown in the fission yeast *Schizosaccharomyces pombe*. *Current Genetics* **8**, 99-105.

12. **Mackay, E. M. & Pateman, J. A. (1982).** The regulation of urease activity in *Aspergillus nidulans*. *Biochemical Genetics* **20**, 763-776.
13. **Mackay, E. M. & Pateman, J. A. (1980).** Nickel requirement of a urease-deficient mutant in *Aspergillus nidulans*. *Journal of General Microbiology* **116**, 249-251.
14. **Meyer-Bothling, L. E., Polacco, J. C. & Cianzio, S. R. (1987).** Pleiotropic soybean mutants defective in both urease isozymes. *Molecular and General Genetics* **209**, 432-438.
15. **Lee, M. H., Pankratz, H. S., Wang, S., Scott, R. A., Finnegan, M. G., Johnson, M. K., Ippolito, J. A., Christianson, D. W. & Hausinger, R. P. (1993).** Purification and characterization of *Klebsiella aerogenes* UreE protein: a nickel-binding protein that functions in urease metallocenter assembly. *Protein Science* **2**, 1042-1052.
16. **Saraste, M., Sibbald, P. R. & Wittinghofer, A. (1990).** The P-loop—a common motif in ATP- and GTP- binding proteins. *Trends in Biochemical Sciences* **15**, 430-434.
17. **Lee, M. H., Mulrooney, S. B. & Hausinger, R. P. (1990).** Purification, characterization, and in vivo reconstitution of *Klebsiella aerogenes* urease apoenzyme. *Journal of Bacteriology* **172**, 4427-4431.
18. **Wu, L.-F. (1992).** Putative nickel binding sites of microbial proteins. *Research in Microbiology* **143**, 347-351.
19. **Lutz, A., Jacobi, A., Schlensog, V., Böhm, R., Sawers, G. & Böck, A. (1991).** Molecular characterization of an operon (*hyp*) necessary for the activity of the three hydrogenase isoenzymes in *Escherichia coli*. *Molecular Microbiology* **5**, 123-135.
20. **Waugh, R. & Boxer, D. H. (1986).** Pleiotropic hydrogenase mutants of *Escherichia coli* K-12: growth in the presence of nickel can restore hydrogenase activity. *Biochimie* **68**, 157-166.
21. **Maier, T., Jacobi, A., Sauter, M. & Böck, A. (1993).** The product of the *hypB* gene, which is required for nickel incorporation into hydrogenases, is a novel guanine nucleotide-binding protein. *Journal of Bacteriology* **175**, 630-635.
22. **Mulrooney, S. B., Pankratz, H. S. & Hausinger, R. P. (1989).** Regulation of gene expression and cellular localization of cloned *Klebsiella aerogenes* (*K. pneumoniae*) urease. *Journal of General Microbiology* **135**, 1769-1776.

23. **Weatherburn, M. W.** (1967). Phenol-hypochlorite reaction for determination of ammonia. *Analytical Chemistry* **39**, 971-974.
24. **Park, I.-S. & Hausinger, R. P.** (1995). Requirement of carbon dioxide for in vitro assembly of the urease nickel metallocenter. *Science* **267**, 1156-1158.

CHAPTER 4

PURIFICATION AND ACTIVATION PROPERTIES OF URED-UREF-UREASE APOPROTEIN COMPLEXES

These studies were published in the Journal of Bacteriology, 178: 5417-5421, 1996.

ABSTRACT

In vivo assembly of the *Klebsiella aerogenes* urease nickel metallocenter requires the presence of UreD, UreF, and UreG accessory proteins and is further facilitated by UreE. Prior studies had shown that urease apoprotein exists in an uncomplexed form as well as in a series of UreD-urease (I.-S. Park, M. B. Carr, and R. P. Hausinger, Proc. Natl. Acad. Sci. USA 91:3233-3237, 1994) and UreD-UreF-UreG-urease (I.-S. Park, and R. P. Hausinger, J. Bacteriol. 177:1947-1951, 1995) apoprotein complexes. This study demonstrates the existence of a distinct series of complexes comprised of UreD, UreF, and urease apoprotein. These novel complexes exhibited activation properties that were distinct from urease and UreD-urease apoprotein complexes. Unlike the previously described species, the UreD-UreF-urease apoprotein complexes were resistant to inactivation by NiCl₂. The bicarbonate concentration dependence for UreD-UreF-urease apoenzyme activation was significantly decreased compared to that of the urease and UreD-urease apoproteins. Western blot (immunoblot) analyses with polyclonal anti-urease and anti-UreD antibodies indicated that UreD is masked in the UreD-UreF-urease complexes, presumably by UreF. I propose that the binding of UreF modulates the UreD-urease apoprotein activation properties by excluding nickel ions from binding to the active site until after formation of the carbamylated lysine metallocenter ligand.

INTRODUCTION

Urease is a nickel-containing enzyme that catalyzes the hydrolysis of urea and serves as a virulence factor in microorganisms that are associated with urinary stone formation, gastric ulceration, and other human health concerns (2, 7). Crystallographic analysis of *Klebsiella aerogenes* urease revealed that the three structural subunits (encoded by *ureA*, *ureB*, and *ureC*) associate into a trimer of trimers [(UreA-UreB-UreC)₃] with each UreC subunit containing a novel bi-nickel metallocenter (3). The two nickel ions, separated by 3.5 Å, are bridged by a carbamylated lysine residue. Ni-1 is tricoordinate, bound by the carbamate and two histidine ligands, whereas Ni-2 is pentacoordinate, including the carbamate, two histidines, an aspartate, and a solvent molecule as ligands. The apoprotein, formed in cells grown in the absence of nickel ion or generated in accessory gene deletion mutants (5), is nearly identical to holoprotein in structure but lacks the metal ions and the bound carbon dioxide.

K. aerogenes urease apoprotein, here termed Apo, can be partially activated *in vitro* by incubation with nickel ions in bicarbonate-containing buffers (14). Carbon dioxide, in equilibrium with bicarbonate, reversibly reacts with the active-site lysine residue to form the requisite carbamate ligand. The concentration of carbon dioxide required for half-maximal activation is 0.2%, or approximately sevenfold the atmospheric concentration of this gas. Under optimal conditions, only 10-15% of the Apo is activated. The activation reaction competes with nickel binding to noncarbamylated protein and with nonproductive nickel binding to carbamylated protein (15). An additional complication is that several other metal

ions compete with nickel to form inactive metal-substituted species. Direct activation of Apo likely does not occur to any significant extent in the cell (reviewed in reference 8).

Cellular activation of *K. aerogenes* urease requires the participation of three accessory proteins (UreD, UreF, and UreG) and is aided by a fourth (UreE) (5). These peptides are encoded by genes located in the same cluster (*ureDABCEFG*) as those encoding the enzyme subunits (5, 9). On the basis of its ability to bind nickel ions (6), UreE is suggested to play a role involving nickel donation or storage. In contrast, the other accessory proteins are thought to function as complexes with the urease subunits. Both *ureD* and *ureF* possess non-consensus ribosome binding sites and are expressed at very low levels in the cell. Changing the ribosome binding site and initiation codon for *ureD* to yield a more consensus-like sequence resulted in the synthesis of high levels of UreD, shown to be present in a series of complexes containing the trimeric Apo [(UreA-UreB-UreC)₃] binding one, two, or three UreD peptides (12). For convenience, these UreD-urease apoprotein complexes will be called D-Apo. Incubation of D-Apo with bicarbonate and nickel ions leads to UreD dissociation and partial activation, accounting for approximately 30% of the available apoprotein (14). As found for Apo, nonproductive reactions compete with the activation process. These reactions include nickel binding to the noncarbamylated D-Apo, nickel binding improperly to the carbamylated species, and binding of other metal ions to form inactive metal-substituted proteins (15). The formation of D-Apo is not sufficient to account for activation of urease in the cell. Another series of Apo complexes containing UreD, UreF, and UreG has been detected and is able to be activated (13). Since all of these components are required for generating active urease *in vivo*, the UreD-UreF-

UreG-Apo complexes (DFG-Apo) were suggested to serve as the key cellular urease activation machinery. These complexes are present at minute levels in the cell and their properties have not been well characterized (11). The specific roles for UreD, UreF, and UreG in these complexes are unknown.

To better define the functions of the individual accessory proteins, we have identified, purified, and characterized the properties of a new series of complexes comprised of UreD, UreF, and the urease subunits. The UreD-UreF-Apo complexes (DF-Apo) have activation properties that are distinct from those of Apo or D-Apo species and provide insight into the role of UreF.

MATERIALS AND METHODS

Bacterial strains and plasmid constructions. All molecular biology methods followed the general protocols outlined in Sambrook *et al.* (16).

Three constructs were generated in which *ureF* was overexpressed in a background containing all or most of the other urease genes, with *ureD* also expressed at high levels in two cases (Fig. 1). First, the 1.68-kbp *SalI* fragment of pKAU17 (10) was blunt ended with Klenow fragment and ligated to phosphorylated *NdeI* linker (5'-ACCATATG-3'). The resulting product was digested with *NdeI* and *AvrII*, and the 670-bp fragment was ligated to the 5.7-kbp *NdeI-NheI* fragment of pET-11a (Novagen, Madison, WI), thus placing *ureF* under the control of the T7 promoter. This construct, pETF, was transformed into

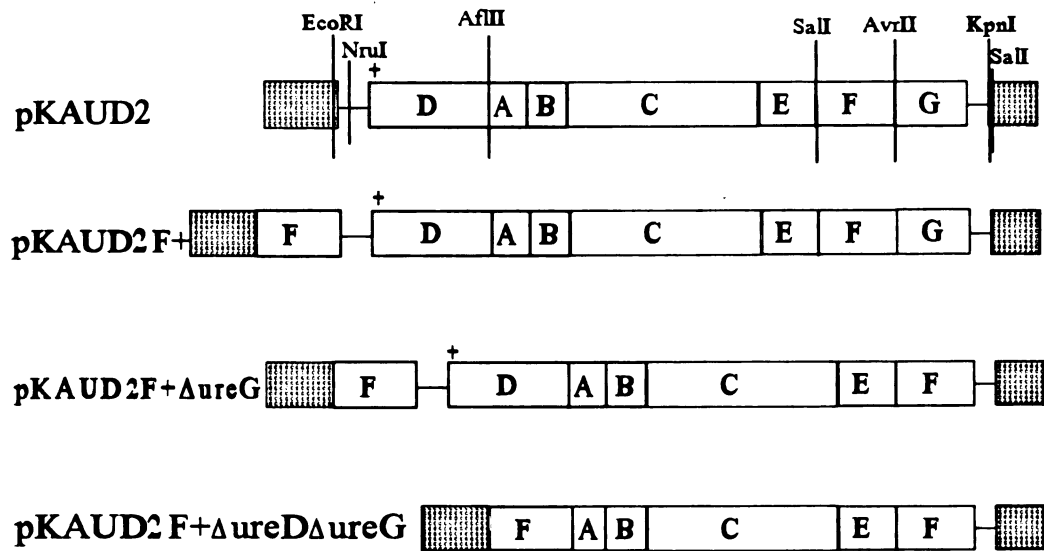


Figure 1. Schematic representations of several plasmids utilized in these studies. The pKAUD2 or pKAU17 map shows several restriction sites used for plasmid constructions as well as the gene arrangements in the plasmids. Transcription proceeds from left to right. Note that pKAUD2 (12) is identical to pKAU17 (10), except it is modified in the *ureD* ribosome-binding site region and initiation codon in order to overexpress *ureD* (shown as +). The pUC8 vector is indicated by (▨).

Escherichia coli BL21(DE3) (Novagen, Inc.). The 740-bp *Xba*I-*Bam*HI fragment of pETF was inserted into the blunt-ended *Eco*R1 site of pKAUD2 (12) to form pKAUD2F+. A *ureG* deletion derivative of this plasmid, pKAUD2F+ Δ *ureG*, was obtained by religation of the blunt-ended 8-kbp *Avr*II-*Kpn*I fragment. The double deletion mutant, pKAUD2F+ Δ *ureD Δ *ureG*, was constructed by digesting plasmid pKAUD2F+*ureG* with *Nru*I and *Afl*III, filling in the *Afl*III 5' overhang, and ligating the 7.1-kbp fragment ends. These plasmids were transformed into *E. coli* DH5 α .*

Culture conditions and cell disruption. *E. coli* DH5 α (pKAUD2F+) or its derivatives were grown at 30 or 37 °C to late stationary phase in Luria-Bertani (LB) broth supplemented with 100 μ g ampicillin per ml, harvested by centrifugation, and suspended in PEDG (18 mM potassium phosphate [pH 7.4], 0.09 mM EDTA, 0.09 mM dithiothreitol, 10% glycerol) buffer. Resuspended cells were disrupted by two to three passages through a French pressure cell at 18,000 lb/in² (1 lb/in² = 6.89 kPa), supplemented with 1 mM phenylmethylsulfonyl fluoride, and separated into extracts and pellet fractions by centrifugation at 100,000 x *g* for 45 min at 4 °C.

Purification of DF-Apo. Starting with *E. coli* DH5 α (pKAUD2F+*ureG*) cell extracts, the DF-Apo was purified by successive chromatography on DEAE-Sephadex, Mono Q, and Superose 6 resins. The sample was applied to a DEAE-Sephadex column (2.5 x 19 cm; Pharmacia Biotech, Piscataway, NJ) equilibrated in PEDG buffer, and proteins were eluted from the column by using a 400-ml linear salt gradient to 0.5 M KCl in

the same buffer. Fractions containing the DF-Apo were pooled, dialyzed against PEDG buffer, and applied to a Mono Q HR 10/10 (Pharmacia Biotech) column equilibrated with the same buffer. The proteins were eluted with a linear salt gradient to 1 M KCl in PEDG buffer. DF-Apo eluted from the column at 0.4-0.6 M KCl. Fractions containing the desired proteins were pooled, dialyzed against 18 mM phosphate [pH 7.4] buffer containing 0.09 mM EDTA, 0.09 mM dithiothreitol, and 0.1 M KCl. The protein pool was concentrated in a Centriprep-10 or -30 (Amicon, Beverly, MA) to 4 mls and chromatographed, via 2 runs, on a Superose 6 column (1.6 x 49 cm; Pharmacia Biotech) equilibrated in the same buffer.

Polyacrylamide gel electrophoresis. Sodium dodecyl sulfate (SDS)-polyacrylamide gel electrophoresis was carried out by using the buffers described by Laemmli (4) and included 4.5% and 13.5% polyacrylamide stacking and running gels. Nondenaturing gels used the same buffers without detergent and consisted of 3% and 6% polyacrylamide stacking and running gels. The gels were either stained with Coomassie brilliant blue or electroblotted onto nitrocellulose, probed with anti-*K. aerogenes* urease antibodies (10) or anti-*K. aerogenes* UreD antibodies (17), and visualized by using anti-rabbit immunoglobulin G-alkaline phosphatase conjugates (1). The band intensities of Coomassie-stained gels were determined with an AMBIS (San Diego, CA) gel scanner. For calculation of the ratios of UreD, UreF, and UreC, M_r values of 29,300, 27,000, and 60,300 were used.

Urease activity assays. Urease activity was measured by quantitating the rate of ammonia release from urea by formation of indophenol, which was monitored at 625 nm (19). One unit of urease activity was defined as the amount of enzyme required to hydrolyze 1 μ mole of urea per min at 37 °C. The standard assay buffer consisted of 25 mM HEPES (*N*-2-hydroxyethylpiperazine-*N'*-2-ethanesulfonic acid; pH 7.75), 0.5 mM EDTA, and 50 mM urea. Protein concentrations were determined by a commercial assay (Bio-Rad, Hercules, CA) with a bovine serum albumin standard.

Activation of urease apoproteins. Routine Apo, D-Apo, and DF-Apo activation buffer consisted of 100 mM HEPES (pH 8.3), 150 mM NaCl, 100 mM NaHCO₃, and 100 μ M NiCl₂ (15). For specific experiments, the conditions were modified by varying the bicarbonate or nickel ion concentrations, adding other metal ions to the activation buffer, or incubating samples in the presence of metal ions prior to addition of bicarbonate.

RESULTS AND DISCUSSION

Purification and characterization of UreD-UreF-urease apoprotein complexes.

E. coli DH5 α (pKAUD2F+ Δ ureG) synthesized high levels of the urease subunits, UreD, and UreF. When cells were grown in the absence of nickel ions these peptides were found to copurify during DEAE-Sepharose, Mono Q, and Superose 6 chromatographies as illustrated by denaturing polyacrylamide gel electrophoretic analysis of the resulting protein pools (Fig 2, lanes 2-5). On the basis of the staining intensities, the composition of the last pool was

calculated to be 0.86-0.89 UreD and 0.78-0.81 UreF per UreC. The broad elution profile from the gel permeation column suggested that multiple DF-Apo species were present. Results from nondenaturing polyacrylamide gel electrophoretic analyses were consistent with the presence of three DF-Apo complexes when proteins were visualized by probing with anti-urease immunoglobulin G (Fig. 3A, lane 3). The electrophoretic migration positions of these complexes corresponded to those described previously for the D-Apo complexes (12), as shown in Figure 3A, lane 2. Surprisingly, however, anti-UreD antibodies failed to detect cross-reactive material associated with the DF-Apo bands (Fig. 3B, lane 3), whereas the D-Apo species were detected (Fig. 3B, lane 2). (When the same fractions were analyzed by Western blot [immunoblot] analysis of a denaturing gel, UreD was clearly detected by these antibodies [data not shown]). After incubation with nickel ions in activation buffer, the three DF-Apo species collapsed to form a band that migrated at the position of urease and Apo (Fig. 3A, lane 4 and Fig. 3C), similar to the results reported for D-Apo (12). Addition of bicarbonate alone had no effect on the band migration. Two bands (labelled X in Fig. 3) that migrated more slowly than urease, but slightly faster than the 1 UreD-Apo species were detected by Coomassie staining of the activated DF-Apo species. These bands did not cross-react with anti-urease or anti-UreD antibodies. As observed previously in cell extracts from *E. coli* DH5(pKAU17) (13), a slowly migrating band (labelled Y in Fig. 3) cross-reacted with anti-urease and anti-UreD antibodies. Two-dimensional gels (data not shown) indicated that the predominant protein in this band is that observed just below UreC in Figure 2. N-terminal sequence analysis of this peptide revealed a sequence consistent with that of GroEL (XXKDVKF). Purified *E. coli* GroEL

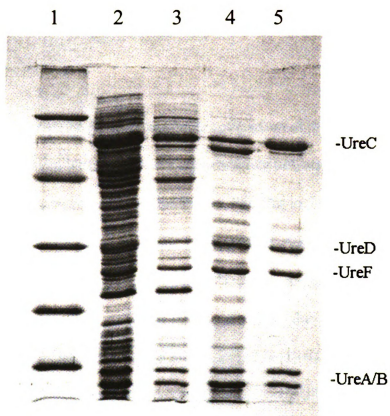
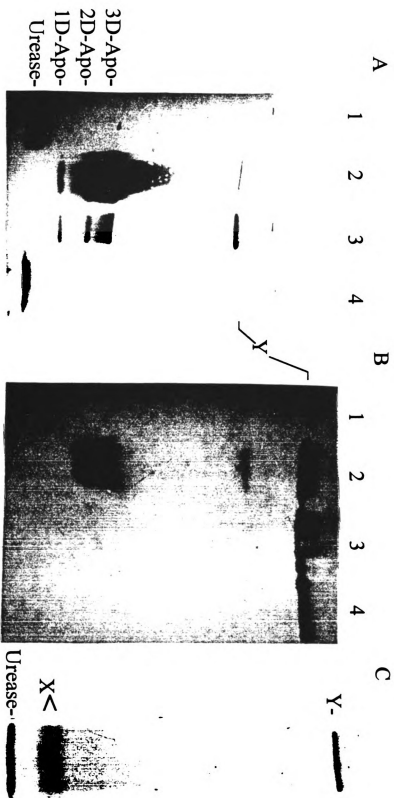


Figure 2. Partial purification of the DF-Apo as analyzed by SDS/polyacrylamide gel electrophoresis. Samples included: lane 1, molecular weight markers (phosphorylase *b*, M_r 97,400; bovine serum albumin, M_r 66,200; ovalbumin, M_r 45,000; carbonic anhydrase, M_r 31,000; soybean trypsin inhibitor, M_r 21,000; and lysozyme, M_r 14,400); lane 2, *E. coli* DH5 α (pKAUD2F+ $\Delta ureG$) cell extracts; lane 3, DEAE-Sepharose pool; lane 4, Mono Q pool; lane 5, Superose 6 pool.

FIG. 3. Native polyacrylamide gel electrophoretic comparison of the D-Apo and DF-Apo samples. **Panel A.** Western blot analysis of a nondenaturing polyacrylamide gel visualized with anti- *K. aerogenes* urease antibodies. Samples included: lane 1, 10 µg Apo; lane 2, 10 µg of D-Apo complexes; lane 3, 20 µg of DF-Apo; lane 4, 10 µg of DF-Apo complexes incubated in activation buffer at 37 °C for 90 minutes. **Panel B.** Western blot comparison using anti-UreD antibodies for samples as in panel A. **Panel C.** Coomassie-stained native gel with the same protein sample as shown in lane 4 of panel A. The migration positions for Apo and D-Apo containing 1, 2, and 3 UreD per trimeric urease [(UreA-UreB-UreC)₃] (12) are indicated. The band labelled Y contains GroEL that crossreacts with anti-urease and anti-UreD antibodies.



was found to electrophorese at positions corresponding to these bands on native and denaturing gels, and both antibodies were observed to cross-react with authentic GroEL. I conclude that GroEL is present at substoichiometric levels in our preparations of D-Apo and DF-Apo.

From the results described above, I conclude that the DF-Apo species represent the trimeric Apo [(UreA-UreB-UreC)₃] with 1, 2, or 3 each of UreD and UreF peptides bound. On the basis of Western blot analyses, I suggest that the UreF peptides mask the UreD peptides; i.e., anti-UreD antibodies fail to detect the UreD that is present in the DF-Apo although the peptide is recognized in D-Apo. Although DF-Apo and D-Apo complexes appear to migrate identically when examined by native gel electrophoresis, slight changes in size are detected when these samples are examined by gel permeation chromatography. It is likely that the DF-Apo complexes were unknowingly observed before. In prior studies that sought to examine the requirements for D-Apo formation, deletion mutants in *ureE*, *ureF*, or *ureG* were studied by immunological methods using *E. coli* cells containing the *K. aerogenes* urease gene cluster (13). Although the D-Apo complexes in $\Delta ureF$ mutant cells comigrated with complexes from control and $\Delta ureE$ or $\Delta ureG$ mutant cells during electrophoresis, the absence of UreF led to an apparent diminishment in gel chromatography size that was attributed to a conformational change induced by UreF. The present findings allow reinterpretation of the prior results: the control and $\Delta ureE$ or $\Delta ureG$ mutants actually formed DF-Apo and only the $\Delta ureF$ mutant cells formed D-Apo.

To examine whether UreD was needed for UreF to form a complex with the urease subunits, pKAUD2F+ $\Delta ureD\Delta ureG$ was constructed. Cells containing this plasmid were

disrupted, and extracts were chromatographed on DEAE-Sepharose and Mono Q columns. The urease subunits eluted from these resins as noncomplexed species and UreF appeared to be almost entirely insoluble. Furthermore, when *ureF* was expressed separately from the genes encoding the urease subunits, the gene product was exclusively located in the insoluble fraction (data not shown).

Activation properties of DF-Apo. When standard Apo activation conditions were used, the DF-Apo pool was activated to a specific activity value of 800 ± 100 U/mg of total protein (e.g., see closed triangles in Fig. 4 and Fig. 5A). This level of activation was very similar to that observed for D-Apo and about twice that obtained for Apo (14, 15). For comparison, native urease isolated from *K. aerogenes* possesses a specific activity of $\sim 2,500$ U/mg of protein (18). The rate of DF-Apo activation, however, was significantly slower than that observed with either of the other apoproteins when assessed under similar conditions. For example, 60-90 min was required for half-maximal activation of DF-Apo, compared with 15-20 min for the Apo and D-Apo species (14).

The nickel and bicarbonate concentration dependencies were significantly altered for the new species compared to the corresponding properties for Apo and D-Apo. As shown in Fig. 4, the nickel ion concentration exhibited a marked effect on the DF-Apo activation rate, with increasing rates observed to $500 \mu\text{M}$ and slight inhibition observed at 1 mM NiCl_2 . In contrast, the Apo and D-Apo species exhibit maximal activation rates at $\sim 60 \mu\text{M NiCl}_2$ and are inhibited by nickel ion concentrations above $300 \mu\text{M Ni}$ (14). For DF-Apo, half-maximal levels of activity were achieved at $\sim 5 \text{ mM}$ added bicarbonate when

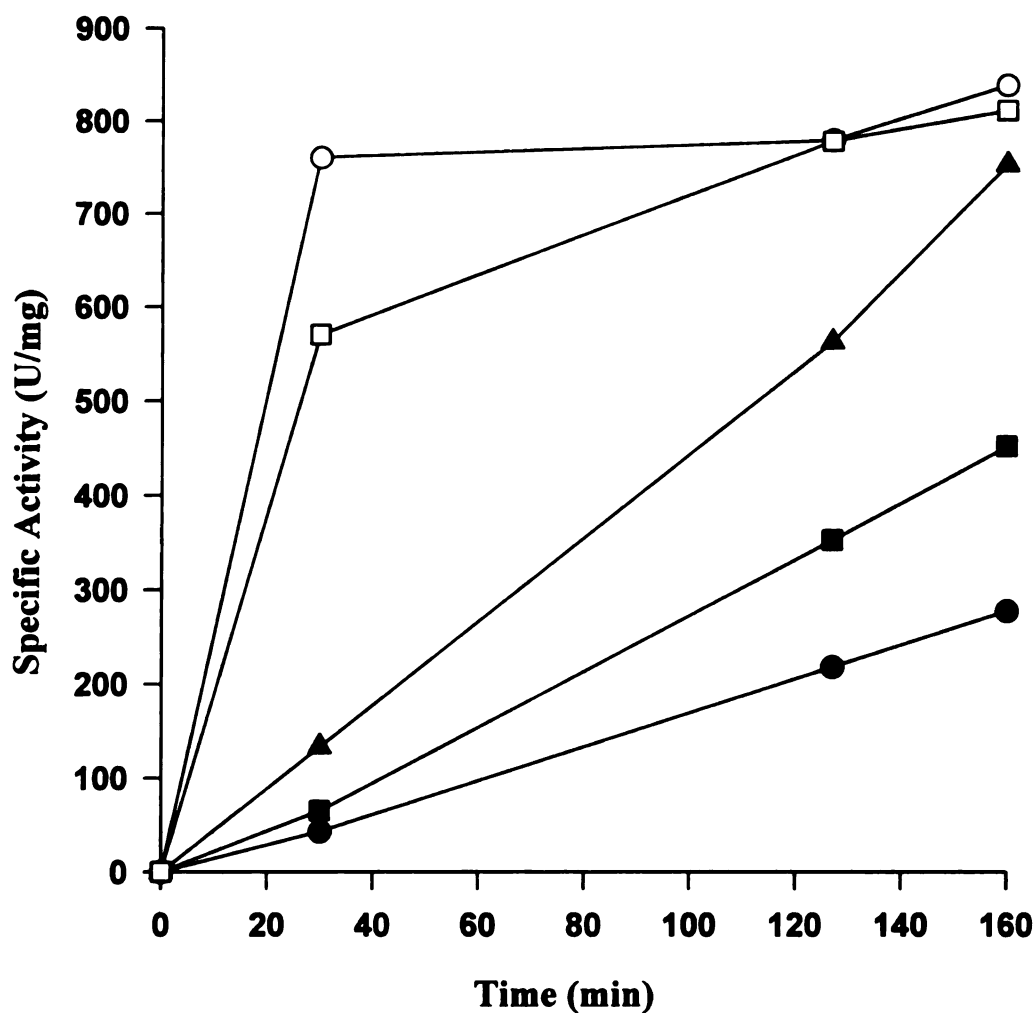


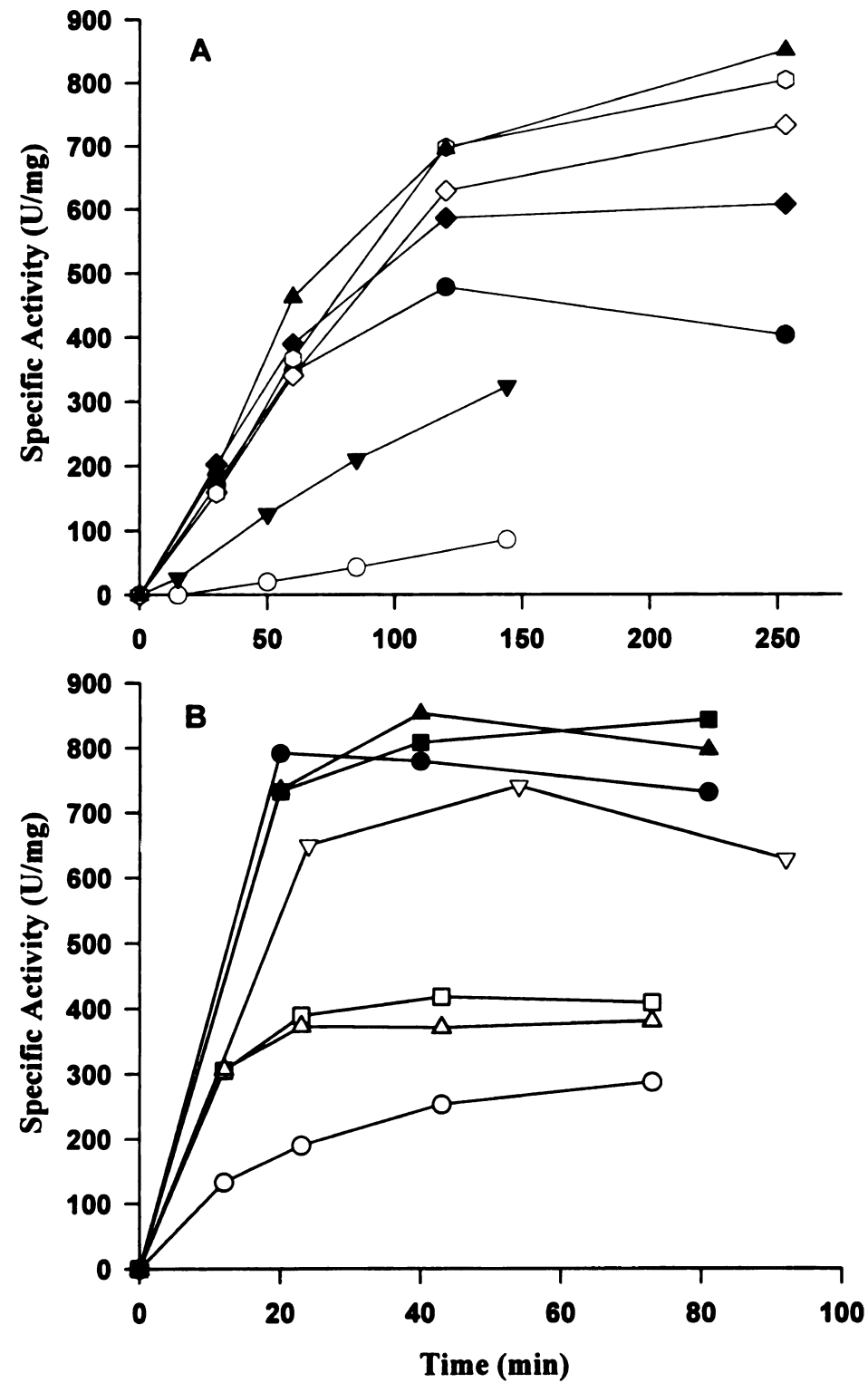
Figure 4. Nickel ion concentration dependence of activation for the DF-Apo. The purified sample (0.1 mg/ml) was incubated at 37 °C in 100 mM HEPES (pH 8.3) buffer containing 150 mM NaCl, 100 mM NaHCO₃ and 25 (●), 50(■), 100(▲), 500 (○), or 1000 (□) μM NiCl₂. Aliquots were removed at the indicated times and the samples were assayed for urease activity.

using 100 μM NiCl_2 (Fig. 5A) or at ~ 250 μM sodium bicarbonate when 500 μM NiCl_2 (Fig. 5B) was used. These results contrast those obtained with Apo and D-Apo species, which exhibit half-maximal activation in the presence of approximately 10 mM bicarbonate.

As another measure to compare activation properties of DF-Apo versus Apo and D-Apo species, the ability for various metal ions to inhibit the activation process was studied. Prior incubation of DF-Apo with nickel ions in the absence of added bicarbonate led to only a slight reduction in its ability to be activated (Fig. 6). Prior work demonstrated that these same conditions greatly reduced the activation competence of Apo and D-Apo (15). On the other hand, DF-Apo was almost completely inhibited by prior incubation with 100 μM zinc, cobalt, or copper ions (Fig. 6), similar to the behavior of Apo and D-Apo samples (15). As observed with the previously characterized species, inhibition of DF-Apo resulted when activation was carried out with buffers containing 100 or 500 μM NiCl_2 and varied concentrations of zinc ions (Fig. 7). For example, only about 50% of the urease in the pool was activated with 100 μM NiCl_2 in the presence of ~ 3.3 μM zinc ions. In the presence of 500 μM NiCl_2 , a slightly higher concentration of zinc ion (4.3 μM) was required to inhibit activation by 50%.

Function of UreF. The enhanced activation properties of DF-Apo over D-Apo and Apo (i.e., an increased resistance to nickel ion inhibition and a decreased bicarbonate concentration dependence) provide compelling evidence that this novel complex is biologically relevant. Although DF-Apo may not exist to any significant extent in the cell, it may occur as an intermediate to formation of the DFG-Apo species and it appears to

FIG. 5. Bicarbonate ion concentration dependence of activation for the DF-Apo. The sample (0.1 mg/ml) was incubated at 37 °C in 100 mM HEPES (pH 8.3) buffer containing 150 mM NaCl, 100 (upper panel) or 500 μ M (lower panel) NiCl₂, and the following concentrations of NaHCO₃: 0 (○), 0.1 (Δ), 0.25 (□), 1 (▽), 2 (▼), 5 (●), 10 (◆), 25 (◇), 50 (■), 75 (○), or 100 (▲) mM added NaHCO₃.



provide insight into the role of UreF. I propose that UreF modulates the activation process primarily by eliminating the binding of nickel ions to noncarbamylated protein. This change greatly facilitates formation of the carbamylated protein, which in turn results in a lowered bicarbonate requirement. As in the Apo and D-Apo species (15), however, the carbamylated DF-Apo protein is likely to bind nickel ions to yield two states, only one of which is active. Thus, *in vitro* activation of DF-Apo yields a final specific activity that falls far short of that observed (~2,500 U/mg) in fully active enzyme (18). The ratio of active to inactive nickel-containing carbamylated protein arising from DF-Apo is likely to be similar to that generated from D-Apo, based on their similar final specific activities of ~800 U/mg total protein. In addition to eliminating the interaction of nickel ions with noncarbamylated urease apoprotein, an added consequence of forming the DF-Apo is to reduce the overall activation rate by approximately fivefold. Additional studies are needed to elucidate how UreF acts to preclude nickel ion from binding to the noncarbamylated apoenzyme complex, and why zinc, cobalt, and copper ions do not appear to be similarly excluded. Furthermore, it will be important to purify the DFG-Apo species and characterize how its activation properties compare to those of Apo, D-Apo, and now DF-Apo.

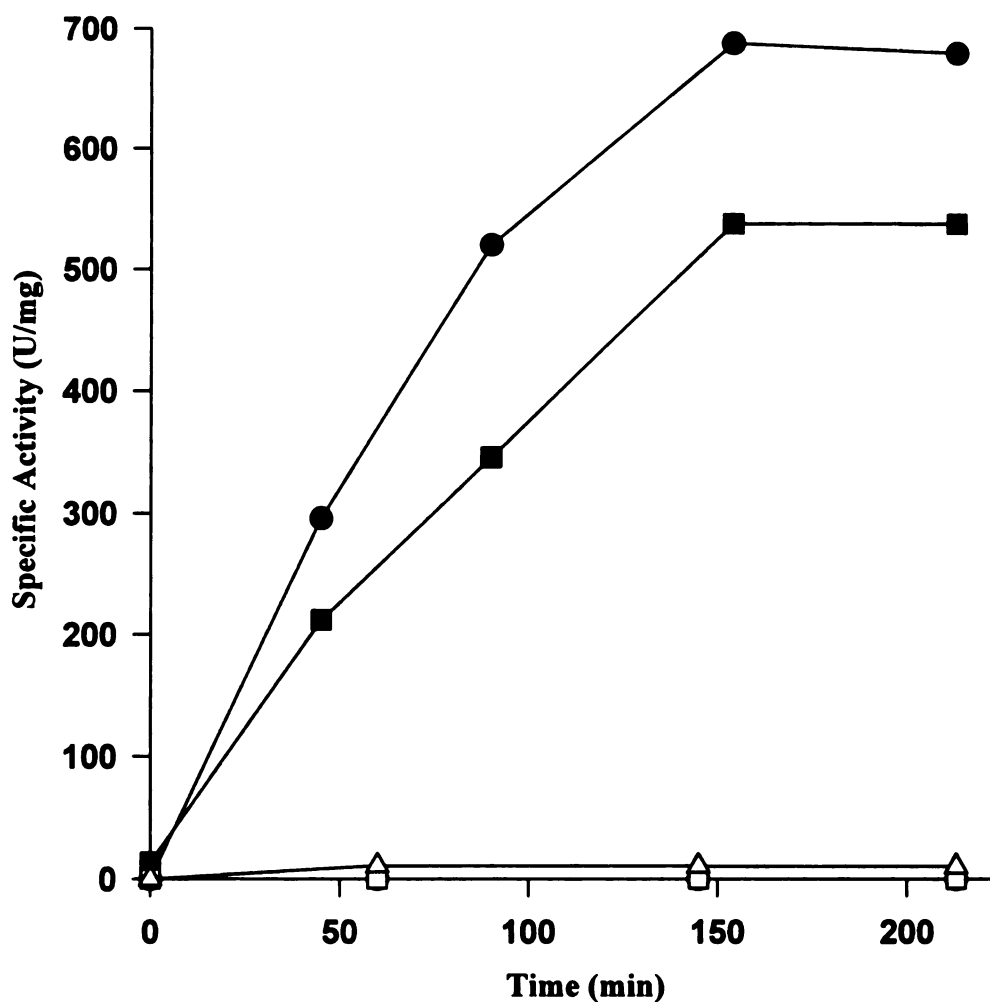


Figure 6. Effect of incubation of DF-Apo with metal ions prior to activation by NiCl₂ and bicarbonate. The sample (0.5 mg/ml) was incubated at 37 °C in buffer containing 100 mM HEPES (pH 8.3) and 150 mM NaCl with no metal (●) or with 100 μM NiCl₂ (■), ZnCl₂ (○), CoCl₂ (Δ), or CuCl₂ (□). After 80 minutes an aliquot of each mixture was activated in 100 mM HEPES (pH 8.3) buffer containing 150 mM NaCl, 100 μM NiCl₂, and 100 mM NaHCO₃, and samples were assayed for urease at the indicated timepoints.

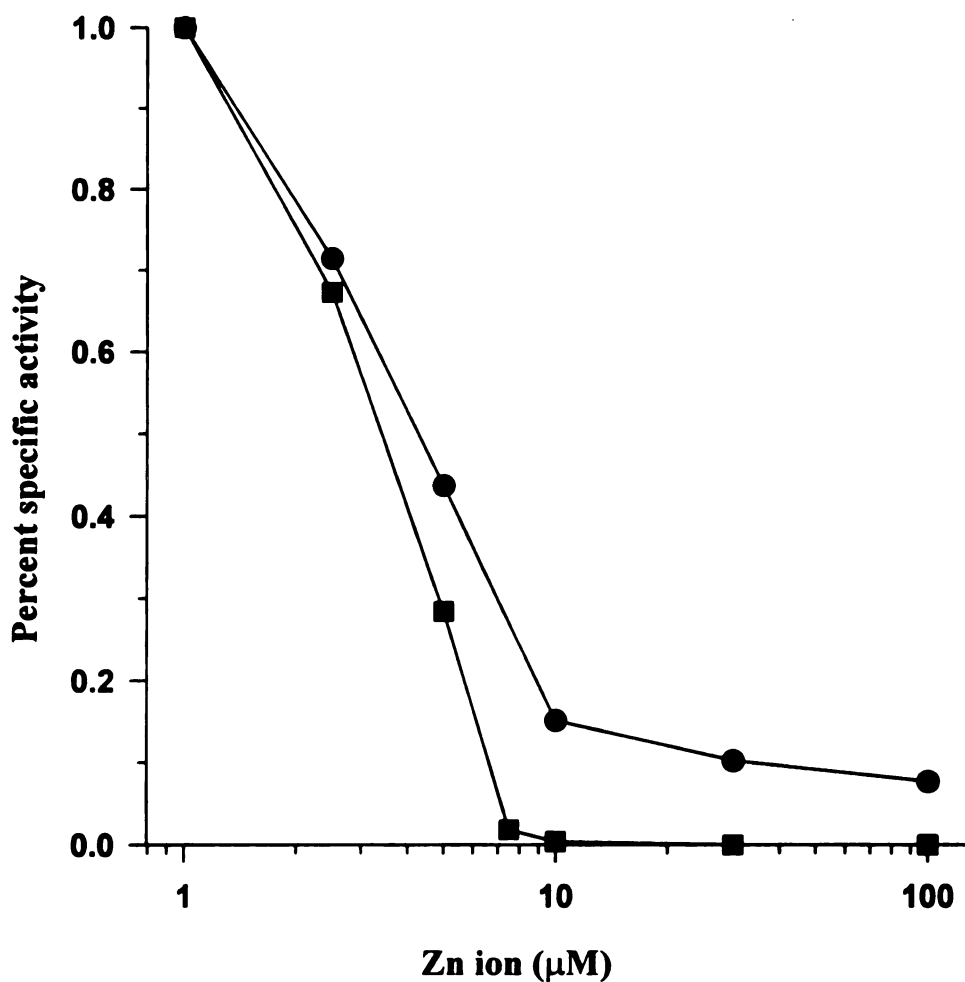


Figure 7. Effect of zinc ion concentration on DF-Apo activation. The sample (0.1 mg/ml) was incubated in activation buffer containing 100 (■) or 500 (●) μM NiCl₂ and the indicated concentrations ZnCl₂. The percent specific activity, based on a sample containing no zinc ions, was determined after 4 hours incubation.

REFERENCES

1. **Blake, M. S., Johnston, K. H., Russel-Jones, G. L. & Gotschlich, E. C. (1984).** A rapid, sensitive method for detection of alkaline phosphatase-conjugated anti-antibody on western blots. *Analytical Biochemistry* **136**, 175-179.
2. **Hausinger, R. P. (1993).** Urease. In *Biochemistry of Nickel*, pp. 23-57. New York: Plenum Publishing Corp.
3. **Jabri, E., Carr, M. B., Hausinger, R. P. & Karplus, P. A. (1995).** The crystal structure of urease from *Klebsiella aerogenes*. *Science* **268**, 998-1004.
4. **Laemmli, U. K. (1970).** Cleavage of structural proteins during the assembly of the head of bacteriophage T4. *Nature (London)* **227**, 680-685.
5. **Lee, M. H., Mulrooney, S. B., Renner, M. J., Markowicz, Y. & Hausinger, R. P. (1992).** Sequence of *ureD* and demonstration that four accessory genes (*ureD*, *ureE*, *ureF*, and *ureG*) are involved in nickel metallocenter biosynthesis. *Journal of Bacteriology* **174**, 4324-4330.
6. **Lee, M. H., Pankratz, H. S., Wang, S., Scott, R. A., Finnegan, M. G., Johnson, M. K., Ippolito, J. A., Christianson, D. W. & Hausinger, R. P. (1993).** Purification and characterization of *Klebsiella aerogenes* UreE protein: a nickel-binding protein that functions in urease metallocenter assembly. *Protein Science* **2**, 1042-1052.
7. **Mobley, H. L. T., Island, M. D. & Hausinger, R. P. (1995).** Molecular biology of microbial ureases. *Microbiological Reviews* **59**, 451-480.
8. **Moncrief, M. B. C. & Hausinger, R. P. (1996).** Nickel incorporation into urease. In *Mechanisms of Metallocenter Assembly*, pp. 151-171. Edited by R. P. Hausinger, G. L. Eichhorn & L. G. Marzilli. New York: VCH Publishers.
9. **Mulrooney, S. B. & Hausinger, R. P. (1990).** Sequence of the *Klebsiella aerogenes* urease genes and evidence for accessory proteins facilitating nickel incorporation. *Journal of Bacteriology* **172**, 5837-5843.
10. **Mulrooney, S. B., Pankratz, H. S. & Hausinger, R. P. (1989).** Regulation of gene expression and cellular localization of cloned *Klebsiella aerogenes* (*K. pneumoniae*) urease. *Journal of General Microbiology* **135**, 1769-1776.
11. **Park, I.-S. (1994).** Thesis. East Lansing, MI: Michigan State University.

12. **Park, I.-S., Carr, M. B. & Hausinger, R. P.** (1994). *In vitro* activation of urease apoprotein and role of UreD as a chaperone required for nickel metallocenter assembly. *Proceedings of the National Academy of Sciences* **91**, 3233-3237.
13. **Park, I.-S. & Hausinger, R. P.** (1995). Evidence for the presence of urease apoprotein complexes containing UreD, UreF, and UreG in cells that are competent for *in vivo* enzyme activation. *Journal of Bacteriology* **177**, 1947-1951.
14. **Park, I.-S. & Hausinger, R. P.** (1995). Requirement of carbon dioxide for *in vitro* assembly of the urease nickel metallocenter. *Science* **267**, 1156-1158.
15. **Park, I.-S. & Hausinger, R. P.** (1996). Metal ion interactions with urease and UreD-urease apoproteins. *Biochemistry* **35**, 5345-5352.
16. **Sambrook, J., Fritsch, E. F. & Maniatis, T.** (1989). *Molecular cloning: a laboratory manual*, 2nd edn. Cold Spring Harbor, NY: Cold Spring Harbor Laboratory.
17. **Taha, T. & Hausinger, R. P.** (1996). Unpublished observations.
18. **Todd, M. J. & Hausinger, R. P.** (1987). Purification and characterization of the nickel-containing multicomponent urease from *Klebsiella aerogenes*. *Journal of Biological Chemistry* **262**, 5963-5967.
19. **Weatherburn, M. W.** (1967). Phenol-hypochlorite reaction for determination of ammonia. *Analytical Chemistry* **39**, 971-974.

CHAPTER 5

CHARACTERIZATION OF UREG, IDENTIFICATION OF A URED-UREF-UREG COMPLEX, AND EVIDENCE THAT A FUNCTIONAL NUCLEOTIDE-BINDING SITE IS REQUIRED FOR *IN VIVO* METALLOCENTER ASSEMBLY OF UREASE

ABSTRACT

Previous studies have indicated that urease metallocenter assembly in *Klebsiella aerogenes* requires the presence of several accessory proteins (UreD, UreE, UreF, UreG) in addition to the urease structural subunits. UreG was isolated by using a novel purification procedure that included sequential ion exchange chromatographic steps that used phosphate buffers containing or lacking 20 percent glycerol. The protein was shown to be a monomer of $M_r = 21,814 \pm 20$ by using a combination of gel filtration chromatography and mass spectrometry. Although it contains a P-loop motif typically found in nucleotide-binding proteins, UreG did not bind or hydrolyze ATP or GTP and it exhibited no affinity for ATP- and GTP-linked agarose resins. Site-directed mutagenesis of *ureG* allowed the production of altered UreG proteins at the P-loop motif. Substitution of alanine at positions Lys-20 or Thr-21 resulted in the production of inactive urease in cells grown in the presence of nickel, indicating the importance of an intact P-loop for UreG function *in vivo*. These mutant cells were unable to synthesize the UreD-UreF-UreG-urease apoprotein complexes, thought to be the key activation complexes in the cell. A novel complex containing UreD, UreF, and UreG (termed DFG complex) was detected in cells carrying the urease gene cluster with deletions of *ureE* and the urease structural genes. The DFG complex was found to be in the insoluble fraction upon cell lysis, but was solubilized by addition of Triton X-100. Following DEAE-Sepharose chromatography and removal of detergent, the DFG complex bound to an ATP-linked agarose resin. In cells containing a UreG P-loop variant, the DFG complex was formed but it did not bind to the nucleotide-linked resin. These results

suggest that the UreG P-loop motif is essential for nucleotide binding in the DFG complex and that nucleotide hydrolysis may be required for *in vivo* metallocenter assembly.

INTRODUCTION

In vivo activation of *Klebsiella aerogenes* urease involves the participation of four accessory proteins: UreD, UreE, UreF, and UreG (1). Although the precise function of these proteins in urease nickel metallocenter assembly has not been established, UreE has been shown to be a nickel-binding protein (2), and a series of UreD-urease (D-Apo) (3), UreD-UreF-urease (DF-Apo) (4, Chapter 4), and UreD-UreF-UreG-urease (DFG-Apo) (5) apoprotein complexes have been identified. The auxiliary proteins within these complexes alter the activation properties of the urease apoprotein (Apo) and allow the cell to obtain fully active enzyme. Apo activation has been studied *in vitro* and shown to require the presence of carbon dioxide (6). Structural studies have demonstrated that the essential CO₂ is used to form a carbamylated lysine at the active site which functions as a bridging ligand to the requisite nickel ions (7).

Of the four urease accessory proteins, UreG is the most highly conserved (Chapter 1, see section II.F) and the only one of this group that exhibits clear sequence homology to other proteins. For example, UreG contains a P-loop motif that is typically found in ATP- and GTP-binding proteins (8) where it functions in nucleotide binding. The presence of this putative nucleotide-binding site in UreG might be related to the *in vivo* energy requirement for urease activation (9). Besides the limited similarity to the P-loop motif in various proteins, the entire UreG protein from *K. aerogenes* is approximately 25% identical to the sequence of the *Escherichia coli* *hypB* gene product (10). This gene is part of the *hydrogenase pleiotropic operon* required for activation of the three nickel-containing

hydrogenases found in *E. coli*. HypB plays a role in nickel-ion processing based on the demonstration that mutations in *hypB* can be complemented by addition of high levels of nickel ion to the growth medium (11). *E. coli* HypB has been purified and found to bind and hydrolyze GTP (12). These findings raise the possibilities that UreG may bind nucleotides and catalyze nucleotide hydrolysis as part of its role in facilitating urease metallocenter assembly.

Here, I describe the purification and characterization of UreG and I provide evidence from site-directed mutagenesis studies that the P-loop motif is needed for UreG to function *in vivo* in metallocenter assembly. In addition, I demonstrate the presence of a complex (termed DFG) containing UreD, UreF, and UreG. Partially purified DFG complex is shown to bind to a nucleotide-linked resin, whereas DFG complex obtained from a P-loop variant lacks the ability to bind to this resin. These studies highlight the importance of the P-loop motif within UreG and identify a novel complex of the urease accessory proteins.

MATERIALS AND METHODS

Bacterial strains and plasmid construction. All molecular biology methods followed the general methods outlined in Sambrook *et al.* (13). All plasmids were transformed into *E. coli* DH5 α .

To test the necessity for the P-loop motif in UreG, two mutants were created in which Lys-20 was changed to Ala (K20A) or Thr-21 was changed to Ala (T21A). A 1.5-kb *SalI-KpnI* fragment of pKAU17 (14) was subcloned into M13mp18 and mutagenized

by the method of Kunkel *et al.* (15). Uracil-containing single-stranded template DNA was prepared from *E. coli* CJ236 [*dut1 ung1 thi-1 relA1/pCJ105(cam^rF')*]. By using oligonucleotide primers 5'-TCGGCTCCGGTGCAACCGCTCTGC-3' or 5'-GCTCCGGTAAAGCCGCTCTGCTG-3' (the underlined bases represent changes from the wild-type sequence), the phage DNA was mutagenized and the mutant phage were isolated in *E. coli* MV1193 (Δ [*lac-proAB*] *rpsL thi endA spcB15 hsdR4 Δ [*srl-recA*]306::*Tn10[te^r]* F' [*traD36 proAB⁺ lacI^q lacZ* Δ M15]). Mutants were identified by sequence analysis using Sequenase 2.0 (United States Biochemical) and the single-strand DNA sequence method of Sanger *et al.* (16). The 840-bp *AvrII-KpnI* fragment was subcloned back into pKAU17 to generate pKAU17K20A or pKAU17T21A and the sequence was confirmed by double-strand DNA sequencing methods. The 2.4-kb *BamHI-KpnI* fragments of pKAU17K20A and pKAU17T21A were also subcloned into the 5.7-kb *BamHI-KpnI* fragment of pKAUD2, containing a mutated *ureD* promoter region to allow overexpression of this gene (3), to generate pKAUD2K20A or pKAUD2T21A.*

Plasmids were also constructed with *ureG* or a mutated *ureG* gene for study of the DFG complex. The construct pKAUD2F+ Δ *ureA* Δ *ureB* Δ *ureC* Δ *ureE* containing only *ureD*, *ureF*, and *ureG* was created by taking the 5.4-kb *AflIII-BlnI* fragment of pKAUD2F+ (17), blunt-ending with Klenow fragment, and religating the ends. The pKAUD2F+T21A Δ *ureA* Δ *ureB* Δ *ureC* Δ *ureE* plasmid was constructed by ligating a blunt-ended 8.2-kb *EcoRI* fragment of pKAUD2T21A to a blunt-ended 740-bp *XbaI-BamHI* pETF fragment (4) containing the overexpressed *ureF* gene. This plasmid,

pKAUD2F+T21A, was digested with *Afl*III and *Bln*I, the 5.4-kb fragment was blunt ended with Klenow, and the ends were ligated together. For routine purification of UreG, I made use of plasmid pKAUG-1 containing only *ureG* (17). This plasmid was constructed by isolating the 4.1 kb *Ksp*I-*Eco*R1 from pKAUD2 (3), blunt-ending with Klenow, and ligating the ends together.

Culture Conditions. All cultures were grown at either 30 °C or 37 °C to late stationary phase in 3 liters of Luria-Bertani (LB) broth supplemented with 100 µg ampicillin per ml. *E. coli* DH5 cells containing plasmids pKAUG-1, pKAU17K20A, pKAU17T21A, pKAUD2K20A, or pKAUD2T21A were harvested by centrifugation and resuspended in 30 mls PEB (20 mM phosphate [pH 7.4], 1 mM EDTA, 1 mM 2-mercaptoethanol) buffer. *E. coli* DH5 cells containing plasmids pKAUD2F+ Δ *ureA* Δ *ureB* Δ *ureC* Δ *ureE* or pKAUD2F+T21A Δ *ureA* Δ *ureB* Δ *ureC* Δ *ureE* were harvested by centrifugation and resuspended in 30 mls of HMDG (25 mM HEPES [pH 7.4], 5 mM MgCl₂, 0.5 mM dithiothreitol, 10 percent glycerol) buffer.

Purification of UreG. *E. coli* DH5 α cells carrying plasmid pKAUG-1 were resuspended in PEB buffer, supplemented with 1 mM phenylmethylsulfonyl fluoride, and disrupted by passage through a French pressure cell (American Instrument Co., Silver Spring, MD) at 18,000 lb/in² (1 lb/in² = 6.89 kPa). Cell extracts, obtained after centrifugation at 100,000 x g for 45 minutes at 4 °C, were applied to a DEAE-Sepharose column (2.5 x 19 cm;

Pharmacia Biotech, Piscataway, NJ) that had been equilibrated with PEB, and proteins were eluted by using a 400-ml linear salt gradient to 0.5 M KCl in the same buffer. Fractions containing UreG (eluting at approximately 0.1-0.2 M KCl) were pooled, dialyzed against PEB buffer containing 20 % glycerol, and applied to a Mono Q HR 10/10 (Pharmacia Biotech) column equilibrated with the same buffer containing 20% glycerol. Flow-through fractions containing UreG were pooled, dialyzed against PEB buffer to remove the glycerol, and applied to the re-equilibrated Mono Q column in PEB buffer. A linear salt gradient to a concentration of 1 M KCl in PEB was used to elute UreG at approximately 0.1-0.4 M KCl. Samples containing UreG were pooled, concentrated, dialyzed against 25 mM HEPES buffer (pH 7.4) containing 1 mM EDTA, 1 mM 2-mercaptoethanol, and 0.1 M KCl, and subjected to Superose 12 chromatography in this same eluent. For subunit molecular weight determination, matrix-assisted laser desorption ionization time-of-flight mass spectrometry was used. A 0.6 μ g sample of purified UreG was loaded onto Zetabind nylon membrane, dried, washed with water, and mixed with one μ l of sinapinic acid (18). The sample was run on a Vestec LaserTec Research time-of-flight mass spectrometer (Vestec, Houston, TX) equipped with a nitrogen laser (model VSL-337ND, Laser Science, Newton, MA).

Partial purification of the DFG complex. Three liters of cells of *E. coli* DH5 α carrying plasmids pKAUD2F+ Δ ureA Δ ureB Δ ureC Δ ureE or pKAUD2F+T21A Δ ureA Δ ureB Δ ureC- Δ ureE were resuspended in HMDG buffer, supplemented with 1 mM phenylmethylsulfonyl fluoride, and disrupted by passage through a French pressure cell at 18,000

lb/in². The sample was centrifuged at 27,000 x g for 45 minutes at 4 °C and the supernatant was removed. The pellet was washed with 20 ml of HMDG buffer, recentrifuged as stated above, and the supernatant was removed. The pellet was suspended in 20 ml HMDG buffer containing 0.5% (w/v) Triton X-100 or Tween 20 and incubated at 4 °C for 17 h. After centrifugation at 27,000 x g for 45 min, the supernatant fraction containing the DFG complex was removed. The solubilized protein sample was applied to a DEAE-Sepharose column (2.5 x 19 cm) that had been equilibrated with HMDG buffer containing detergent, and the proteins were eluted by using a 400-ml linear salt gradient to 0.5 M KCl in the same buffer. Fractions containing DFG were pooled, dialyzed against HMDG buffer with 0.5% detergent, and added to a column of Extracti-Gel D Detergent Removing Gel (1.7 x 7 cm; Pierce, Rockford, IL). The flow-through fractions containing DFG complex were pooled and added to ribose hydroxyl-linked GDP-, ribose hydroxyl-linked GTP-, or N-6-linked ATP-agarose resins (Sigma Chemical, St. Louis, MO) that had been equilibrated in HMDG buffer. Columns were washed with HMDG buffer and proteins were eluted with 10 mM ATP or 1 M KCl in HMDG buffer.

Preparation of polyclonal antibodies against UreG. Antibodies were generated in a white, female, New Zealand rabbit by injecting 200 µl (2.5 mg/ml) of purified native UreG in phosphate-buffered saline that was emulsified with the same volume of TiterMax adjuvant (Vaxcel, Norcross, GA). The rabbit was boosted after 23 days, and after 97 days the immunoglobulin G fraction was purified from the serum using the E-Z-Sep kit

(Pharmacia Biotech). Antibodies were titrated by using standard dot blot (19) and immunoblotting techniques (20).

Polyacrylamide gel electrophoresis. Sodium dodecyl sulfate (SDS)-polyacrylamide gel electrophoresis was carried out by using the buffers of Laemmli (21) and included 4.5% and 12.5% polyacrylamide stacking and running gels. Nondenaturing gels used the same buffers without SDS and consisted of 3% and 6% polyacrylamide stacking and running gels. Denaturing gels were stained with Coomassie brilliant blue, while nondenaturing gels were electroblotted onto nitrocellulose, probed with either polyclonal anti-*K. aerogenes* urease antibodies (14) or anti-*K. aerogenes* UreG antibodies, and visualized using goat anti-rabbit immunoglobulin G-alkaline phosphatase conjugates (Sigma Chemical, St. Louis, MO). When testing for the presence of biotin, blots were probed and detected with ExtrAvidin-alkaline phosphatase (Sigma Chemical). Cytochrome c-biotin labeled protein (Sigma Chemical) was used as a positive control. The band intensities of Coomassie-stained gels were determined with an AMBIS (San Diego, CA) gel scanner. For calculation of the ratios of UreD, UreF, and UreG, M_r values of 29,300, 27,000, and 21,800 were used.

Urease activity assays. Urease activity was measured by quantitating the rate of ammonia release from urea by formation of indophenol, which was monitored at 625 nm (22). One unit of urease activity was defined as the amount of enzyme required to

hydrolyze 1 μ mole of urea per minute at 37 °C. The standard assay buffer consisted of 25 mM HEPES (pH 7.75), 0.5 mM EDTA, and 50 mM urea. Protein concentrations were determined by a commercial assay (Bio-Rad, Hercules, CA) with bovine serum albumin standard.

Equilibrium dialysis determination of nucleotide binding. Nucleotide binding was determined by equilibrium dialysis using 50 mM sodium phosphate (pH 7.2) buffer containing 1 mM $MgCl_2$, 0.5% NaCl, and the desired nucleotide or 50 mM Tris (pH 7.5), 100 mM NaCl, 5 mM $MgCl_2$, 0.09 mM dithiothreitol, and 0.09 mM EDTA and the desired nucleotide. [^{14}C]ATP (44 mCi/mmol; ICN Pharmaceuticals, Costa Mesa, CA) or [^{14}C]GTP (13.5 Ci/mmol; ICN Pharmaceuticals) was diluted with various concentrations of unlabeled ATP or GTP, respectively. The protein concentration was 2 μ M or 6 μ M. Free ligand equilibrium was attained in an equilibrium dialyzer (Hoeffer Scientific, San Francisco, CA) using Spectrapor 2 dialysis membranes at 4 °C for approximately 14 hours. Samples of 100 μ l were removed from each compartment and radioactivity was measured in a liquid scintillation counter.

Chromatographic measurement of nucleotide hydrolysis. The rates of hydrolysis of ATP and GTP were analyzed by using a C_{18} reverse-phase HR 5/5 column (Pharmacia Biotech) equilibrated with buffer containing 19% acetonitrile, 30 mM potassium phosphate, and 10 mM tetrabutylammonium phosphate (pH 2.65) (23) or analyzed by a

Mono Q HR 10/10 column equilibrated with 20 mM phosphate (pH 7.3). For reverse-phase chromatography, 0.033 μ M of UreG, 0.6 mM ATP, and 10 mM MgCl_2 in 0.1 M potassium phosphate buffer (pH 7.3) were incubated at room temperature for 1-13 hours. Reactions were quenched with two volumes of column equilibration buffer and 1/10 of the sample was chromatographed. GTP hydrolysis was measured using Mono Q chromatography. [^3H]GTP was diluted with unlabeled GTP to a final concentration of 5 μ M and incubated at room temperature with 1.2 μ M of UreG, 10 mM MgCl_2 , and 50 mM Tris (pH 8.0). At various time intervals, samples were removed and chromatographed on the Mono Q column. Radioactivity in the resulting fractions was detected using a liquid scintillation counter.

Carbonic anhydrase assay. Carbonic anhydrase activity was tested by monitoring the hydrolysis of *p*-nitrophenyl acetate at 400 nm and 25 °C (24).

RESULTS

UreG purification and characterization. UreG was purified from *E. coli* cells containing pKAUG-1 by using a combination of DEAE-Sepharose, Mono Q, and Superose 12 chromatographies (Fig. 1). From a one liter culture about 10-15 mg of UreG was recovered. A novel step in the purification process involved sequential Mono Q chromatography of the sample in the presence and then absence of 20% glycerol in phosphate buffer. UreG exhibited little affinity for the Mono Q column in the presence of

glycerol (Fig. 1, lane 4), but bound tightly to the resin when the glycerol was removed by dialysis. This behavior was only observed when using phosphate buffers (i.e., the protein was retained by the column in HEPES buffer containing 20% glycerol). UreG also tended to smear when chromatographed on the Mono Q column in the absence of glycerol. For most applications, the protein was essentially homogenous after the second Mono Q chromatography step (Fig. 1, lane 5); however, a Superose 12 column was added as an additional purification step to prepare the sample for use in antibody production. The estimated size of native UreG based on the gel filtration chromatography results was approximately 19.1 kDa. A more precise size estimate of UreG was determined by using matrix-assisted laser desorption ionization time-of-flight electrospray-mass spectrometry. UreG was shown to possess an M_r of $21,814 \pm 20$ which agrees well with the expected size ($M_r = 21,812$) for protein lacking the N-terminal methionine based on the translated DNA sequence (25).

To begin to characterize the function of UreG, I examined the properties of the purified protein: its ability to bind or hydrolyze nucleotides, its carbonic anhydrase activity, and its biotin content. The presence of the P-loop motif in the UreG sequence is consistent with a role in nucleotide binding; however, no detectable ATP- or GTP-binding was observed using equilibrium dialysis methods, and no nucleotide hydrolysis was detected using two chromatographic procedures. Since high levels of CO_2 are known to be required for carbamylation of Lys-217 in the urease apoprotein (6) in order to form the binuclear active site (7), I tested whether UreG possessed carbonic anhydrase activity (to provide CO_2 from bicarbonate) or whether it contained a cofactor that could function

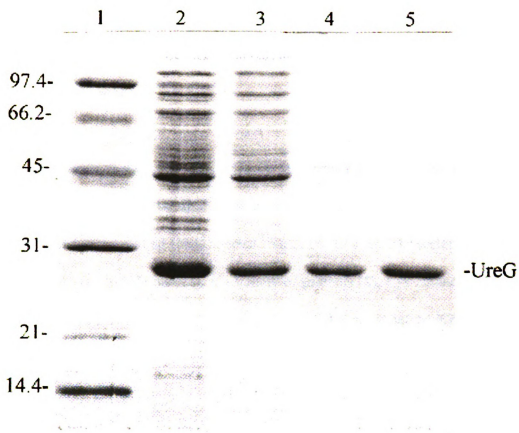


Figure 1. Purification of UreG as monitored by SDS/polyacrylamide gel electrophoresis. Samples included: lane 1, molecular weight markers (phosphorylase *b*, M_r 97,400; bovine serum albumin, M_r 66,200; ovalbumin, M_r 45,000; carbonic anhydrase, M_r 31,000; soybean trypsin inhibitor, M_r 21,000; and lysozyme, M_r 14,400); lane 2, *E. coli*(pKAUG-1) cell extracts; lane 3, DEAE-Sepharose pool; lane 4, first Mono Q pool using buffer containing glycerol; lane 5, second Mono Q pool using glycerol-free buffer.

to deliver CO₂. No carbonic anhydrase activity was detected, and UreG did not contain biotin when analyzed by Western blot (immunoblot) analysis using avidin-linked alkaline phosphatase (data not shown). The latter result was consistent with mass spectrometric size analyses (see above).

Site-directed mutagenesis of UreG. To further assess the importance of the highly conserved P-loop motif in UreG, I used site-directed mutagenesis methods to prepare constructs that formed altered UreG species. Since the Lys and Thr residues in the motif are essential for nucleotide binding in a variety of proteins (8), Lys-20 and Thr-21 of the UreG P-loop motif were changed independently to Ala to generate K20A and T21A forms of this protein. The two mutated genes were subcloned back into pKAU17 and pKAUD2. The UreG P-loop variants did not affect formation of the D-Apo or DF-Apo complexes, but they prevented formation of DFG-Apo when *E. coli* cells containing pKAUD2K20A or pKAUD2T21A were grown in the absence of nickel (Fig. 2). Moreover, the P-loop specific alterations to pKAU17 and pKAUD2 resulted in the complete loss of urease activity when cells were grown in LB containing nickel (data not shown).

Partial purification and characterization of the DFG complex. Since direct purification and characterization of the DFG-Apo complexes (thought to be the key activation complexes in the cell) remain an intractable problem, I examined the feasibility

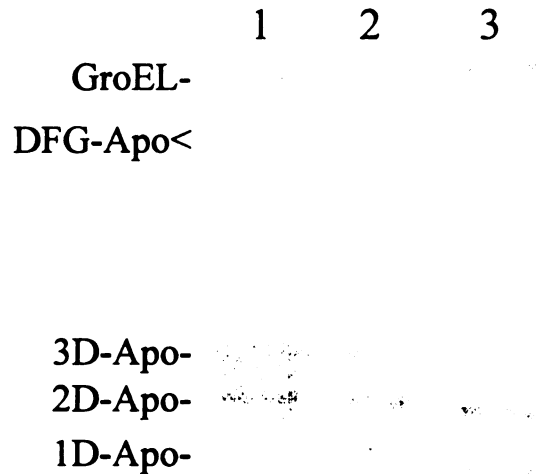


Figure 2. Effects of alterations to the UreG P-loop on formation of urease apoprotein complexes. Cell extracts were analyzed on a nondenaturing polyacrylamide gel and probed with anti-*K. aerogenes* urease antibodies. Lanes: 1, 40 μ g of cell extracts from *E. coli*(pKAUD2); 2, 40 μ g of cell extracts from *E. coli*(pKAUD2K20A); 3, 40 μ g of cell extracts from *E. coli*(pKAUDT21A). The positions of the co-migrating D-Apo and DF-Apo complexes (containing one, two, or three UreD or UreD and UreF molecules per urease apoprotein trimer; 3, 4) and the DFG-Apo complexes (5) are indicated. The anti-urease antibodies cross-react with GroEL that is present in these extracts (4).

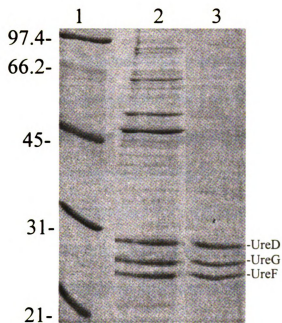


Figure 3. Analysis of the UreD-UreF-UreG complex bound to an ATP-linked agarose resin as analyzed by SDS/polyacrylamide gel electrophoresis. Samples included: lane 1, molecular weight markers; lane 2, Extracti-Gel DFG pool; lane 3, sample eluted from ATP-linked agarose resin by 1 M KCl in HMDG buffer.

of first characterizing the heterotrimeric accessory protein complex. The DFG complex was partially purified from *E. coli* cells containing pKAUD2F+ $\Delta ureA\Delta ureB\Delta ureC\Delta ureE$ using detergent solubilization, DEAE-Sepharose, and Extracti-Gel D chromatography. Based on staining intensities, the DFG complex consisted of 0.847-0.848 UreD and 0.818-0.819 UreF per UreG. The resulting DFG pool was added to various nucleotide-linked agarose resins to test for nucleotide-binding capabilities. The DFG complex did not bind to GDP- or GTP-linked agarose resins, but a variable portion of it was bound to an ATP-linked agarose column. The bound complex eluted from the column upon addition of HMDG buffer containing 1 M KCl (Fig. 3) or 10 mM ATP (data not shown). If samples were not first chromatographed on a DEAE-Sepharose column, the DFG complex did not bind to the ATP-linked agarose resin consistent with the removal of a competing ligand during ion-exchange chromatography. Interaction with the nucleotide-resin also required the removal of detergent. The detergent-free complex was rather unstable and UreD precipitated out of solution in less than one week.

E. coli cells containing pKAUD2F+T21A $\Delta ureA\Delta ureB\Delta ureC\Delta ureE$ were examined to determine whether the DFG complex was able to form and to determine whether it had similar properties when the UreG was altered at the P-loop motif. The cells were cultured and proteins were purified as described above. In cells containing the UreG P-loop variant, the DFG complex was formed (data not shown); however, the complex did not bind to the ATP-linked agarose resin as observed with the wild-type DFG (data not shown).

DISCUSSION

UreG purification and partial characterization. The *ureG* gene is expressed at high levels in *K. aerogenes*. Since this protein is required for functional nickel insertion into the urease active site and contains a sequence suggestive of function (i.e., a P-loop motif) its purification and characterization was a logical step in examining metallocenter assembly. UreG was purified by using a novel purification procedure in which addition and then removal of 20 percent glycerol from a phosphate buffer resulted in greatly altered ion-exchange chromatographic properties of the protein. It is unclear how glycerol affects the chromatographic behavior of UreG; however, this type of result is not unprecedented. For example, the presence of solvent-excluding reagents like polyethylene glycol was found to affect the self-association of Rubisco activase so that the molecular mass was two- to four-fold higher in the presence of this reagent, and the enzyme exhibited higher ATPase and Rubisco activating properties in addition to possessing increased affinity for ATP and Rubisco (26). The structural changes in UreG appear to depend on the additional presence of phosphate, perhaps due to phosphate binding at the UreG P-loop motif. Note, however, that when purified UreG was subjected to gel filtration chromatography in the presence of 20% glycerol and 20 mM phosphate, UreG was still present as a monomer. Several different types of columns were examined for their abilities to purify UreG. Despite possessing a P-loop motif, UreG did not bind to ATP- or GTP-linked agarose resins. Similarly, an Affi-Gel blue gel (BioRad) column which has been found to bind several nucleotide-requiring proteins did not bind

the protein. Although DEAE-Sepharose and Mono Q ion exchange resins were successfully used for UreG isolation, the protein tended to smear when chromatographed on anionic exchangers.

Further characterization of purified UreG focused on its possible involvement in providing CO₂ for carbamylation of Lys-217, which then serves as a nickel ligand. Specifically, I tested UreG for the presence of biotin and carbonic anhydrase activity. Neither biotin, a carrier of CO₂ (reviewed in 27), nor carbonic anhydrase activity was associated with purified UreG from *E. coli* cells containing pKAUG-1. One caveat to note is that the UreG tested in these experiments was produced independently of the other urease structural and accessory proteins. Possibly one or more of the additional accessory proteins, such as UreF, must be co-produced in growing cells in order to supply or link biotin to UreG or to result in generation of carbonic anhydrase activity associated with this protein.

The requirement of the P-loop motif for UreG function. Although UreG contains a P-loop motif, which is commonly found in nucleotide-binding proteins (8), I was unable to detect nucleotide binding to or hydrolysis by this protein. This result contrasts with the situation found in the *E. coli* HypB protein (10), to which UreG exhibits 25 percent identity. *E. coli* HypB binds and hydrolyzes GTP, likely related to its suggested role in nickel ion processing (11). It should be noted that HypB from *Rhizobium leguminosarum* does not bind or hydrolyze GTP or ATP (28), even though its proposed nucleotide binding domain is absolutely conserved. In the cases of the *R. leguminosarum* HypB and

the *K. aerogenes* UreG, it is possible that additional accessory proteins must be present for nucleotide binding and hydrolysis to be observed. An appealing model is that the UreG P-loop motif is involved in the observed *in vivo* energy requirement for urease activation.

To further assess the importance of UreG P-loop motif, site-directed mutagenesis was performed to replace either of two conserved residues (Lys-20 and Thr-21), acting to bind the Mg-nucleotide complex, by Ala. *E. coli* cells containing the urease gene cluster with these mutations and grown in the presence of nickel lacked urease activity. The cell extracts were activated *in vitro*, presumably from D-Apo or DF-Apo complexes which are unaffected in the UreG P-loop variants. Using immunoblot analysis, I demonstrated that DFG-Apo complexes were not present at detectable levels in soluble extracts of the P-loop variants. In summary, these data indicate that a functional P-loop motif in UreG is essential for *in vivo* incorporation of nickel into the urease active site and may be important for DFG-Apo formation or stability.

The DFG complex. A complex containing 1 UreD and UreF, per UreG protein was detected in *E. coli* cells carrying the urease gene cluster with deletions in the urease subunits and *ureE* genes. This complex was observed in the insoluble fraction upon cell lysis and centrifugation, but was solubilized upon addition of detergent to this protein pool. Following DEAE-Sepharose and Extracti-Gel D chromatographies, DFG was shown to bind to an ATP-linked agarose resin. A P-loop variant in UreG did not affect formation of the DFG complex, indicating that nucleotide binding is not required for

UreD, UreF, and UreG association. The complex did not, however, bind to the ATP-linked agarose resin. This data supports the idea that a functional UreG P-loop is essential for nucleotide-binding of the DFG complex, but is not essential for its formation.

Although the DFG complex was observed under highly artificial conditions and I have not demonstrated the presence of such a species in cells containing the wild-type urease gene cluster, these studies may provide significant clues related to the *in vivo* urease metallocenter assembly mechanism. For example, DFG-Apo, the urease apoprotein complex that has been proposed to be the key species needed for *in vivo* activation (5), could be formed by the association of urease apoprotein with the DFG complex, rather than by a stepwise assembly of Apo to D-Apo (3), to DF-Apo (4), to DFG-Apo (5) species. The evidence that DFG complex binds nucleotides via its P-loop provides strong support that nucleotide-dependent metallocenter assembly will be associated with the DFG-Apo species.

REFERENCES

1. **Lee, M. H., Mulrooney, S. B., Renner, M. J., Markowicz, Y. & Hausinger, R. P.** (1992). Sequence of *ureD* and demonstration that four accessory genes (*ureD*, *ureE*, *ureF*, and *ureG*) are involved in nickel metallocenter biosynthesis. *Journal of Bacteriology* **174**, 4324-4330.
2. **Lee, M. H., Pankratz, H. S., Wang, S., Scott, R. A., Finnegan, M. G., Johnson, M. K., Ippolito, J. A., Christianson, D. W. & Hausinger, R. P.** (1993). Purification and characterization of *Klebsiella aerogenes* UreE protein: a nickel-binding protein that functions in urease metallocenter assembly. *Protein Science* **2**, 1042-1052.
3. **Park, I.-S., Carr, M. B. & Hausinger, R. P.** (1994). *In vitro* activation of urease apoprotein and role of UreD as a chaperone required for nickel metallocenter assembly. *Proceedings of the National Academy of Sciences* **91**, 3233-3237.
4. **Moncrief, M. B. C. & Hausinger, R. P.** (1996). Purification and activation properties of UreD-UreF-urease apoprotein complexes. *Journal of Bacteriology* **178**, 5417-5421.
5. **Park, I.-S. & Hausinger, R. P.** (1995). Evidence for the presence of urease apoprotein complexes containing UreD, UreF, and UreG in cells that are competent for *in vivo* enzyme activation. *Journal of Bacteriology* **177**, 1947-1951.
6. **Park, I.-S. & Hausinger, R. P.** (1995). Requirement of carbon dioxide for *in vitro* assembly of the urease nickel metallocenter. *Science* **267**, 1156-1158.
7. **Jabri, E., Carr, M. B., Hausinger, R. P. & Karplus, P. A.** (1995). The crystal structure of urease from *Klebsiella aerogenes*. *Science* **268**, 998-1004.
8. **Saraste, M., Sibbald, P. R. & Wittinghofer, A.** (1990). The P-loop--a common motif in ATP- and GTP- binding proteins. *Trends in Biochemical Sciences* **15**, 430-434.
9. **Lee, M. H., Mulrooney, S. B. & Hausinger, R. P.** (1990). Purification, characterization, and *in vivo* reconstitution of *Klebsiella aerogenes* urease apoenzyme. *Journal of Bacteriology* **172**, 4427-4431.
10. **Lutz, A., Jacobi, A., Schlensog, V., Böhm, R., Sawers, G. & Böck, A.** (1991). Molecular characterization of an operon (*hyp*) necessary for the activity of the

- three hydrogenase isoenzymes in *Escherichia coli*. *Molecular Microbiology* **5**, 123-135.
11. **Waugh, R. & Boxer, D. H.** (1986). Pleiotropic hydrogenase mutants of *Escherichia coli* K-12: growth in the presence of nickel can restore hydrogenase activity. *Biochimie* **68**, 157-166.
 12. **Maier, T., Jacobi, A., Sauter, M. & Böck, A.** (1993). The product of the *hypB* gene, which is required for nickel incorporation into hydrogenases, is a novel guanine nucleotide-binding protein. *Journal of Bacteriology* **175**, 630-635.
 13. **Sambrook, J., Fritsch, E. F. & Maniatis, T.** (1989). *Molecular cloning: a laboratory manual*, 2nd edn. Cold Spring Harbor, NY: Cold Spring Harbor Laboratory.
 14. **Mulrooney, S. B., Pankratz, H. S. & Hausinger, R. P.** (1989). Regulation of gene expression and cellular localization of cloned *Klebsiella aerogenes* (*K. pneumoniae*) urease. *Journal of General Microbiology* **135**, 1769-1776.
 15. **Kunkel, T. A.** (1985). Rapid and efficient site-specific mutagenesis without phenotypic selection. *Proceedings of the National Academy of Sciences* **82**, 488-492.
 16. **Sanger, F., Nicklen, S. & Coulson, A. R.** (1977). DNA sequencing with chain-terminating inhibitors. *Proceeding of the National Academy of Sciences* **74**, 5463-5467.
 17. **Park, I.-S.** (1994). Thesis. East Lansing, MI: Michigan State University.
 18. **Zaluzec, E. J., Gage, D. A. & Watson, J. J.** (1994). Quantitative assessment of cysteine and cystine in peptides and proteins following organomercurial derivatization and analysis by matrix-assisted laser desorption ionization mass spectrometry. *Journal of the American Society for Mass Spectrometry* **5**, 359-366.
 19. **Cleveland, P. H., Wickham, M. G., Goldbaum, M. H., Ryan, A. F. & Worthen, D. M.** (1981). Rapid and efficient immobilization of soluble and small particulate antigens for solid phase radioimmunoassay. *Journal of Immunoassay* **2**, 117-136.
 20. **Engvall, E. & Perlmann, P. J.** (1972). Enzyme-linked immunosorbent assay, ELISA. III. Quantitation of specific antibodies by enzyme-labeled anti-immunoglobulin in antigen-coated tubes. *Journal of Immunology* **109**, 129-135.
 21. **Laemmli, U. K.** (1970). Cleavage of structural proteins during the assembly of the head of bacteriophage T4. *Nature (London)* **227**, 680-685.

22. **Weatherburn, M. W.** (1967). Phenol-hypochlorite reaction for determination of ammonia. *Analytical Chemistry* **39**, 971-974.
23. **Coleman, J. P., White, W. B., Egestad, B., Sjøvall, J. & Hylemon, P. B.** (1987). Biosynthesis of a novel bile acid nucleotide and mechanism of 7 α -dehydroxylation by an intestinal *Eubacterium* species. *Journal of Biological Chemistry* **262**, 4701-4707.
24. **Pocker, Y. & Deits, T. L.** (1982). Effects of pH on the anionic inhibition of carbonic anhydrase activities. *Journal of the American Chemical Society* **104**, 2424-2434.
25. **Mulrooney, S. B. & Hausinger, R. P.** (1990). Sequence of the *Klebsiella aerogenes* urease genes and evidence for accessory proteins facilitating nickel incorporation. *Journal of Bacteriology* **172**, 5837-5843.
26. **Salvucci, M. E.** (1992). Subunit interactions of rubisco activase: polyethylene glycol promotes self-association, stimulates ATPase and activation activities, and enhances interactions with rubisco. *Archives of Biochemistry and Biophysics* **298**, 688-696.
27. **Knowles, J. R.** (1989). The mechanism of biotin-dependent enzymes. *Annual Review of Biochemistry* **58**, 195-221.
28. **Rey, L., Imperial, J., Palacios, J.-M. & Ruiz-Argueso, T.** (1994). Purification of *Rhizobium leguminosarum* HypB, a nickel-binding protein required for hydrogenase synthesis. *Journal of Bacteriology* **176**, 6066-6073.

CHAPTER 6

PURIFICATION OF UREF AND CHARACTERIZATION OF NON-NATIVE URED-UREF-UREG-UREASE APOPROTEIN COMPLEXES

ABSTRACT

Urease nickel metallocenter assembly in *Klebsiella aerogenes* requires the presence of UreD, UreF, and UreG accessory proteins and is further facilitated by UreE. Urease apoprotein exists in an uncomplexed form as well as in a series of complexes including a UreD-UreF-UreG-urease apoprotein complex (I.-S Park, and R. P. Hausinger, J. Bacteriol. 177:1947-1951, 1995). In this study, *ureF* was overexpressed in the absence and presence of the other urease genes. UreF was shown to be highly insoluble in the absence of the other urease components and required detergent for solubilization. In contrast, when produced as part of a thioredoxin-UreF fusion protein, the sample was soluble and was readily purified. Overexpression of *ureF* along with the other urease genes resulted in formation of a UreD-UreF-UreG-urease apoprotein species that was distinct in chromatographic and electrophoretic behavior from the *in vivo* species identified earlier. The final level of activation, the nickel ion and bicarbonate dependencies, and the metal ion inactivation properties of this species were not enhanced over the properties observed for urease and UreD-urease apoprotein complexes. I conclude that the UreD-UreF-UreG-urease apoprotein studied in this paper is unlike the form involved in urease activation *in vivo*.

INTRODUCTION

Urease nickel metallocenter assembly in *Klebsiella aerogenes* is a complicated process that requires three accessory proteins (UreD, UreF, and UreG) and is facilitated by a fourth protein (UreE) (reviewed in 1). In addition to the accessory protein requirement, CO₂ is necessary to bridge the two active site nickels in the form of a carbamylated lysine (2). The accessory proteins are encoded in the same gene cluster as the three urease structural genes (*ureA*, *ureB*, *ureC*). The roles of the accessory proteins in metallocenter assembly are unclear. UreE is a nickel-binding protein (3) and is thought to function as a nickel donor. The three required accessory proteins participate in several complexes that contain UreD and urease apoprotein (D-Apo) (4), UreD, UreF, and urease apoprotein (DF-Apo) (5, Chapter 4), UreD, UreF, UreG, and urease apoprotein (DFG-Apo) (6), or a complex containing UreD, UreF, and UreG (DFG) (Chapter 5). UreF, when present in the DF-Apo complex, precludes nickel from binding to the urease active site until Lys-217 is carbamylated. UreG contains a P-loop motif, typically found in nucleotide-binding proteins, and suggestive evidence indicates that this motif is essential for *in vivo* incorporation of nickel into the active site (Chapter 5).

In order to better understand the *in vivo* metallocenter assembly process for urease, I enhanced cellular synthesis of UreF in the absence and the presence of the other urease components. These studies were designed to facilitate the purification and characterization of UreF and DFG-Apo. I have found that UreF is highly insoluble in the absence of the other urease components, and I've overcome this limitation by causing the cells to synthesize a thioredoxin-UreF fusion protein that I have purified. Furthermore, I have

shown that overexpression of *ureF* along with the other urease genes led to the formation of DFG-Apo complexes that are distinct in its properties from those described earlier (6) and is probably not relevant to the cellular activation process.

MATERIALS AND METHODS

Bacterial strains and plasmid construction. All molecular biology methods followed the general methods outlined in Sambrook *et al.* (8). Plasmid pKAUD2F+, containing overexpressed *ureF* and a mutated *ureD* promoter region to allow overexpression of this gene, has been described previously (5). This plasmid was transformed into *Escherichia coli* DH5 α .

To facilitate UreF purification, three methods were examined to optimize *ureF* expression. The 1.68-kbp *SalI* fragment of pKAU17 (9) was blunt ended with Klenow fragment and ligated to phosphorylated *NdeI* linker (5'-ACCATATG-3'). The resulting product was digested with *NdeI* and *AvrII* and the 670-bp fragment was ligated to the 5.7-kbp *NdeI-NheI* fragment of pET-11a (Novagen, Madison, WI), thus placing *ureF* under the control of a T7 promoter. This construct, pETF, was transformed into *E. coli* BL21(DE3) (Novagen). Alternatively, a *ureF* gene fusion with a 5' terminal extension was generated by blunt-ending the 670-bp *SalI-BlnI* fragment of pKAU17 with Klenow fragment and inserting it into the 3.4-kbp *BamHI*-digested and blunt-ended vector pQE-32 (Qiagen, Chatsworth, CA). This construct, pQEF, was transformed into *E. coli* M15[pREP4]. Finally, the 670-bp *SalI-AvrII* fragment of pKAU17 was ligated to the 4.4-kbp *XhoI-XbaI*

fragment of pThioHis C (Invitrogen, San Diego, CA). This construct, pThioHisF, was transformed into *E. coli* DH5 α .

Culture conditions and cell disruption. All cultures were grown in Luria-Bertani (LB) broth supplemented with 100 μ g ampicillin per ml. *E. coli* cells containing pETF or pThioHisF were grown at 37 °C until they reached an OD₆₀₀ of ~0.6. Isopropyl β -D-thiogalactopyranoside (IPTG) was added (1 mM final concentration) and the cells were grown for an additional 3-5 h at 30 or 37 °C. The cells were harvested by centrifugation and suspended in HEDG (25 mM HEPES [pH 7.4], 1 mM EDTA, 1 mM dithiothreitol, and 20% glycerol) buffer for cells containing pETF or in binding (20 mM sodium phosphate [pH 7.8], 500 mM NaCl, 10% glycerol) buffer for cells with pThioHisF. *E. coli* M15[pREP4] cells containing pQEF were grown in LB at 30 °C until an OD₆₀₀ of ~0.7-0.9, induced with 2 mM IPTG, and cultured for an additional 5 hours. Cells were harvested by centrifugation and suspended in PNC (20 mM NaHPO₄ [pH 8.0], and 300 mM NaCl) buffer. *E. coli* DH5 α (pKAUD2F+) was grown at 30 or 37 °C to late stationary phase, harvested by centrifugation, and suspended in PEDG (18 mM potassium phosphate [pH 7.4], 0.09 mM EDTA, 0.09 mM dithiothreitol, and 10% glycerol) buffer. Resuspended cells were disrupted by 2-3 passages through a French pressure cell at 18,000 lb/in² (1 lb/in² = 6.89 kPa), supplemented with 1 mM phenylmethylsulfonyl fluoride, and separated into extracts and pellet fractions by centrifugation at 100,000 x g for 45 min at 4 °C.

Partial purification of UreF. UreF was enriched from disrupted cell pellets of a 150 ml culture of *E. coli* BL21(DE3) containing pETF. The pellet was washed with 20 ml of HEDG buffer, centrifuged at 26,000 x g for 45 minutes, and the supernatant was removed. The sample was suspended in 20 ml HEDG buffer containing 0.5% (w/v) Triton X-100 and incubated at 37 °C for 30 min or at 4 °C for 17 h. After centrifugation at 26,000 x g for 20 min, the supernatant fraction containing UreF was added to a column of Extracti-Gel D Detergent Removing Gel (1.7 x 7 cm; Pierce, Rockford, IL). The flow-through fractions containing UreF protein were concentrated and subjected to Superose 12 chromatography (1.6 x 48.5 cm; Pharmacia Biotech, Piscataway, NJ) in HEDG buffer containing 0.1 M KCl.

His-tagged, UreF fusion protein was enriched from disrupted cell pellets of a 100 ml culture of *E. coli* M15[pREP4] carrying pQEF. The cell pellet was resuspended in PNC buffer containing 0.5% Triton X-100 and solubilized as described above. The supernatant fraction was applied to a nickel-charged nitrilotriacetic acid resin (1.7 x 2 cm; Qiagen). After washing the column with 500 ml of PNC buffer supplemented with 0.5% Triton X-100 and 10% glycerol, the bound proteins were eluted from the column with PNC buffer containing 1 M imidazole.

UreF fused to a thioredoxin protein was purified from a 2-liter culture of *E. coli* carrying pThioHisF. Cell extracts were chromatographed on a ProBond nickel-charged Sepharose resin (1.5 x 6.8 cm, Invitrogen) equilibrated in binding buffer. The column was washed with binding buffer until the A_{280} was less than 0.01. The column was then washed with 20 mM sodium phosphate (pH 6.0), 500 mM NaCl, and 10% glycerol until the A_{280}

was less than 0.01. The column was washed with 50 mls of binding buffer to raise the pH back up to pH 7.8, and then proteins were eluted with binding buffer containing 50 mM imidazole. Fractions containing ThioHisF were pooled and dialyzed against 20 mM sodium phosphate (pH 7.8), 0.1 mM dithiothreitol, and 10% glycerol. The sample was applied to a Mono Q HR 10/10 (Pharmacia Biotech) column equilibrated with the same buffer. The proteins were eluted with a linear salt gradient to 1 M KCl in the same buffer. Fractions containing ThioHisF were pooled and reapplied to the ProBond resin and chromatographed again as described above to remove proteins that bound nonspecifically to the initial ProBond column.

Enrichment of DFG-Apo. Cell extracts from a 3-liter culture of *E. coli* DH5 α (pKAUD2F+) were used to enrich a series of DFG-Apo complexes. The sample was applied to a DEAE-Sepharose column (2.5 x 19 cm; Pharmacia Biotech) equilibrated in PEDG buffer, and proteins were eluted from the column by using a 400-ml linear salt gradient to 0.5 M KCl in the same buffer. Fractions containing the DFG-Apo were pooled, dialyzed against PEDG buffer, and applied to a Mono Q HR 10/10 (Pharmacia Biotech) column equilibrated with the same buffer. The proteins were eluted with a linear salt gradient to 1 M KCl in PEDG buffer. DFG-Apo eluted from the column at 0.4-0.6 M KCl. Fractions containing the desired proteins were pooled, dialyzed against PEDG containing 0.1 M KCl. The protein pool was concentrated in a Centriprep-10 or -30 (Amicon, Beverly, MA) to 4 mls and chromatographed, via 2 runs, on a Superose 6 column (Pharmacia Biotech, 1.6 x 49 cm) equilibrated in the same buffer.

Polyacrylamide gel electrophoresis. Sodium dodecyl sulfate (SDS)-polyacrylamide gel electrophoresis was carried out by using the buffers described by Laemmli (10) and included 4.5% and 12.5% polyacrylamide stacking and running gels. Nondenaturing gels used the same buffers without detergent and consisted of 3% and 6% polyacrylamide stacking and running gels. The gels were either stained with Coomassie brilliant blue or electroblotted onto nitrocellulose, probed with anti-*K. aerogenes* urease antibodies (9), and visualized by using anti-rabbit immunoglobulin G-alkaline phosphatase conjugates (11). When testing for the presence of biotin, blots were probed and detected with ExtrAvidin-alkaline phosphatase (Sigma Chemical). The band intensities of Coomassie-stained gels were determined with an AMBIS (San Diego, CA) gel scanner. For calculation of the ratios of UreD, UreF, UreG, and UreC, M_r values of 29,300, 27,000, 21,800 and 60,300 were used.

Urease activity assays. Urease activity was measured by quantitating the rate of ammonia release from urea by formation of indophenol, which was monitored at 625 nm (12). One unit of urease activity was defined as the amount of enzyme required to hydrolyze 1 μ mole of urea per min at 37 °C. The standard assay buffer consisted of 25 mM HEPES (pH 7.75), 0.5 mM EDTA, and 50 mM urea. Protein concentrations were determined by using a commercial assay (Bio-Rad, Hercules, CA) with a bovine serum albumin standard.

Activation of urease apoprotein. Routine urease apoprotein activation buffer consisted of 100 mM HEPES (pH 8.3), 150 mM NaCl, 100 mM NaHCO₃, and 100 μM NiCl₂ (2). For specific experiments, the conditions were modified by varying the bicarbonate or nickel ion concentrations, adding other metal ions to the activation buffer, or incubating samples in the presence of metal ions prior to addition of bicarbonate.

RESULTS AND DISCUSSION

High level synthesis and partial purification of UreF. UreF, a protein that is absolutely required for *in vivo* activation of urease (reviewed in 1), has not been purified or characterized from any microorganism. *K. aerogenes* UreF purification has been confounded by the low expression level of the corresponding gene in the wild type microorganism and in *E. coli* cells carrying the *K. aerogenes* urease gene cluster (13). Analogous to the situation for *ureD*, another essential urease accessory protein, *ureF*, possesses a non-consensus ribosome binding site. Unlike the case with *ureD* (4), however, alterations to the *ureF* ribosome binding site by site-directed mutagenesis did not result in the synthesis of high levels of the gene product (14). Three alternative strategies were devised to allow high level synthesis of the *ureF* gene product in the absence of the other urease components.

In *E. coli*(pETF), *ureF* expression was regulated through an IPTG-inducible T7 RNA polymerase acting on a T7 promoter located immediately upstream from the cloned gene. When induced with IPTG, high level synthesis of UreF was observed (Fig. 1, lane 2).

The desired protein, however, was not in the soluble cell extracts (Fig. 1, lane 3). In the case of cells grown at 30 °C, but not for 37 °C-grown cells, about 50 % of UreF was solubilized from the pellet by incubation in buffer containing 0.5% Triton X-100 (Fig. 1, lane 4). The identity of the predominant band was confirmed to be UreF by *N*-terminal amino acid sequence analysis (data not shown). Upon removal of detergent, the solubility of UreF decreased and further purification efforts were hindered. The protein sample appeared to smear during chromatography on ion exchange or hydrophobic columns. Size exclusion chromatography revealed the presence of an aggregated form containing UreF as well as other peptides.

An alternative approach to UreF purification made use of *E. coli* M15[pREP4] cells carrying pQEF where *ureF* expression is controlled by an IPTG-regulated T5 promoter. In this construct, UreF was synthesized at high levels as a fusion protein with an *N*-terminal extension containing six histidine residues. The presence of the His-tag did not enhance solubility of UreF and the fusion protein was found in the pellet fraction after cell lysis and centrifugation (data not shown). As observed for the pETF-encoded UreF protein, Triton X-100 treatment solubilized a portion of His-tagged UreF. The His-tag was ineffective for protein purification when using a nickel-charged nitrilotriacetic acid column, possibly due to aggregation of proteins in the sample and the propensity of UreF to precipitate out of solution.

A third construct containing *ureF* was generated by creating a gene fusion of a thioredoxin gene containing a nickel binding site and *ureF*. This ThioHisF fusion protein was observed in cell extracts and was purified using a nickel-affinity and anion exchange

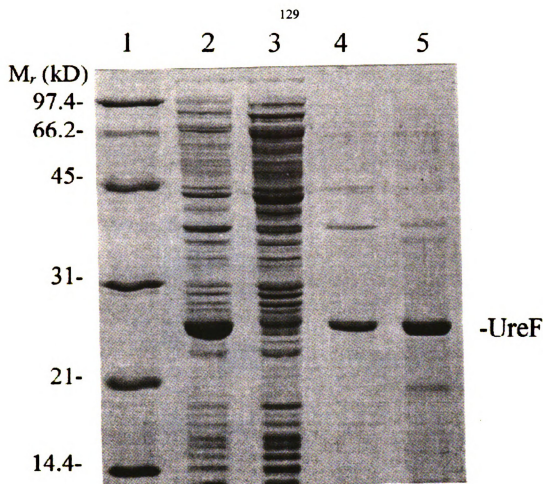


Figure 1. SDS/polyacrylamide gel electrophoretic analysis of UreF solubilization. Samples included: lane 1, molecular weight markers (phosphorylase *b*, M_r 97,400; bovine serum albumin, M_r 66,200; ovalbumin, M_r 45,000; carbonic anhydrase, M_r 31,000; soybean trypsin inhibitor, M_r 21,000; and lysozyme, M_r 14,400); lane 2, disrupted cell suspension from *E. coli* BL21(DE3)[pETF]; lane 3, soluble cell extracts; lane 4, solubilized sample after treating lysed cell pellets with HEDG buffer containing 0.5% Triton X-100; lane 5, pellet remaining after partial solubilization of UreF.

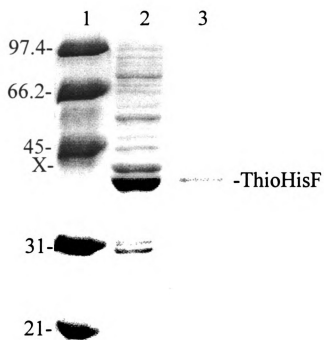


Figure 2. Purification of ThioHisF as analyzed by SDS/polyacrylamide gel electrophoresis. Samples included: lane 1, molecular weight markers; lane 2, first ProBond ThioHisF pool; lane 3, second ProBond ThioHisF pool.

chromatographies. Chromatography on the nickel-affinity column resulted in partial purification of ThioHisF (Fig. 2, lane 2). The bound proteins eluted from the column at a very low imidazole concentration (< 50 mM) so purification of ThioHisF using an imidazole gradient was not very helpful. ThioHisF was chromatographed on a Mono Q column to remove the protein, labelled X (Fig. 2, lane 2), that co-eluted with ThioHisF off the ProBond column. Mono Q fractions containing ThioHisF were pooled and reapplied to the nickel-affinity resin and purified as described for the first ProBond chromatography step. This was done to remove proteins that bound non-specifically during the first ProBond chromatography procedure. The ThioHisF protein was reasonably pure (Fig. 2, lane 3) and remained soluble throughout the purification procedure. Since high levels of CO₂ are known to be required for carbamylation of Lys-217 in the urease apoprotein (2) in order to form the binuclear active site (15), I tested whether the UreF fusion protein possessed a cofactor that could function to deliver CO₂. The ThioHisF protein did not contain biotin when analyzed by Western blot (immunoblot) analysis using avidin-linked alkaline phosphatase (data not shown). The fusion protein does, however, contain an enterokinase cleavage site that was used to release UreF from the thioredoxin. Protease treatment resulted in cleavage of thioredoxin from UreF, and UreF remained soluble. After gel filtration to remove the enterokinase protein (M_r 43,000) and the thioredoxin fusion partner (M_r 14,400), UreF (M_r 27,000) may then be used to make antibodies or be used for crystallization trials. This method provides the first soluble purification scheme for UreF.

Enrichment of DFG-Apo. A series of urease apoprotein complexes containing UreD, UreF, and UreG were previously described (6), but these species were present at levels too low to allow purification and detailed characterization. Because the prior complexes were observed in cells that synthesized high levels of urease subunits, UreD, and UreG, the limiting component for their formation appeared to be UreF. In an effort to optimize synthesis of these complexes, I constructed plasmid pKAUD2F+ and used it to purify DFG-Apo.

E. coli(pKAUD2F+) cells synthesized high levels of urease, UreD, UreF, and UreG. The four proteins were soluble in extracts and co-eluted during purification using DEAE-Sephacrose, Mono Q, and Superose 6 chromatographies (Fig. 3). Size exclusion chromatography results, however, indicated the presence of multiple, very large species ($M_r > 670,000$) that eluted at and near the void volume of the Superose 6 column, in contrast to the reported behavior for DFG-Apo (6). Nondenaturing gel electrophoretic analysis revealed that much of the protein did not enter the running gel and the protein that did electrophorese migrated very slowly (data not shown), again differing from the DFG-Apo properties (6). Due to these differences the species purified here are designated DFG-Apo* to distinguish them from the DFG-Apo complexes observed *in vivo* in cells not overexpressing *ureF*. Based on gel scanning analysis of Coomassie blue-stained bands on an SDS/polyacrylamide gel, there appeared to be an average of 1.16-1.19 UreD, 0.93-0.96 UreG, and 0.77-0.81 UreF per UreC protein in the DFG-Apo* pool. Efforts to disrupt the aggregated complex or to further resolve the complex from contaminating proteins led to diminishment in intensity

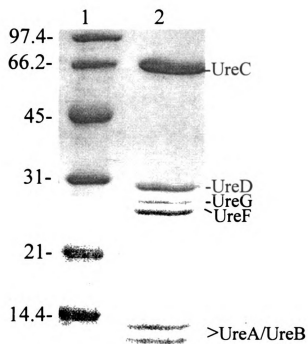


Figure 3. Analysis of DFG-Apo complex purified from *E. coli*(pKAUD2F+) by SDS/polyacrylamide gel electrophoresis. Samples included: lane 1, molecular weight markers; lane 2, Superose 6 pool.

of the UreG peptide compared to the UreD, UreG, and urease peptides when examined by SDS/polyacrylamide gel analysis (data not shown).

The DFG-Apo* complexes were shown to be activation competent, yielding 450-600 U/mg of total protein when using standard activation conditions that had been optimized for activating D-Apo and Apo. The level and rate of activation of DFG-Apo* complexes are similar to that observed for D-Apo (4). The bicarbonate (Fig. 4) and nickel concentration (Fig. 5) dependencies of the DFG-Apo* were similar to those observed for both Apo and D-Apo (2, 4), exhibiting half-maximal activation at ~25 mM added bicarbonate and ~75 μ M NiCl₂. The ability of various metal ions to inhibit activation of DFG-Apo was studied since previous work on Apo and D-Apo had demonstrated inhibition by nickel ion as well as other divalent metals (16). Prior incubation of the DFG-Apo* pool with either 100 or 500 μ M NiCl₂ for 80 minutes resulted in a 40-70% or 50-80% decrease respectively in the extent of urease activation when subsequently incubated in the presence of both nickel ions and bicarbonate (data not shown). The extent of activation varied from one purification to another, perhaps due to different levels of UreG in the complex pools. Although the DFG-Apo* complexes are able to be activated *in vitro*, the final level of activation and the nickel ion and bicarbonate dependencies for these complexes are not enhanced over the properties observed for activation of Apo and D-Apo. I believe that the present DFG-Apo* species are not significant to urease metallocenter assembly. Rather, I suspect that these species likely represent non-native aggregates with limited function for urease assembly.

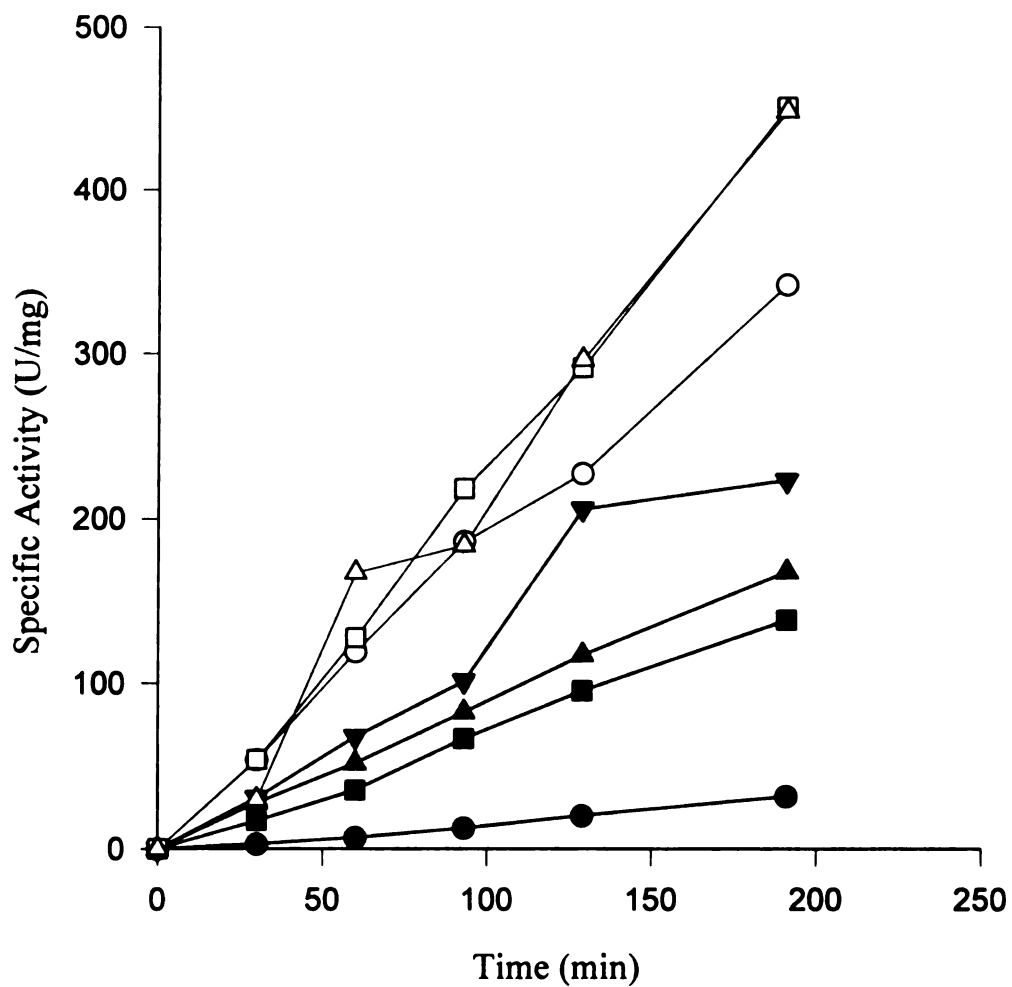


Figure 4. Bicarbonate ion concentration dependence of activation for the DFG-Apo*. The sample (0.5 mg/ml) was incubated at 37 °C in 100 mM HEPES (pH 8.3) buffer containing 150 mM NaCl, 100 μ M NiCl₂, and the following concentrations of NaHCO₃: 0 (●), 5 (■), 10 (▲), 25 (▼), 50 (○), 75 (□), or 100 (Δ) mM added NaHCO₃.

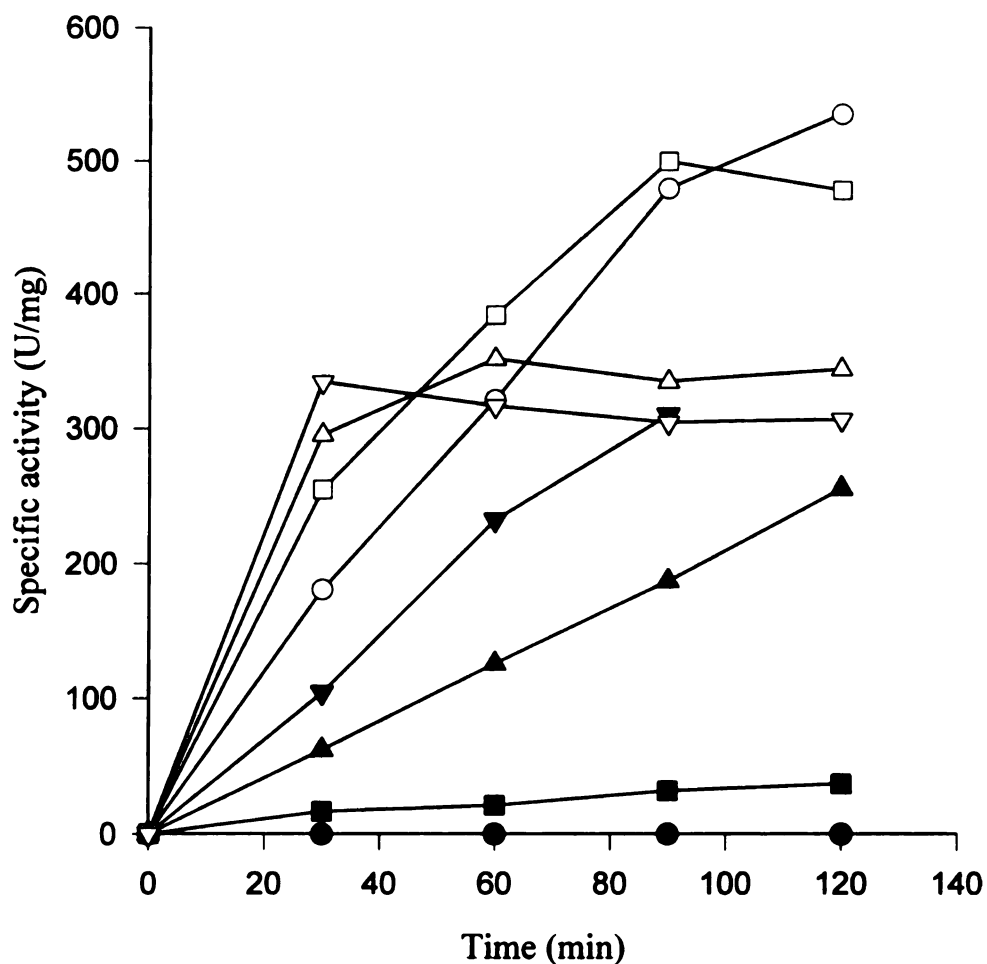


Figure 5. Nickel ion concentration dependence of activation for the DFG-Apo*. The purified sample (0.1 mg/ml) was incubated at 37 °C in 100 mM HEPES (pH 8.3) buffer containing 150 mM NaCl, 100 mM NaHCO₃ and 0 (●), 25 (■), 50 (▲), 75 (▼), 100 (○), 200 (□), 500 (Δ), or 1000 (▽) μM NiCl₂. Aliquots were removed at the indicated times and the samples were assayed for urease activity.

REFERENCES

1. **Moncrief, M. B. C. & Hausinger, R. P.** (1996). Nickel incorporation into urease. In *Mechanisms of Metallocenter Assembly*, pp. 151-171. Edited by R. P. Hausinger, G. L. Eichhorn & L. G. Marzilli. New York: VCH Publishers.
2. **Park, I.-S. & Hausinger, R. P.** (1995). Requirement of carbon dioxide for in vitro assembly of the urease nickel metallocenter. *Science* **267**, 1156-1158.
3. **Lee, M. H., Pankratz, H. S., Wang, S., Scott, R. A., Finnegan, M. G., Johnson, M. K., Ippolito, J. A., Christianson, D. W. & Hausinger, R. P.** (1993). Purification and characterization of *Klebsiella aerogenes* UreE protein: a nickel-binding protein that functions in urease metallocenter assembly. *Protein Science* **2**, 1042-1052.
4. **Park, I.-S., Carr, M. B. & Hausinger, R. P.** (1994). *In vitro* activation of urease apoprotein and role of UreD as a chaperone required for nickel metallocenter assembly. *Proceedings of the National Academy of Sciences* **91**, 3233-3237.
5. **Moncrief, M. B. C. & Hausinger, R. P.** (1996). Purification and activation properties of UreD-UreF-urease apoprotein complexes. *Journal of Bacteriology* **178**, 5417-5421.
6. **Park, I.-S. & Hausinger, R. P.** (1995). Evidence for the presence of urease apoprotein complexes containing UreD, UreF, and UreG in cells that are competent for in vivo enzyme activation. *Journal of Bacteriology* **177**, 1947-1951.
7. **Lee, M. H., Mulrooney, S. B. & Hausinger, R. P.** (1990). Purification, characterization, and in vivo reconstitution of *Klebsiella aerogenes* urease apoenzyme. *Journal of Bacteriology* **172**, 4427-4431.
8. **Sambrook, J., Fritsch, E. F. & Maniatis, T.** (1989). *Molecular cloning: a laboratory manual*, 2nd edn. Cold Spring Harbor, NY: Cold Spring Harbor Laboratory.
9. **Mulrooney, S. B., Pankratz, H. S. & Hausinger, R. P.** (1989). Regulation of gene expression and cellular localization of cloned *Klebsiella aerogenes* (*K. pneumoniae*) urease. *Journal of General Microbiology* **135**, 1769-1776.
10. **Laemmli, U. K.** (1970). Cleavage of structural proteins during the assembly of the head of bacteriophage T4. *Nature (London)* **227**, 680-685.

11. **Blake, M. S., Johnston, K. H., Russel-Jones, G. L. & Gotschlich, E. C. (1984).** A rapid, sensitive method for detection of alkaline phosphatase-conjugated anti-antibody on western blots. *Analytical Biochemistry* **136**, 175-179.
12. **Weatherburn, M. W. (1967).** Phenol-hypochlorite reaction for determination of ammonia. *Analytical Chemistry* **39**, 971-974.
13. **Lee, M. H., Mulrooney, S. B., Renner, M. J., Markowicz, Y. & Hausinger, R. P. (1992).** Sequence of *ureD* and demonstration that four accessory genes (*ureD*, *ureE*, *ureF*, and *ureG*) are involved in nickel metallocenter biosynthesis. *Journal of Bacteriology* **174**, 4324-4330.
14. **Park, I.-S. (1994).** Thesis. East Lansing, MI: Michigan State University.
15. **Jabri, E., Carr, M. B., Hausinger, R. P. & Karplus, P. A. (1995).** The crystal structure of urease from *Klebsiella aerogenes*. *Science* **268**, 998-1004.
16. **Park, I.-S. & Hausinger, R. P. (1996).** Metal ion interactions with urease and UreD-urease apoproteins. *Biochemistry* **35**, 5345-5352.

CHAPTER 7

ADDITIONAL STUDIES

A. Identification of a series of urease apoprotein forms. During routine purification of urease apoprotein (termed Apo) from *Escherichia coli* pKAU22 Δ ureD (1), a unique series of bands were observed when purified Apo was analyzed on a nondenaturing polyacrylamide gel electrophoresis (Fig. 1, lane 2). When activated by the addition of nickel and bicarbonate, the Apo species did not collapse completely. The four major species remained while some of the larger less prevalent species disappeared (data not shown). To determine how these species were formed, I tested for collapse of the Apo forms by incubating purified protein for 1 hour at 37 °C in 18 mM phosphate (pH 7.3), 1 mM EDTA, 1 mM dithiothreitol (DTT) and various compounds such as KCl, hydroxylamine, glycerol, and additional quantities DTT and EDTA. The incubated samples were subjected to nondenaturing polyacrylamide gel electrophoresis (Fig. 1). DTT collapsed the species down to the form typically observed for holo- or apoprotein (Fig. 1, lane 7). One mM DTT was present at all stages of the Apo purification procedure, so it is unclear why additional incubation with 10 mM DTT would collapse the species. Incubation with glycerol (Fig. 1, lane 4), sodium bicarbonate (Fig. 1, lane 5), KCl (Fig. 1, lane 6), EDTA (Fig. 1, lane 8), and hydroxylamine (data not shown) did not affect Apo species formation. As observed with DTT, 2-mercaptoethanol was also able to collapse the Apo species. These results suggest that disulfide bonds may be involved in the Apo species formation.

Since the data suggested that DTT might be reducing disulfide bonds in the Apo species, I speculated that a particular Cys in the Apo might be involved. I decided to test for Apo species formation using a plasmid containing a mutated Cys (C319A) at the active site

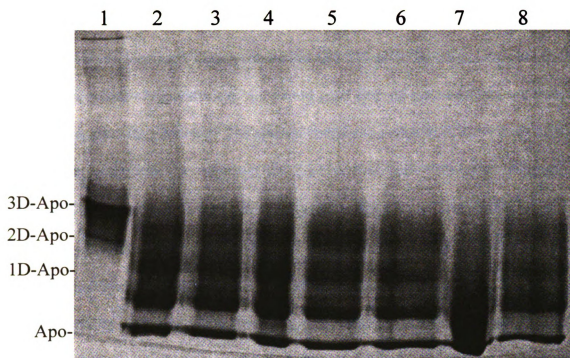


Figure 1. Nondenaturing polyacrylamide gel electrophoretic analysis of Apo. Purified Apo was incubated in 18 mM phosphate (pH 7.4), 0.1 M KCl, 0.09 mM EDTA, 1 mM dithiothreitol with various compounds at 37 °C for 1 hour then analyzed on a 6% native polyacrylamide gel. Samples included: lane 1, D-Apo complexes; lane 2, Apo not incubated at 37 °C; lane 3, Apo only; lane 4, Apo with 20% glycerol; lane 5, Apo with 150 mM NaHCO₃; lane 6, Apo with 0.4 M KCl; lane 7, Apo with 1 mM dithiothreitol; lane 8, Apo with 10 mM EDTA.

(3). The plasmid containing C319A was chosen because Cys-319 is the only Cys located in the active site and it was mutagenized previously. The presence of a flexible loop over the active site (4) would support the hypothesis that Cys 319 could be interacting with another Cys located outside of the active site. I removed *ureD* from the plasmid to prevent possible D-Apo complexes from forming. The plasmid containing a pKAU17C319A *ureD* deletion mutant was constructed by religating the 7.5-kbp *NruI-SacI* blunt-ended fragment of pKAU17C319A and transforming *E. coli* DH5 α . When the C319 purified Apo was analyzed by nondenaturing polyacrylamide gel electrophoresis, the species pattern observed previously for wild-type Apo was not detected (Fig. 2, lane 2). Instead, bands were detected that corresponded to the expected Apo/holoprotein band position (labelled Apo), but also additional bands (labelled X*) were detected. The bands labelled X* electrophoresed at the same position where bands were observed previously when DF-Apo complexes were activated with nickel and bicarbonate. These bands were labelled X (5, Chapter 6, Fig. 3C) and were found to contain urease when analyzed by 2-dimensional polyacrylamide gel electrophoresis. The bands observed with C319A Apo were also found to contain urease (data not shown), and incubation with 10-100 mM DTT did not alter the C319A Apo species. This suggests that Cys-319 may play a role in these species formation possibly by disulfide formation and these results might explain why dithiothreitol collapses the species.

It was puzzling why these species are forming and why the crystal structure of Apo didn't identify any difference between holourease and Apo with the exception of nickel being absent from the active site and Lys-217 not being carbamylated (6). Apo utilized to make the crystals was purified from cells containing all the accessory proteins. When Apo

was purified from *E. coli*(pKAU22), these Apo species were not detected and a single Apo band was detected on native gels (data not shown). When the additional Apo species were observed, Apo was purified from a *ureD* gene deletion mutant (Fig. 1). UreD could still possibly have a role as a chaperonin involved in preventing these species from forming. UreD may prevent disulfide bond formations with Cys-319 by stabilizing or controlling the flexible loop's structure over the active site. One could imagine UreD functioning as a doorman and controlling the influx of essential molecules such as nickel and bicarbonate while preventing unwanted guests such as other metal ions and potentially reactive sulfhydryl groups. Evidence for this is supported from studies showing that the presence of UreD in the UreD-Apo complexes appears to reduce the rate of Apo interaction with nickel as well as other metal ions (7). Due to the absence of UreD in the cell, these Apo species may be inactive forms of urease that may contain disulfide groups and may also contain nonproductive-bound nickel or other metal ions. Cross-linking studies have shown that UreD interacts with the β subunit of urease. The active site is located in the α subunit, but when looking at the crystal structure, $[(\alpha\beta\gamma)_3]$, UreD associated with the β subunit of one $(\alpha\beta\gamma)$ trimer may interact with the α subunit of the adjacent trimer. Crystallization of the D-Apo complexes will undoubtedly provide insight into UreD's role in metallocenter assembly.

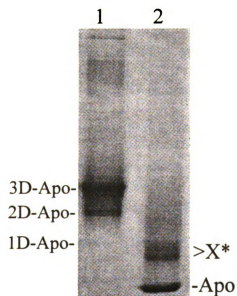


Figure 2. Nondenaturing polyacrylamide gel electrophoretic analysis of purified Apo from *E. coli*(pKAU17C319A Δ ureD). Samples include; lane 1, D-Apo complexes, and lane 2, purified C319A Apo.

B. Incubation of Apo and UreD-UreF-UreG complex. In Chapter 6, I attempted to purify the UreD-UreF-UreG-Apo (termed DFG-Apo) species by overexpressing *ureF* in a strain already overexpressing *ureD*. Unfortunately, the complexes observed (termed DFG-Apo*) were not the species observed *in vivo* (2) and are probably not relevant to the cellular activation process. I wanted to test the theory that UreD-UreF-UreG (DFG) complex might bind to Apo to form the *in vivo* DFG-Apo. The urease metallocenter assembly model suggests that the DFG-Apo species might be constructed in this manner. I attempted to form the *in vivo* DFG-Apo species by incubating purified Apo and partially purified DFG together. The sample was incubated overnight at 4 °C and then subjected to Superose 12 chromatography. Fractions off the column were analyzed by denaturing polyacrylamide gel electrophoresis (Fig. 3, lanes 3-7). DFG and some Apo co-eluted during gel filtration. [Note: When ATP was included in the sample, there was no detectable difference in the Superose 12 chromatogram or protein banding patterns on native and denaturing gels (data not shown)]. Fractions were also analyzed by nondenaturing polyacrylamide gel electrophoresis, transferred to nitrocellulose, and analyzed by immunoblot analysis visualized with anti *K. aerogenes* urease antibodies (Fig. 4). Samples containing Apo, UreD, UreF, and UreG contained a band (labelled X, Fig. 4, lanes 4-5) that migrated at a position more closely resembling the DFG-Apo species observed *in vivo*. This band was not detected when Apo and DFG samples were analyzed separately by immunoblot analysis (data not shown). Interestingly, a band that migrated at approximately the same position as 1D-Apo was also observed (Fig. 4, lanes 4-6). There are two possible explanations for formation of 1D-Apo. First, DFG-Apo

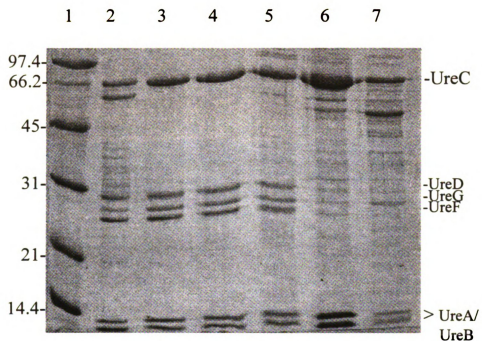


Figure 3. SDS/polyacrylamide electrophoretic analysis of Apo and DFG pool after Superose 12 chromatography. Samples included: lane 1, molecular weight markers (phosphorylase *b*, M_r 97,400; bovine serum albumin, M_r 66,200; ovalbumin, M_r 45,000; carbonic anhydrase, M_r 31,000; soybean trypsin inhibitor, M_r 21,000; and lysozyme, M_r 14,400); lane 2, DFG-Apo*; lanes 3-7, successive Superose 12 fractions of the Apo and DFG mixture.

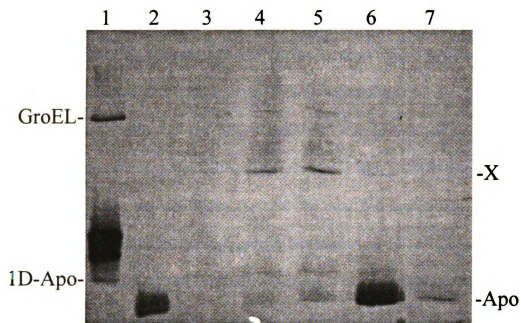


Figure 4. Native polyacrylamide gel electrophoretic analysis of Apo and DFG pool after Superose 12 chromatography. Western blot analysis of a nondenaturing polyacrylamide gel visualized with anti-*Klebsiella aerogenes* urease antibodies. Samples included: lane 1, D-Apo; lane 2, Apo; lanes 3-7, same samples analyzed in Fig. 2, lanes 3-7.

may have formed, but UreF and UreG dissociated from the complex resulting in D-Apo. This seems unlikely because one would expect to see 3D- and 2D-Apo complexes also. Another possibility is that some UreD dissociated from DFG and bound to Apo to form 1D-Apo. I did not perform immunoblot analysis with anti-*K. aerogenes* UreD antibodies to be sure this band contains UreD. Addition of DFG to Apo provides evidence supporting the model that Apo and DFG can interact to form DFG-Apo, at least *in vitro*. This procedure may be utilized in the future to characterize DFG-Apo since overexpression of *ureD*, *ureF*, *ureG*, and the urease structural subunits (plasmid pKAUD2F+) produces an anomalous DFG-Apo* species *in vivo* (Chapter 6).

Since formation of the *in vivo* DFG-Apo complexes *in vitro* appeared to be a possible prospect with Apo and DFG complexes, I tested for formation of the DFG-Apo complexes by incubating the DF-Apo complexes (5) with partially purified UreG under the same experimental conditions used for the Apo and the DFG complexes. When analyzed by gel filtration chromatography, association of DF-Apo and UreG did occur (data not shown), but the complexes observed were the multiple, very large species observed with the DFG-Apo* complexes in *E. coli*(pKAUD2F+) (Chapter 6). These results suggest that stepwise addition of accessory proteins to Apo *in vitro* may not form the DFG-Apo observed *in vivo*, and formation of the DFG complex followed by incubation with Apo may be the most logical approach *in vitro* to form the DFG-Apo complexes.

REFERENCES

1. **Lee, M. H., Mulrooney, S. B., Renner, M. J., Markowicz, Y. & Hausinger, R. P.** (1992). Sequence of *ureD* and demonstration that four accessory genes (*ureD*, *ureE*, *ureF*, and *ureG*) are involved in nickel metallocenter biosynthesis. *Journal of Bacteriology* **174**, 4324-4330.
2. **Park, I.-S. & Hausinger, R. P.** (1995). Evidence for the presence of urease apoprotein complexes containing UreD, UreF, and UreG in cells that are competent for in vivo enzyme activation. *Journal of Bacteriology* **177**, 1947-1951.
3. **Martin, P. R. & Hausinger, R. P.** (1992). Site-directed mutagenesis of the active site cysteine in *Klebsiella aerogenes* urease. *Journal of Biological Chemistry* **267**, 20024-20027.
4. **Jabri, E., Carr, M. B., Hausinger, R. P. & Karplus, P. A.** (1995). The crystal structure of urease from *Klebsiella aerogenes*. *Science* **268**, 998-1004.
5. **Moncrief, M. B. C. & Hausinger, R. P.** (1996). Purification and activation properties of UreD-UreF-urease apoprotein complexes. *Journal of Bacteriology* **178**, 5417-5421.
6. **Jabri, E. & Karplus, P. A.** (1996). Structures of the *Klebsiella aerogenes* urease apoenzyme and two active-site mutants. *Biochemistry* **35**, 10616-10626.
7. **Park, I.-S. & Hausinger, R. P.** (1996). Metal ion interactions with urease and UreD-urease apoproteins. *Biochemistry* **35**, 5345-5352.

CHAPTER 8

CONCLUSIONS AND FUTURE PROSPECTS

The initial goal of this work was to try and characterize two of the accessory proteins, UreG and UreF, required for urease metallocenter assembly in *Klebsiella aerogenes*. Although I was unable to fully characterize both of these proteins individually, I was able to identify several complexes in which these proteins play an important role. Characterization of these complexes helped to identify the roles of these proteins in the context of all the protein players in this complicated production.

Crystallization of urease was essential for resolving the structure of the holoenzyme, and its active site environment. I provided urease and Seleno-methionine-containing urease to Dr. Andy Karplus for crystallographic analysis. The X-ray crystal structure analysis of *K. aerogenes* has been resolved to 2.2 Å. The enzyme functions as a tightly packed trimer of trimers $[(\alpha\beta\gamma)_3]$ containing three bi-nickel active sites. The two nickel ions per active site are located 3.5 Å apart and are bridged by a carbamate formed on Lys-217. A solvent molecule is tightly bound to one metal ion and appears to partially bridge to the second. One nickel ion possesses a distorted trigonal bipyramidyl or distorted square pyramidyl geometry and the five ligands include His-134, His-136, Asp-360, Lys-217 carbamate, and water (or hydroxide). The second nickel ion possesses pseudotetrahedral geometry and is liganded by His-246, His-272, Lys-217 carbamate, and solvent in partial occupancy. In addition to the metallocenter ligands, the crystal structure reveals several additional residues worth noting. His-219 is appropriately positioned to stabilize substrate binding to the fourth ligand position of the second nickel ion. His-320 is located near the bi-nickel center and is likely to participate in catalysis. Finally, Cys-319 is within the active site environment, but does not play a catalytic role.

Catalysis has been suggested to proceed by urea binding in *O*-coordination to the fourth coordination site of the second nickel ion with stabilization rendered by His-219. The solvent molecule that is now solely coordinated to the first nickel ion is thought to carry out nucleophilic attacks on the bound urea to form a tetrahedral intermediate. Elimination of ammonia from the intermediate is facilitated by proton donation from His-320 acting as a general acid, and carbamate is released.

My studies on the activity of urease in the crystalline state found that the enzyme has less than 0.05% of the activity observed for the soluble enzyme under standard assay conditions. The trace amounts of activity observed arise from limited enzyme activity at the crystal surfaces or trace levels of enzyme dissolved into the crystal storage buffer. This data support the necessity for a conformational change during urea catalysis.

I overexpressed *ureF* and partially purified UreF in its insoluble form using Triton X-100. UreF was also purified as part of a thioredoxin fusion protein which was found in the soluble portion of the cell, unlike wild-type UreF. Overexpression of *ureF* and *ureD* in a *ureG* deletion mutant resulted in production of a series of UreD-UreF-urease apoprotein (DF-Apo) complexes. These complexes exhibited activation properties distinct from urease (Apo) and UreD-urease (D-Apo) apoprotein complexes. These complexes were resistant to inactivation by NiCl₂ and exhibited a decreased bicarbonate requirement. Immunoblot analysis with polyclonal anti-urease and anti-UreD antibodies indicated that in these complexes UreD is masked, presumably by UreF, and the DF-Apo complexes migrate at the same positions as D-Apo complexes during nondenaturing polyacrylamide gel electrophoresis. One of the most interesting results from the DF-Apo

characterization studies is the ability of the complexes to preclude nickel ions from the active site but the inability to preclude other divalent metal ions. The mechanism by which DF-Apo can distinguish between the nickel and other metal ions is unknown. Once carbamylation of Lys-217 has occurred, UreF may detect this and conformational change occurs within the complex and Ni ion is permitted to enter the active site to form the urease metallocenter. The D-Apo portion of the complexes could then permit nickel ions to enter followed by UreD and UreF dissociation from holourease. I propose that UreF is the key component involved in precluding nickel ions from binding to the active site until the carbamylated lysine metallocenter is formed. I suspect that UreF functions within complexes rather than as the free protein.

Since UreG is produced in large quantities in the cell and it contains a nucleotide-binding motif typically observed in nucleotide binding proteins, I attempted to purify and characterize UreG. I hypothesized that UreG may assist in CO₂ delivery to the active site in an energy-dependent manner. Purified UreG did not bind or hydrolyze nucleotides, contain biotin, nor exhibit carbonic anhydrase activity. Mutations in the UreG P-loop motif do, however, eliminate detectable urease activity *in vivo* when cells were grown in the presence of nickel. These results support work done by Mann Lee in which he identified an *in vivo* energy requirement for urease activity. Although UreG did not bind or hydrolyze nucleotides, I suspected that UreG may only exhibit nucleotide binding and hydrolysis activities when complexed with other proteins (see below).

In addition to characterizing UreG, I identified a complex containing UreD, UreF, and UreG (DFG) in urease deletion mutants. The partially purified complex bound to an

ATP-linked agarose resin. Formation of DFG was not affected by mutations in the UreG P-loop motif; however, this species was incapable of binding to an ATP-linked agarose resin. I propose UreG is unable to bind and hydrolyze nucleotides unless complexed with other accessory proteins. DFG may modulate the ability of UreG to bind and hydrolyze nucleotides. UreG may act as a molecular switch where the binding and hydrolysis of nucleotide triphosphate to nucleotide diphosphate triggers the on and off states of UreG. UreD and UreF may function as nucleotide release proteins, similar to guanine nucleotide release proteins, or nucleotide hydrolysis activating proteins such as GTPase activating proteins observed in eukaryotes (1). UreD and UreF in the DFG complex may regulate metallocenter assembly by modulating the relative concentration of active UreG (NTP-bound) and inactive form (NDP-bound) in the cell (Fig. 1). An important experiment will be to test DFG for NTP binding and hydrolysis, but also add NTP to DFG and look for dissociation of UreD or UreF from the complex. Once NTP is bound to UreG, the protein functioning as the nucleotide release protein may dissociate. It is also possible that the proteins only dissociate from UreG after interaction with Apo (i.e., in the DFG-Apo complexes).

In an attempt to characterize DFG-Apo, I partially purified the complexes in an *Escherichia coli* strain that overexpressed *ureD* and *ureF* as well as the other urease genes. These complexes were distinct from those identified *in vivo* previously by Il-Seon Park. The complexes formed a large aggregate that migrated very slowly during nondenaturing gel electrophoretic analysis. The activation competency, bicarbonate and nickel requirements, and metal inactivation studies were similar to those observed for D-

Apo. Not only were these complexes distinct from those observed previously, characterization of these complexes did not provide any insight into the possible role of this species. I conclude that the complex I characterized is not relevant to the *in vivo* urease activation pathway and results from nonspecific protein interactions probably due to the overexpression of *ureF* in the cell. However, *in vitro* studies involving the incubation Apo and DFG together did provide some encouraging results. It appeared that DFG-Apo was formed and its band pattern on a nondenaturing gel was similar to the DFG-Apo complexes that were observed *in vivo*. This procedure might be used to form enough DFG-Apo so that NTP binding and hydrolysis studies can be performed.

By combining studies done by me and by other members in the lab, a pathway describing *in vivo* urease metallocenter assembly has been proposed (Fig. 2; also depicted in Chapter 1). Nickel ions enter the cell by utilization of a nickel or less selective metal ion transport system. UreE (ⓔ) binds 6 nickel per dimer and is thought to donate nickel ions to Apo present in the DFG-Apo species. Formation of DFG-Apo is thought to arise from sequential binding of UreD, UreF, and UreG to Apo or from binding of the pre-formed DFG complex to Apo. Interaction of DFG-Apo with UreE results in insertion of nickel into the active site along with CO₂. Interaction of DFG-Apo and UreE has not yet been detected so this aspect of the model still needs to be tested. Nucleotide hydrolysis is probably involved at this stage, but it is unknown whether the energy requirement is for UreE nickel donation, CO₂ delivery, or removal of an incorrectly bound metal from Apo. The CO₂ delivery system for this process is unknown but accessory proteins are most

likely involved. Once nickel and CO₂ have been successfully inserted into the active site, the accessory proteins dissociate from urease and functional holoprotein is formed.

Important questions need to be addressed in order to better understand urease metallocenter assembly. The DFG complex needs to be more fully characterized including testing for CO₂ binding, carbonic anhydrase activity, and K_m determination for binding nucleotide using equilibrium dialysis methods. The DFG-Apo observed *in vivo* needs to be characterized. Does UreG have NTP hydrolysis capabilities in this species and does this complex directly interact with UreE? Another key question is how CO₂ gets into the active site. Are accessory proteins involved or does it simply diffuse into the active site? Initially I had thought that by purifying the individual accessory proteins and characterizing them, the roles of these proteins in urease metallocenter assembly would be easily identified. The difficulties in purification and characterization of UreF and UreG made me realize that this would not be the best approach. The identification of the different complexes provided a new direction in my research for understanding the roles of the accessory proteins. Hopefully my work has helped to shape an *in vivo* urease metallocenter assembly model that is more detailed and more intriguing than when I started working on this project.

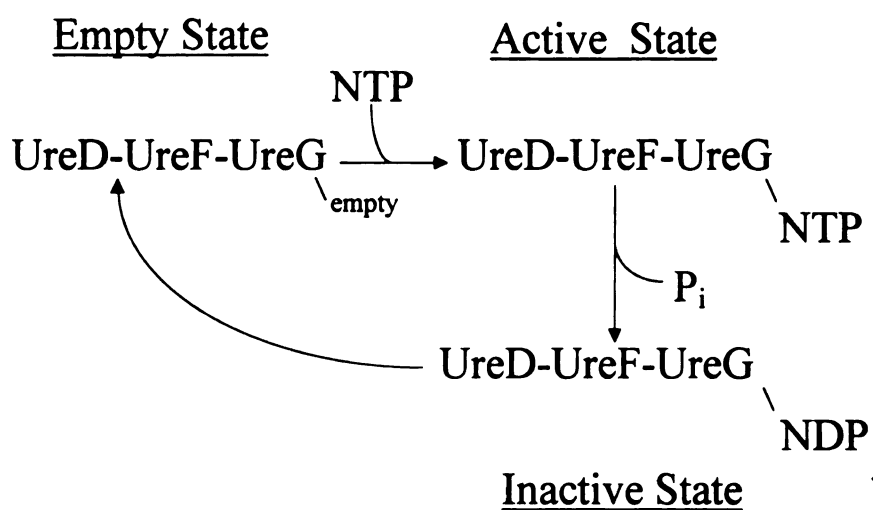
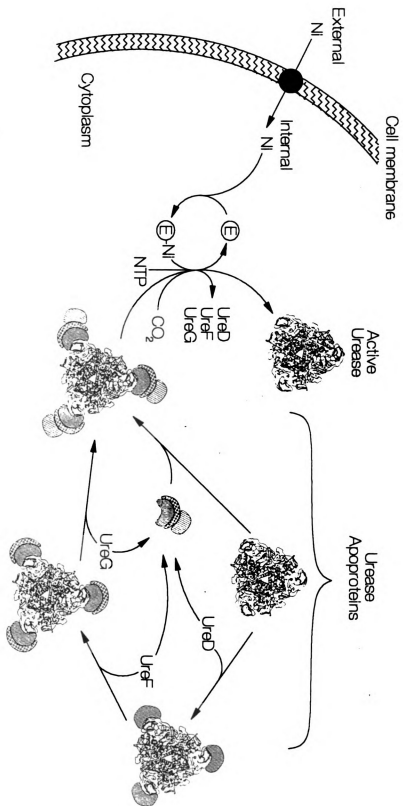


Figure 1. Proposed nucleotide hydrolysis scheme for the DFG complex. The proposed scheme for the DFG complex involves three different states of UreG: empty, active, and inactive. It is unclear whether UreD or UreF dissociates from UreG at any of these stages. The process may only occur if DFG is associated with Apo (i.e., in the DFG-Apo complexes).

Figure 7. Model for *in vivo* urease metallocenter assembly. The incorporation of nickel into urease apoprotein *in vivo* is proposed to occur by a complex process involving four accessory proteins: UreD, UreE, UreF, and UreG. Nickel enters the cell using a nickel transport system. UreE (\oplus) functions as the putative nickel donor and delivers nickel ions to the DFG-Apo complex. The model proposes that Apo either sequentially binds UreD, UreF, and UreG, or it binds the DFG complex to form the DFG-Apo complex. Insertion of nickel and CO₂ into the active site may require nucleotide hydrolysis in which UreG may play a role. Formation of holourease results in dissociation of the accessory proteins from the enzyme.



REFERENCES

1. **Bourne, H. R., Sanders, D. A. & McCormick, F.** (1990). The GTPase superfamily: a conserved switch for diverse cell functions. *Nature* **348**, 125-132.

APPENDIX I

Reprinted (abstracted/excerpted) with permission from Jabri, E., Carr, M. B., Hausinger, R. P. & Karplus, P. A. (1995). The crystal structure of urease from *Klebsiella aerogenes*. *Science* 268, 998-1004, Copyright 1996 American Association for the Advancement of Science.

The Crystal Structure of Urease from *Klebsiella aerogenes*

Evelyn Jabri, Mary Beth Carr, Robert P. Hausinger, P. Andrew Karplus*

The crystal structure of urease from *Klebsiella aerogenes* has been determined at 2.2 Å resolution and refined to an *R* factor of 18.2 percent. The enzyme contains four structural domains: three with novel folds playing structural roles, and an ($\alpha\beta$)₂ barrel domain, which contains the bi-nickel center. The two active site nickels are 3.5 Å apart. One nickel ion is coordinated by three ligands (with low occupancy of a fourth ligand) and the second is coordinated by five ligands. A carbamylated lysine provides an oxygen ligand to each nickel, explaining why carbon dioxide is required for the activation of urease apoenzyme. The structure is compatible with a catalytic mechanism whereby urea ligates Ni-1 to complete its tetrahedral coordination and a hydroxide ligand of Ni-2 attacks the carbonyl carbon. A surprisingly high structural similarity between the urease catalytic domain and that of the zinc-dependent adenosine deaminase reveals a remarkable example of active site divergence.

Urease (urea amidohydrolase; E.C. 3.5.1.5), a nickel-dependent metalloenzyme, catalyzes the hydrolysis of urea to form ammonia and carbon dioxide (1) with a rate approximately 10¹⁴ times the rate of the uncatalyzed reaction. In 1926, urease was isolated from seeds of the jack bean plant (*Canavalia ensiformis*) as a pure, crystalline enzyme by Sumner (2). These crystals, the first obtained for a known enzyme, played a decisive role in proving the proteinaceous nature of enzymes. Approximately 50 years later, jack bean urease was identified as the first nickel metalloenzyme (3). Nickel has since been found to be a component of hydrogenases for which a crystal structure was recently reported (4), methyl coenzyme M reductases, and carbon monoxide dehydrogenases (5).

Nickel-dependent ureases have been isolated from various bacteria, fungi, and higher plants (1). Their primary environmental role is to allow the organism to use external and internally generated urea as a nitrogen source (6) and, in plants, urease probably also participates in systemic nitrogen transport pathways and possibly acts as a toxic defense protein (7). In agricultural settings, rapid hydrolysis of fertilizer urea by soil bacterial ureases results in unproductive volatilization of nitrogen and in ammonia toxicity or alkaline-induced plant damage. Agricultural trials have shown that urease inhibitors can be combined with fertilizer to increase the overall efficiency of nitrogen

utilization (6). Medically, bacterial ureases are important virulence factors. They are implicated in the formation of infection-induced urinary stones (accounting for 15 to 20 percent of all urinary stones), catheter encrustation, pyelonephritis, and hepatic encephalopathy (6). The urealytic *Helicobacter pylori* has also been implicated in peptic ulceration and possibly stomach cancer formation (8). Although some inhibitors of urease are used in treatment, more than half of the patients experience adverse side effects. The commonly used inhibitor, acetohydroxamic acid, depresses bone marrow biosynthesis, inhibits DNA synthesis, and is teratogenic in high doses (9).

The best characterized bacterial urease is that from *Klebsiella aerogenes*. The native enzyme has three subunits, α (60.3 kD, UreC), β (11.7 kD, UreB), and γ (11.1 kD, UreA), reportedly associating with ($\alpha\beta\gamma$)₂ stoichiometry (10). Jack bean urease, the benchmark for comparison, exists as a trimer or hexamer of identical 91-kD subunits (11). Despite the apparent variation in quaternary structure, amino acid sequence comparison shows that ureases are homologous, sharing more than 50 percent sequence identity (11, 12). The presence of multiple distinct gene products related to portions of the jack bean sequence has also been observed for other bacterial ureases. This clear correspondence between the sequence of the single subunit plant urease and the two or three subunit bacterial ureases indicates the occurrence of a gene fusion or disruption events during the evolution of this enzyme (1). Urease does not show significant sequence similarity with other proteins.

The stoichiometry of nickel and its role in the catalytic activity of the *K. aerogenes* and jack bean ureases have been extensive-

ly studied (1). Stoichiometric analysis of inhibitor binding to urease (13) and spectroscopic analysis of thiol inhibited urease (14, 15) have shown that both ureases contain a bi-nickel center per active site. This metallocenter is directly involved in binding of substrates and inhibitors (16). Recent evidence has been obtained showing that nickel binding to urease requires CO₂ incorporation probably involving a protein nucleophile (pK_a > 9.0) (17).

Despite the availability of crystals for nearly 70 years, a structure of jack bean urease has not been determined. We have reproduced the octahedral crystals of jack bean urease and obtained crystals of *K. aerogenes* urease (18). Whereas the jack bean urease crystals diffract only to ~3.0 Å, those of *K. aerogenes* urease diffract beyond 2.0 Å resolution and can provide a detailed view of the structure and active site. We describe here the crystal structure of this nickel metalloenzyme (urease, from the bacterium *K. aerogenes*) at 2.2 Å resolution.

Structure determination. Crystals of *K. aerogenes* urease, selected site-directed mutants (19), urease apoenzyme (nickel-free) (20), and selenomethionine (Se-Met) urease (21) were grown under the same conditions (18). The phases were determined by multiple isomorphous replacement (MIR) at 3.0 Å resolution with five heavy atom derivatives and inclusion of the anomalous signal (AS) and solvent flattening (SF) (Table 1). Although connectivities and side chain densities were ambiguous in the initial electron density map, the positions of most of the β strands and α helices were clear.

An initial Ca trace (720 atoms) from the MIR-AS-SF minimap was used to build a polyaniline chain (22) that served as the starting point for interactive model building (23). Difference maps for the urease apoenzyme and three histidine to alanine mutants at the active site (His²¹³⁴, His²¹¹⁹, and His²¹²⁰) (19) provided unambiguous starting points for the insertion of sequence. Later, the positions of Se-Met difference peaks (21) and the heavy atom binding sites served as additional guides for placing sequence. Seven rounds of model building, refinement (24), and phase combination at 3.0 Å resolution (25, 26) led to a map in which the complete polypeptide chains, except the last five residues of the β subunit, could be traced unambiguously. Refinement of this model and phase extension to 2.0 Å resolution were completed by means of the simulated annealing and positional refinement protocols of X-PLOR (27). As refinement progressed, excess density at the N ϵ atom of Lys²¹¹⁷ became stronger and took on a well-defined branched shape connecting the lysine to both nickel ions (see below). In view of the recently documented

E. Jabri and P. A. Karplus are in the Section of Biochemistry, Molecular and Cell Biology, Cornell University, Ithaca, NY, 14853, USA. M. B. Carr and R. P. Hausinger are in the Departments of Microbiology and Biochemistry, Michigan State University, East Lansing, MI 48824-1101, USA.

*To whom correspondence should be directed.

requirement of CO₂ for nickel binding (17), we modeled this density as a carbamate derivative of Lys²¹⁷, from here on referred to as Lys^{217*}. In the course of refinement, changes in the density near the active site led us to suspect that the five crystals merged in the original native data set (Nat1) (Table 1) might not be perfectly isomorphous. Difference Fourier analysis with the unmerged data sets allowed us to group equivalent data sets on the basis of the absence (Nat2) or presence (Nat3) of excess active site density. Two structures were subsequently refined with gradient minimization in X-PLOR. The Nat2 structure, in which a water molecule is bound to Ni-2, was refined at 2.2 Å resolution with an *R* factor of 18.2 percent and *R*_{free} of 23.2 percent (Table 1). The Nat3 structure, in which an unidentified ligand bridges the nickel ions, was refined at 2.0 Å resolution with an *R* of 18.5 percent and *R*_{free} of 22.5 percent. Aside from small differences at the active site, the Nat2 and Nat3 structures are equivalent. The uninterpreted density at the active site in the Nat3 structure is the appropriate size for a urea molecule or a HCO₃⁻. The protein models had good geometry (28), and most heavy atom positions were near Cys, Arg, Gln, and Asp residues. The final electron density map was consistently of high quality (see below) except in the region of residues α316 to α336 where the density was sparse and the refined model had high temperature factors.

Overall structure. *Klebsiella aerogenes* urease is a tightly associated trimer of (αβγ)-units in a triangular arrangement (Fig. 1A). This (αβγ)₃ stoichiometry differs from the proposed (αβ₂γ₂)₂ structure that was based on the relative intensities of subunit bands in Coomassie blue stained gels coupled with gel filtration chromatographic and native gel electrophoretic analysis (10). All three subunits make extensive contacts to build the trimer: each α subunit packs between the two symmetry related α subunits, and contacts two β subunits and two γ subunits to form the sides of the triangle; each β subunit packs between two adjacent α subunits at the corners of the triangle; and each γ subunit interacts with two α subunits and tightly with two other γ subunits at the crystallographic threefold axis.

Because of the close interactions of the subunits, it is not obvious which α, β, and γ chains make up a primary (αβγ)-unit. However, the (αβγ)-unit discussed below was chosen such that the proximity of the various termini were compatible with the known homology of this urease with the two subunit urease from *H. pylori* (29) and the one subunit urease from jack bean (11). The carboxyl terminus of the γ subunit is 16 Å from the amino terminus of the β subunit, within the distance needed for the

insertion of four residues in the *H. pylori* urease but requiring a looping out of 30 residues of the jack bean sequence. The carboxyl terminus of the β subunit is about 35 Å from the terminus of the α subunit, a distance that would readily allow the inser-

tion of the extra 33 residues that exist in jack bean urease. The high conservation of sequence in all ureases combined with extensive interactions of the trimer suggest that all known ureases adopt a similar trimeric structure. Approximately 3300 Å²

Table 1. Summary of crystallographic data and results. Intensity data were collected at room temperature with a San Diego Multwire Systems Detector (hardware and software) on a Rigaku RU-200 rotating anode x-ray generator (47). Heavy atom derivatives were prepared by soaking crystals at room temperature in crystal storage buffer (100 mM Hepes, pH 7.5, 2.0 M Li₂SO₄) containing the respective heavy atom. Forty heavy atom compounds were screened and five derivatives were obtained. Multiple isomorphous replacement phases, at 3.0 Å including anomalous data (AS), were calculated by means of the program Derfl (48). This initial set of phases was mediocre because the heavy atom derivatives shared common sites and the phasing power beyond ~3.8 Å resolution was weak. The overall figure of merit to 3.0 Å resolution was 0.672. The phases were improved with three rounds of SF with zeroing of electron density at the heavy atom sites to remove heavy atom "ghost" peaks (26). Model building into a 3.0 Å MIR-AS-SF map was done with the programs O (22) and CHAIN (23). The phases were improved with rounds of partial model refinement by means of gradient minimization in the program TNT (24) (33,436 reflections, with weighting to the MIR-AS-SF phases) followed with phase combination by the program SIGMA (25). Phase improvement was evidenced by improved separation of the density of the nickel ions and improved connectivity and side chain densities in regions not included in the model. Upon completion of the chain tracing, refinement was continued with X-PLOR (27). The models for Nat2, Nat3, and apoenzyme were also refined in X-PLOR. The final models for Nat2 and Nat3 include 787 residues and two Ni²⁺ ions. The model for urease apoenzyme contains 787 residues but lacks the two Ni²⁺ ions and the CO₂ modification of Lys²¹⁷.

Data set	Resolution		Reflections			<i>R</i> _{sym} [*]
	(Å)	No. of crystals	Total	Unique	Complete (%)	
<i>Data collection statistics</i>						
Nat1†	2.0	5	663,385	58,463	93	9.5
Nat2	2.2	2	331,399	42,583	92	11.0
Nat3	2.0	3	386,731	56,334	93	8.9
Apoenzyme	2.8		85,114	20,532	95	12.2
HOHgC ₉ H ₄ CO ₂ Na	3.3		18,660	11,027	89	7.5
EuCl ₃	3.3		18,953	12,210	89	6.5
Hg ₂ (CH ₃ COO) ₂	2.5		67,132	28,709	94	7.6
C(HgOOCCH ₃) ₂	2.4		69,997	29,672	93	8.5
(CH ₃) ₂ Pb(CH ₃ COO)	2.4		106,954	23,486	93	7.9
Se-Met	3.0		92,935	20,332	90	14.7

Derivatives	Soaking conditions		<i>R</i> factor versus native (%)	Heavy atom sites	Phasing power vs. resolution‡		
	Conc. (mM)	Time (days)			α-6 Å	6-4 Å	4-3 Å
<i>Phasing statistics</i>							
HOHgC ₉ H ₄ CO ₂ Na	1	5	19.5	a,b	1.30	1.18	0.79
EuCl ₃	10	7	9.5	a,b	1.48	1.31	0.74
Hg ₂ (CH ₃ COO) ₂	Sat'd.	2	15.3	a,b,c,d,e	1.30	1.18	0.83
C(HgOOCCH ₃) ₂	Sat'd.	1	18.3	a,b,c,f,g,h,i,j,k	2.00	1.58	0.97
(CH ₃) ₂ Pb(CH ₃ COO)	10	8	12.5	b,g,i,m,n	1.75	1.49	0.97
FOM§	-	-	-	-	0.825	0.789	0.612

Data set	Resolution (Å)	Reflections (N)	Non-hydrogen atoms	Solvent molecules	<i>R</i> _{int}	<i>R</i> _{free} ¶	rms deviations	
							Bonds (Å)	Angles (deg)
<i>Refinement statistics</i>								
Nat2	10-2.2	41,809	5,964	177	18.2	23.2	0.008	1.88
Nat3	10-2.0	55,572	6,002	215	18.5	22.5	0.008	1.98
Apoenzyme	10-2.8	20,184	5,944	157	18.4	25.7	0.009	1.88

**R*_{sym} = $\sum |I - \langle I \rangle| / \sum I$, where *I* is the integrated intensity of a given reflection. †Nat1 = native data set for MIR analysis. ‡Phasing power is the ratio between the root mean square (rms) of the heavy atom scattering amplitude and the lack of closure error. §FOM is the mean figure of merit (cosine of the estimated phase error). ¶*R*_{free} = $\sum |F_{obs} - F_{calc}| / \sum |F_{obs}|$, where *F* is the structure factor. ¶¶*R*_{free} is the cross-validation *R* factor computed for the test set of reflections (5 percent of the total), which are omitted in the refinement process.

(10 percent) of the α , β , and γ surfaces are buried to form the $(\alpha\beta\gamma)$ -unit, and 19,100 \AA^2 (23 percent) of the $(\alpha\beta\gamma)$ -unit surface is buried when the trimer is in formation.

The $(\alpha\beta\gamma)$ -unit itself forms a T-shaped molecule with dimensions of 75 by 80 by 80 \AA (Fig. 1B). The urease $(\alpha\beta\gamma)$ -unit consists of four structural domains, two in the α

chain and one each in the β and γ chains (Fig. 1, B and C). Three of these domains appear to be unusual types of folds (30). They do not contribute any residues to the active site, but rather have structural roles. The α subunit has an $(\alpha\beta)_6$ barrel domain and a primarily β domain (Fig. 1). The $(\alpha\beta)_6$ barrel is rather elliptical with the

long axis (about 20 \AA) connecting strands 3 and 7. Two extra parallel strands (9 and 10) extend the lower portion of strands 1 to 3, accentuating the flattened appearance of the barrel. The active site is located at the carboxyl termini of the strands, and a helical excursion (H2-H4) between strand 7 and helix 7 forms a "flap" across the active

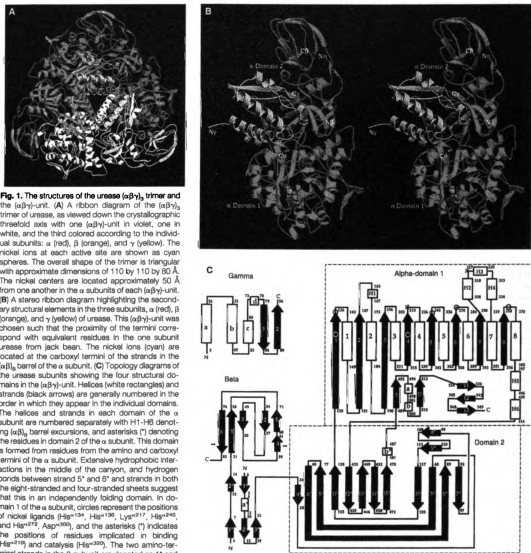


Fig. 1. The structures of the urease $(\alpha\beta\gamma)$ trimer and the $(\alpha\beta\gamma)$ -unit. (A) A ribbon diagram of the $(\alpha\beta\gamma)_3$ trimer of urease, as viewed down the crystallographic threefold axis with one $(\alpha\beta\gamma)$ -unit in violet, one in white, and the third colored according to the individual subunits: α (red), β (orange), and γ (yellow). The nickel ions at each active site are shown as cyan spheres. The overall shape of the trimer is triangular with approximate dimensions of 110 by 110 by 80 \AA . The nickel centers are located approximately 50 \AA from one another in the α subunits of each $(\alpha\beta\gamma)$ -unit. (B) A stereo ribbon diagram highlighting the secondary structural elements in the three subunits, α (red), β (orange), and γ (yellow) of urease. This $(\alpha\beta\gamma)$ -unit was chosen such that the proximity of the termini correspond with equivalent residues in the one subunit urease from jack bean. The nickel ions (open) are located at the carboxyl termini of the strands in the $(\alpha\beta)_6$ barrel of the α subunit. (C) Topology diagrams of the urease subunits showing the four structural domains in the $(\alpha\beta\gamma)$ -unit. Helices (white rectangles) and strands (black arrows) are generally numbered in the order in which they appear in the individual domains. The helices and strands in each domain of the α subunit are numbered separately with H1-H8 denoting $(\alpha\beta)_6$ barrel excursions, and asterisks (*) denoting the residues in domain 2 of the α subunit. This domain is formed from residues from the amino and carboxyl termini of the α subunit. Extensive hydrophobic interactions in the middle of the canyon, and hydrogen bonds between strand 5' and 6' and strands in both the eight-stranded and four-stranded sheets suggest that this is an independently folding domain. In domain 1 of the α subunit, circles represent the positions of nickel ligands β -Ser¹³⁴, His¹³⁶, Lys²¹⁷, His²⁴⁶, and His²⁷⁰, Asp²⁷⁰, and the asterisks (*) indicates the positions of residues implicated in binding β -Ser¹³⁴ and catalysis (β -Ser²⁰⁹). The two amino-terminal strands in the β subunit are denoted as 1' and 2' to distinguish them from the secondary structure in central six strands. Also, in the β subunit a hyphen (-) indicates that strand 4 hydrogen bonds to strand 6. The beginning and end residue numbers are given for each element.

Secondary structures were defined with the use of DSSP (50), and molecular surface areas were calculated using MS (51), (A) and (B) were produced with MOLSCRIPT (52) and rendered with Raster3D (53).

site. Two helices (H5 and H6) and a long loop (residues $\alpha 515$ to $\alpha 532$) cover the amino-terminal end of the barrel. This loop is part of an unusual feature in which the carboxyl terminal 100 residues wrap completely around the ($\alpha 8$)₈ barrel domain. The second β domain is formed by residues $\alpha 33$ to $\alpha 129$ and $\alpha 30$ to $\alpha 488$. Here, eight-stranded and four-stranded mixed β sheets form the walls of a U-shaped canyon. The walls are connected by the long strands 5* and 6* together with strands 10* and 11*, which go down one side and up the other.

The first 15 residues of the β subunit form two antiparallel β sheets with the amino-terminal residues of the α subunit (Fig. 1). The core of the β subunit adopts an imperfect six-stranded antiparallel β jellyroll. The jellyroll is left-handed and may be the first of this kind observed (31). Strand 6 is followed by a long loop that packs against the loops before and after strand 3. The last five residues ($\beta 102$ to $\beta 106$) are disordered. This subunit stabilizes the trimer by associating with domain 2 of its own α subunit and domain 1 of a symmetry related α subunit.

The γ subunit adopts a novel $\alpha\beta$ domain with four helices and two antiparallel strands (Fig. 1). Two of the helices (b and c) and the two strands pack tightly like the helices of a four-helix bundle and have the commonly seen right-handed up-down-up-down topology for that family (32). Helix a is clearly peripheral and helix d is little more than a turn. This subunit facilitates trimer formation through association with the α subunit and the symmetry related γ subunits. The packing of γ subunits at the crystallographic threefold axis is dominated by three copies of helix a, one from each γ subunit, which pack against one another in an almost orthogonal manner.

The nickel center. Spectroscopic studies of jack bean and *K. aerogenes* urease have suggested that the two active site nickels are within approximately 3.5 Å, and that each metal ion is approximately pentacoordinate, with about two imidazoles and additional N or O atoms serving as ligands (14). Site-directed mutagenesis of *K. aerogenes* urease tentatively identified His²⁴⁶, His¹³⁶, and His²¹⁷ as three of the nickel ligands (19).

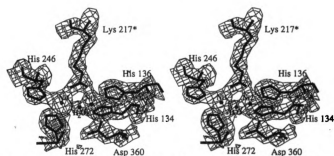


Fig. 2. Stereo diagram of the urease Ni-nickel center showing the carbamylated lysine residue (Lys²¹⁷). The electron density map was calculated with coefficients $2F_o - F_c$, and is shown contoured at 1.5 times the rms density. This figure was produced with CHAIN (23).

Table 2. Coordination geometry at the Ni-nickel center. Coordinate accuracy is approximately 0.2 Å in this region of the structure, as estimated by a Luzzati plot (49).

Metal-ligand	Distance (Å)	Ligand-metal-ligand	Angles (degrees)
Ni1-Lys ²¹⁷ O81	2.0	Lys ²¹⁷ O81-Ni1-His ²⁴⁶ N8	92
Ni1-His ²⁴⁶ N8	2.1	Lys ²¹⁷ O81-Ni1-His ²¹⁷ N6	107
Ni1-His ²¹⁷ N6	2.2	His ²⁴⁶ N8-Ni1-His ²¹⁷ N6	95
Ni2-His ¹³⁶ N4	2.2	His ¹³⁶ N4-Ni2-His ¹³⁴ N2	110
Ni2-His ¹³⁴ N2	2.2	His ¹³⁶ N4-Ni2-Lys ²¹⁷ O82	80
Ni2-Lys ²¹⁷ O82	2.1	His ¹³⁶ N4-Ni2-Mac-1	88
Ni2-Asp ³⁶⁰ O81	2.1	His ¹³⁶ N4-Ni2-Lys ²¹⁷ O82	151
Ni2-Mac-1	2.0	His ¹³⁶ N4-Ni2-Lys ²¹⁷ O82	88
		His ¹³⁶ N4-Ni2-Asp ³⁶⁰ O81	88
Ni1-Ni-2	3.5	His ²⁴⁶ N8-Ni2-Mac-1	92
		Asp ³⁶⁰ O81-Ni2-Lys ²¹⁷ O82	148
		Asp ³⁶⁰ O81-Ni2-Mac-1	98

Our structural results agree reasonably well with these studies (Fig. 2). The nickel ions are well ordered (B factors of about 15.0 Å²) and are 3.5 Å apart. Ni-1 is coordinated by three (two N and one O) ligands: His²⁴⁶ through the N8 atom, His²¹⁷ (33) through N6, and Lys²¹⁷ through O81 of the carbamate (see below). Ni-2 is coordinated by five (two N and three O) ligands: His¹³⁶ and His¹³⁴ both through N4, Asp³⁶⁰ through O81, Wat-1, and Lys²¹⁷ through O82 (Table 2). The geometry for Ni-1 can best be described as pseudotetrahedral with a weakly occupied fourth ligand (34). The geometry for Ni-2 can be described as distorted trigonal bipyramidal or distorted square pyramidal with His¹³⁶ as the apical ligand (Fig. 2 and Table 2).

The presence of a carbamate ligand to the nickel ions would have been surprising if it were not for the recent finding that activation of urease apoenzyme can be achieved *in vitro* only in the presence of CO₂ (17). The activation results and the structure are consistent with the attachment of CO₂ reacting with Lys²¹⁷ prior to nickel binding. The structure of the urease apoenzyme (Table 1) shows no carbamate, suggesting that carbamylation of Lys²¹⁷ occurs readily in aqueous solution, but the binding of nickel ions is required to stabilize the carbamylated form. A similar carbamylated lysine has been observed in another enzyme, namely ribulose-1,5-bisphosphate carboxylase oxygenase (RUBISCO) (35). There, carbamylation is required for the binding of Mg²⁺, which in turn coordinates the substrate. In contrast to urease which binds metal tightly (36), RUBISCO can be readily deactivated by metal chelators. Although urease can be activated *in vitro* by the addition of CO₂, its activation *in vivo* appears to be aided by specific proteins (20, 37).

The use of a carbamate ligand, rather than an Asp or Glu residue, appears to be necessitated by the position of the active site in the ($\alpha 8$)₈ barrel in that shorter Asp or Glu residues would not reach the nickel center. Also, the ability of the carbamate to form resonance isomers that allow higher partial negative charges on the oxygens compared to carboxylic acids may be important in the ligation of the nickels or the modulation of their chemistry.

Active site and catalytic mechanism. Adjacent to the nickel, near Wat-1, is a pocket roughly the size of urea, which is a static structure is sequestered by the side chain of Cys³¹⁹ from a narrow channel leading to the enzyme surface (Fig. 3). However, the H2-H4 flap (residues $\alpha 308$ to $\alpha 336$), which forms one wall of the channel, is highly mobile suggesting that this flap may easily open to allow extensive

access to the active site. In fact, the facile modification of Cys²¹⁹ at the base of the channel by bulky reagents (38) and, in our analysis, by large heavy atom compounds such as C(H₂OOCCH₃), suggests that the channel can readily open.

The putative urea binding pocket is lined by residues from loops 1, 2, 4, 5, 6, 7, and 8 of the (α B)₁ barrel (Fig. 3). These include Ala¹⁶⁷, Gly¹⁷⁷, His²¹⁹, Ala³⁶³, Met³⁶⁴, Cys²¹⁹, and His³²⁰. Three of these residues, His²¹⁹, Cys²¹⁹, and His³²⁰ have been implicated as important by chemical modification and mutagenesis studies. Site-directed mutagenesis of His²¹⁹ to alanine produced an active enzyme with a K_m of 1100 mM compared to 2.3 mM for wild type (19). This result suggests that His²¹⁹ is involved in substrate binding, and in the structure it is positioned 3.1 Å from Ni-1 and 3.7 Å from Ni-2. Furthermore, His²¹⁹ receives a hydrogen bond to N δ from the main chain nitrogen of Asp²²¹ and is therefore protonated on N δ .

Modification of Cys²¹⁹ (or its equivalent residue in jack bean urease) by chemical reagents (11, 38) blocks activity. Dixon and colleagues (39) proposed that a cysteine serves as a general acid in jack bean urease catalysis. Later, mutagenesis studies (36) showed that Cys²¹⁹ is not essential, as an alanine mutation of this residue retained 48 percent of the wild-type activity while mutations to larger residues were more deleterious. The *Staphylococcus xylosum* enzyme does not have a cysteine at this position (40), further supporting the notion that Cys²¹⁹ is not essential for activity. In the structure, Cys²¹⁹ Sy is 4.4 Å from Wat-1. The effect of larger Cys²¹⁹ mutations could easily be caused directly by steric effects or indirectly by changes in the position of the general base, His³²⁰ (see below).

Dienylpyrocarbonate (DEP) modification of the bacterial urease indicated that a histidine with a pK_a of 6.5 is essential for activity (41). Site-directed mutagenesis of His³²⁰ produces an enzyme that is not DEP sensitive and although the mutant has normal nickel content, it has very low (\sim 0.03 percent) activity (19). These results are consistent with His³²⁰ acting as a catalytic base. In the structure, His³²⁰ Ne is 4.8 Å from Ni-1 and 4.3 Å from Wat-1. The pK_a and orientation of His³²⁰ are influenced by hydrogen bonds to the side chains of Asp²²¹ and Arg²³⁶ (Fig. 3).

From the results of biochemical studies, Dixon and colleagues (39) also proposed that a carboxyl group is present at the active site of jack bean urease. In addition, the efficacy of various thiols as inhibitors and the reactivity of thiol-specific modification reagents for inactivating *K. aerogenes* urease are consistent with the presence of a

negatively charged group at the active site (13, 42). The structure confirms the presence of three acidic residues, Gly²²⁰, Asp²²¹, Asp³⁶⁰ and three main chain carbonyl oxygens from residues Ala¹⁶⁷, Gly¹⁷⁷, and Ala³⁶³. The carbonyl oxygens of Gly¹⁷⁷ and Ala³⁶³ serve to hold a water molecule in place, which hydrogen bonds to both Wat-1 and His³²⁰. In a urea-bound enzyme, these carbonyl groups along with that of Ala¹⁶⁷ and possibly O81 of Asp³⁶⁰ may be involved in binding the NH₂ groups of urea.

The structure of *K. aerogenes* urease can accommodate the mechanistic model proposed by Zerner and colleagues for the jack bean enzyme (39). The essence of this proposal is that one nickel ion binds a hydroxide ion, and urea binds to the other nickel, via O-coordination, to polarize the substrate. Based on the structure, Wat-1 would be the hydroxide and the urea oxygen would bind to Ni-1 completing its tetrahedral coordination. Modeling urea in this manner places its oxygen within hydrogen bonding distance of Ne of His²¹⁹ which may aid in orienting and further polarizing the carbonyl of urea and account for the importance of His²¹⁹. The polarized carbonyl of urea is subsequently attacked by a hydroxide, which results in the formation of a tetrahedral intermediate. Zerner's model suggests that a base abstracts a proton from a water molecule to yield a hydroxide. O81 of Asp³⁶⁰ is in a position to activate Wat-1

for attack, whereas the putative catalytic base, His³²⁰ is positioned too far from the attacking hydroxide. For His³²⁰ to act as the catalytic base, it must move upon binding of urea to a position favorable for proton abstraction from Wat-1. The resulting tetrahedral intermediate is thought to decompose, with the participation of a general acid, to ammonia and a Ni-bound carbamate, which subsequently dissociates. At this time, the identity of the general acid present in *K. aerogenes* urease (10) remains unclear.

Although the mechanism outlined above does account for most of the available data, the urease structure is also compatible with alternative models that may involve more structural changes at the active site. For example, urea may displace Wat-1 at Ni-2 and coordinate via the oxygen, or might even bridge both nickels through its carbonyl oxygen. In these cases, there are more possible orientations of bound urea and less can be said about the specific roles for active site residues.

A Zn-metalloenzyme relative. The (α B)₁ barrel observed in the catalytic Ni-binding domain of the α subunit is a rather common topology for proteins, and active debate centers on whether the many (α B)₁ barrels that do not share significant sequence similarity are a result of convergent or divergent evolution (43). Given the lack of recognizable sequence similarity of urease with any other protein, we were surprised

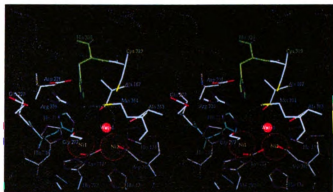


Fig. 3. Stereo diagram of the active site of urease. The nickel ions are sequestered in a pocket from a narrow channel by the side chain of Cys²¹⁹. The channel is formed from residues in the α subunit (His²¹⁹, Lys²¹⁸, Cys²¹⁹, Asp²²⁰, Met²²¹) with some contributions from residues in the α subunit of a symmetry related molecule (His¹⁶⁷, Thr¹⁶⁸, Thr¹⁶⁹). Cys²¹⁹ sits at the base of the channel positioned such that O81 and Sy are 3.6 Å from the plane of the ring of the catalytic base, His³²⁰ (green). Asp²²¹ positions the nickel ligand His²¹⁹ through less commonly observed hydrogen bonding involving the anti-orbital of the carbonyl. His²¹⁹ (cyan) is positioned to donate a hydrogen bond to the substrate and the main chain oxygens of Ala¹⁶⁷, Gly¹⁷⁷, and Ala³⁶³ are positioned to accept hydrogen bonds from water or urea. Nitrogen atoms are blue, oxygen atoms are red, and carbon atoms are gray (His³²⁰, cyan (His²¹⁹), gray (nickel ligands) or white (other active site residues)). Solvent accessible surface area was calculated using a 1.4 Å radius probe. This figure and Fig. 4A were produced with Insight version 2.3.5 (BIOSY).

when a structural comparison with all known protein structures (30) revealed that the ($\alpha\beta$)₂ barrel of the α subunit is strikingly similar to that of adenosine desaminase (ADA), an enzyme containing one zinc per active site. This enzyme catalyzes the deamination of adenosine to yield inosine and ammonia (44), a reaction mechanistically related to that of urease. Both mechanisms involve the attack of a metal coordinated water on the amide carbon to form a tetrahedral intermediate that subsequently degrades to yield NH_3 as one of two products. The nucleophilic water molecule in ADA is stabilized through hydrogen bonds with an aspartic acid and with the catalytic base.

ADA is one of two members of a new class of ($\alpha\beta$)₂ barrels characterized by a unique elliptical barrel axis and a requirement for metal ions (43). The second is the Zn-dependent phosphotriesterase for which the apoenzyme crystal structure was recently determined (45). A superposition of urease and ADA shows that 72 atoms in the strands of the barrel overlap with 1.8 Å root-mean-square (rms) deviation (Fig. 4A). For comparison, the beat overlay with structures of other representative members of the ($\alpha\beta$)₂ barrel family have rms devia-

tions of approximately 3.0 Å (46). The helices in urease and ADA all have the same tilt but are somewhat shifted, so that 90 equivalent residues overlap with 2.8 Å rms deviation. The active sites of urease and ADA also show a high degree of structural similarity (Fig. 4B). The position of the Ni-2 and Wat-1 in urease are structurally equivalent to the zinc ion and the hydrolytic water molecule at the active site of ADA. Ni-2 ligands His^{114} , His^{116} , and Asp^{100} of urease are structurally equivalent to Zn ligands His^{15} , His^{17} , and Asp^{95} of ADA. Lys^{217} in urease is equivalent to Asp^{91} , a residue too short to coordinate the Zn ion. Rather, His^{214} of ADA, structurally equivalent to Ni-1 ligand His^{210} of urease, rotates 90° relative to His^{216} , to take the place of Lys^{217} as a metal ligand. His^{177} , a Ni-1 ligand in urease, is equivalent to His^{19} , the proposed catalytic base in ADA.

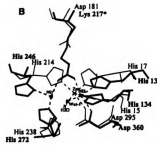
The high degree of global and active site similarity, combined with possible mechanistic similarity, strongly suggests that urease and ADA are homologs. This surprising homology raises some interesting questions: how did urease acquire the requirement for CO_2 activation, and why is the enzyme specific for nickel when zinc or other metals could serve similar functions? Furthermore,

what mechanisms lie behind the emergence of four accessory proteins, UreD, UreE, UreF, and UreG (20, 37), which are required for *in vivo* assembly of urease. Thus, in addition to the utility of this structure for inhibitor design, further study of this system should lead not only to insight into the mechanism and regulation of urease, but also insight into the mechanisms of protein evolution.

REFERENCES AND NOTES

- R. P. Hausinger, *Biochemistry of Nickel* (Plenum Press, New York, 1993), chap. 3.
- J. S. Burmer, *J. Biol. Chem.* **268**, 438 (1993).
- N. E. Dixon, C. Gatzolis, R. L. Blakely, B. Zerner, *J. Amer. Chem. Soc.* **97**, 4131 (1975).
- A. Volzoch et al., *Nature* **375**, 580 (1995).
- R. P. Hausinger, *Biochemistry of Nickel* (Plenum Press, New York, 1993), chap. 4, p. 5.
- H. L. T. Mohler and R. P. Hausinger, *Mol. Microbiol. Rev.* **53**, 85 (1992); H. L. T. Mohler, M. O. Island, R. P. Hausinger, *ibid.*, in press.
- J. C. Polacco and M. A. Holland, in *International Review of Cytology*, K. W. Loon and J. Jenkin, Eds. (Academic Press, San Diego, 1993), p. 20.
- A. Lee, J. Fox, S. Hazell, *Infect. Immun.* **81**, 1601 (1993); J. Fox, S. Hazell, *Microbes* **200**, 159 (1992); M. Marzetti et al., *Cell* **287**, 1655 (1995).
- D. P. Gillies, *Unif. Res.* **7**, 215 (1978).
- M. J. Todd and R. P. Hausinger, *J. Chem. Biol.* **282**, 5095 (1997).
- S. Wang et al., *Inorg. Chem.* **33**, 1569 (1993).
- S. B. Mamonova and R. P. Hausinger, *J. Bacteriol.* **172**, 5837 (1993).
- M. J. Todd and R. P. Hausinger, *J. Biol. Chem.* **264**, 15035 (1989).
- K. Takahashi, T. Suga, G. Maruya, *Eur. J. Biochem.* **175**, 151 (1988).
- M. G. Finnegan et al., *J. Am. Chem. Soc.* **113**, 4000 (1991).
- N. E. Dixon, R. L. Blakely, B. Zerner, *Can. J. Biochem.* **58**, 481 (1980); R. L. Blakely, N. E. Dixon, B. Zerner, *Biochim. Biophys. Acta* **714**, 219 (1983).
- L. S. Park and R. P. Hausinger, *Science* **287**, 1156 (1995).
- E. Jahn, M. H. Lee, R. P. Hausinger, J. A. Karkus, *J. Mol. Biol.* **227**, 634 (1992). Crystals grew in hanging drops equilibrated against 100 mM Hepes (pH 7.5) and 1.8 M Li_2SO_4 . All crystals were isomorphous, having the cubic space group $I2_12_1$ with $a = 170.8$ Å and one catalytic unit per asymmetric unit.
- I. S. Park and R. P. Hausinger, *Protein Sci.* **2**, 1034 (1993). The data statistics for the three mutants are similar to those observed for Nat1. Details of the crystal structure are in preparation.
- M. H. Lee, S. B. Mamonova, M. J. Finver, Y. Mamonova, R. P. Hausinger, *J. Bacteriol.* **174**, 4324 (1992).
- 36-Mer urease was obtained from *K. aerogenes* carrying pKUA19 (20) grown in MOPS minimal medium plus chloramphenicol. When a 1-liter subculture at 37°C reached $A_{600} = 0.8$, the following compounds were added: 30 mg of de-lact, 100 mg of lysine-HCl, 100 mg of inosine, 100 mg of glutathione, 50 mg of leucine, 50 mg of isoleucine, and 50 mg of valine. The culture was grown for an additional 22 hours at 30°C reaching A_{600} of 3.4. Purification was the same as for the holohydrate. The low specific activity observed for the 36-Mer enzyme (207 U/mg) may be due to substitution-induced conformational changes in the active site of the active site base, i.e., His^{190} , placing it in a catalytically unfavorable position. A retrospective analysis shows that 22 of the 23 36-Mer residues have difference peaks $F_o - F_c$ greater than 4.0 times the rms level of the $F_o - F_c$ map. His^{190} is low because of the high mobility of this stretch of residues.
- T. A. Jones, J. Y. Zou, S. W. Cowen, S. W. Kentrup, *Acta Cryst.* **A47**, 110 (1991).
- J. S. Sack, *J. Mol. Cryst. Liq. Cryst.* **8**, 224 (1968).

Fig. 4. Comparison of urease and adenosine desaminase (ADA). (A) An overlay of the ($\alpha\beta$)₂ barrels, according to the strategy of Chothis and Lesk (54). The view is looking from the amino to carboxyl termini of the strands. (B) A stereo-view of the urease active site (thick lines and bold lettering) overlaid onto the ADA active site. Structurally equivalent residues shown (urease/ADA) include $\text{His}^{124}/\text{His}^{15}$, $\text{His}^{126}/\text{His}^{17}$, $\text{Asp}^{100}/\text{Asp}^{95}$, $\text{His}^{177}/\text{His}^{19}$, $\text{His}^{186}/\text{His}^{114}$, and $\text{Lys}^{217}/\text{Asp}^{91}$.



24. D. E. Tronrud, L. F. Ten Eyck, B. W. Matthews, *Acta Crystallogr.* **A43**, 489 (1987). The command file for TNT was modified to include an additional R factor (R_{free}) calculation before initiation of each cycle of refinement. The test data set, generated in X-PLOR, served as the data set for R_{free} calculation while the working data set was used in refinement.
25. R. J. Read, *Acta Crystallogr.* **A46**, 900 (1990). SIGMAA weighted structure factors were used to generate F_{O} , α_{combined} electron density maps for use in fitting.
26. CCP4, "Collaborative Computational Project, Number 4," *ibid.* **D50**, 760 (1994).
27. A. T. Brünger, A. Krukowski, J. W. Erickson, *ibid.* **A48**, 585 (1990).
28. All residues are in the allowed regions of ψ/ϕ angles with seven residues (1.1 percent) falling in the generously allowed regions. Two are in type 2' turns (Ala²²⁴, Phe¹⁹⁹), one is in a type 2 turn (His²⁷²), two are metal ligands (His²⁷², Asp²⁶⁰), and one has a high B factor (Met³¹⁷). Ala²⁶¹ has clear and well-defined density. The model contains three cis-prolines: $\alpha 282$, $\alpha 303$, and $\alpha 470$.
29. C. L. Clayton, M. Pallen, H. Kleenhou, B. W. Wran, S. Tabacqchali, *Nucleic Acid Res.* **18**, 362 (1990); A. Lebligne, V. Cussac, P. Courcoux, *J. Bacteriol.* **173**, 1920 (1991).
30. L. Holm and C. Sander, *J. Mol. Biol.* **233**, 123 (1993); N. S. Boutonnet, M. J. Rooman, M.-E. Ochagavia, J. S. L. Wodak, in preparation; D. F. Fischer, H. Wolfson, S. L. Lin, R. Nussinov, *Protein Sci.* **3**, 769 (1994). A comprehensive search of the Protein Data Bank was done by the three groups cited. The search by L. Holm with the program Dali showed that domain 1 of the α subunit, an $(\alpha\beta)_2$ barrel, is similar to the $(\alpha\beta)_2$ barrel of adenosine deaminase. Domain 2 of the α subunit, the β subunit, and the γ subunit had no closely similar structure.
31. J. S. Richardson, *Adv. Protein Chem.* **34**, 167 (1981).
32. C. Cohen and D. A. D. Parry, *Proteins* **7**, 1 (1990).
33. His²⁷² was not studied by site-directed mutagenesis because it was not conserved in the *Ureaplasma urealyticum* sequence. An analysis of the reported *U. urealyticum* sequence (A. Blanchard, personal communication) indicates that a sequencing error caused a reading frame shift so that about a dozen amino acids, including His²⁷², reported to be distinct compared to other ureases, are in fact conserved.
34. The electron density map shows weak bridging density between Ni-1 and Wat-1. The density is ~ 1.8 Å from Wat-1 and therefore, cannot be a second water molecule at full occupancy. We estimate the position of Wat-1 is highly occupied as it has a reasonable B factor of 7.0 Å². During the other small portion of the time, Wat-1 may instead occupy a position bridging the nickel ions or solely as Ni-1 ligand.
35. F. C. Hartman and M. R. Harpel, *Annu. Rev. Biochem.* **63**, 197 (1993).
36. P. R. Martin and R. P. Hausinger, *J. Biol. Chem.* **267**, 20024 (1992).
37. M. B. Carr and R. P. Hausinger, in *Mechanisms of Metallocenter Assembly*, R. P. Hausinger, G. L. Eichhorn, L. G. Marzilli, Eds. (VCH, New York), in press.
38. M. J. Todd and R. P. Hausinger, *J. Biol. Chem.* **266**, 24327 (1991).
39. N. E. Dixon, P. W. Riddles, C. Gazzole, R. L. Blekeley, B. Zerner, *Can. J. Biochem.* **58**, 1335 (1980).
40. J. Jose, S. Christens, R. Rosenstein, F. Götz, H. Kaltwasser, *FEMS Microbiol. Lett.* **80**, 277 (1991).
41. I. S. Park and R. P. Hausinger, *J. Protein Chem.* **12**, 51 (1993).
42. M. J. Todd and R. P. Hausinger, *J. Biol. Chem.* **266**, 10260 (1991).
43. G. K. Farber and G. A. Petsko, *Trends Biochem. Sci.* **15**, 228 (1990); G. K. Farber, *Curr. Opin. Struct. Biol.* **3**, 409 (1993); D. Reardon and G. K. Farber, *FASEB J.*, in press.
44. D. K. Wilson, F. B. Rudolph, F. A. Quiocho, *Science* **252**, 1278 (1991).
45. M. M. Benning, J. M. Kuo, F. M. Raushel, H. M. Holden, *Biochemistry* **33**, 15001 (1994).
46. E. Jabri and P. A. Karplus, unpublished results.
47. R. C. Hamlin, *Methods Enzymol.* **114**, 416 (1985); N. H. Xuong, C. Nielson, R. Hamlin, D. Anderson, *J. Appl. Crystallogr.* **18**, 342 (1985).
48. R. E. Dickerson, J. E. Weinzierl, R. A. Palmer, *Acta Crystallogr.* **B24**, 997 (1968). Derell is a modified version of a program used in the laboratory of G. E. Schulz.
49. P. V. Luzzati, *Acta Crystallogr.* **5**, 802 (1952).
50. W. Kabsch and C. Sander, *Bio polymers* **22**, 2577 (1983).
51. M. L. Connolly, *Science* **221**, 709 (1983).
52. P. Krauts, *J. Appl. Crystallogr.* **24**, 946 (1991).
53. D. J. Bacon and W. F. Anderson, *J. Mol. Graph.* **6**, 219 (1988); E. A. Merritt and M. E. P. Murphy, *Acta Crystallogr.* **D50**, 869 (1994).
54. L. Chothia and A. Lesk, *EMBO J.* **4**, 823 (1986).
55. We thank I.-S. Park and M. Lee for selected mutant enzymes and apoenzyme, R. Shagita for TAMM and DNA heavy atom compounds, L. Holm, N. Boutonnet, M. Rooman, and D. Fischer for searching the PDB for homologs, S. Ealick for the use of his detector, and B. Carpenter and S. Lippard for helpful discussion of the metal center. Supported by USDA grant 9303870 (P.A.K. and R.P.H.) and by NIH training grant 5T32-GM08384-04 (E.J.). The coordinates and structure factors are deposited in the Protein Data Bank with entry codes 1KAU for Nat2, 2KAU for Nat3, and 3KAU for the apoenzyme.

1 January 1995; accepted 5 April 1995